Fall 2011

A follower load as a muscle control mechanism to stabilize the lumbar spine

Byeong Sam Kim
University of Iowa

A FOLLOWER LOAD AS A MUSCLE CONTROL MECHANISM TO STABILIZE THE LUMBAR SPINE

by

Byeong Sam Kim

An Abstract

Of a thesis submitted in partial fulfillment
of the requirements for the Doctor of
Philosophy degree in Biomedical Engineering
in the Graduate College of
The University of Iowa

December 2011

Thesis Supervisor: Professor Tae-Hong Lim

ABSTRACT

The spine is a long and slender column which supports the upper body. In the 1960s, the compressive force acting on the spine estimated by the intradiscal pressure measured *in vivo* was found to exceed 2600N. However the ligamentous lumbar spine is known to be unstable when subjected to compressive loads of 88 N. It is generally agreed that the ligamentous spine itself is unstable but can be stabilized by the muscle forces (MFs) *in vivo*. Biomechanical loads are known to be closely associated with spinal disorders. Normal spinal loads, however, remains poorly understood due to the lack of knowledge of the MF control mechanism for normal biomechanical functions.

To determine the spinal MFs creating compressive follower loads (CFL) in the lumbar spine in various sagittal postures and to investigate if such MFs can maintain the spinal stability, 3-D optimization and FE models of the spinal system (trunk, lumbar spine, sacrum, pelvis, and 232 muscles) were developed and validated using reported experimental data. Optimization models were used to determine the MFs creating CFLs in the lumbar spine in various sagittal postures from 10° extension to 40° flexion. The deformation of the lumbar spine under these MFs and trunk weight was predicted from FE models. The stable lumbar spine deformation was determined by the resultant trunk sway less than 10 mm.

Optimization solutions of MFs, CFLs, and follower load path (FLP) location were feasible for all studied postures. The FE predictions clearly demonstrated that MFs creating CFLs along the base spinal curve connecting the geometrical centers(GCs) or along a curve in its vicinity (within anterior or posterior shift by 2 mm) produce the stable deformation of the lumbar spine in the neutral standing and flexed postures, whereas the MFs creating the smallest CFLs resulted in the unstable deformation. In case of extended postures, however, it was not possible to find the CFL creating MFs that produce stable

deformation of the extended spine whereas it was possible when stronger muscles were simulated.

The results of this study demonstrate the feasibility for spinal muscles to stabilize the spine via the CFL mechanism. These findings support the hypothesis that CFLs act as muscle control mechanism to stabilize the whole lumbar spine.

Abstract Approved: _____
Thesis Supervisor

_____
Title and Department

_____
Date

A FOLLOWER LOAD AS A MUSCLE CONTROL MECHANISM TO STABILIZE THE LUMBAR SPINE

by

Byeong Sam Kim

A thesis submitted in partial fulfillment
of the requirements for the Doctor of
Philosophy degree in Biomedical Engineering
in the Graduate College of
The University of Iowa

December 2011

Thesis Supervisor: Professor Tae-hong Lim

Graduate College
The University of Iowa
Iowa City, Iowa

CERTIFICATE OF APPROVAL

_____

PH.D. THESIS

_____

This is to certify that the Ph.D. thesis of

Byeong Sam Kim

has been approved by the Examining Committee for the thesis requirement for the Doctor of Philosophy degree in Biomedical Engineering at the December 2011 graduation.

Thesis Committee: _____
Tae-hong Lim, Thesis Supervisor

_____
Kyung K. Choi

_____
M.L. Raghavan

_____
Nicole M. Grosland

_____
Prem S Ramaskrishnan

To my parents, wife and my children

ACKNOWLEDGEMENTS

Many people who have played signifigant roles in the work that is presented in this dissertation. First of all, I would like to thank my advisor Prof. Tae-hong Lim for the support, insight, and encouragement that he provided throughout the years. I am appreciative of the relationship we have developed and I am so blessed to have had a chance to work with him.

I would also like to thank my committee members for evaluating my work. Prof. Kyung K. Choi, Prof. M.L. Raghavan, Prof. Nicole M. Grosland and Prof. Prem S Ramaskrishnan. Thank you for serving on my committee and for providing valuable comments and specific questions for further improvement. Each of you is an expert in your field and I have benefited greatly from the interaction with each of you.

I would like to express my gratitude to Tian for providing assistance in the simulation in this project. I am also grateful for the contribution of the past lab mates; especially to Dr. Kap-soo Han for his contribution to the development of optimization problem in this project and Michael Magnetta for assistance in experiment. It has been a real joy to work with them in this spine lab, and I am grateful for the friendship we have developed.

I am also grateful to the department of Biomedical Engineering for providing the facilities to accomplish my research and teaching assistance ship. Without the help of those mentioned above, my research could not have been undertaken.

Lastly, my wife, children and parents have given me love and support throughout my study in Iowa, and I am thankful for the value they have placed on higher education. Without unwavering support and constant encouragement of my family, my Ph.D work would not have been completed.

TABLE OF CONTENTS

LIST OF TABLES

LIST OF FIGURES

CHAPTER 1

INTRODUCTION

The spine is a long and slender column which supports the upper body. In the 1960s, Nachemson et.al showed that compressive force acting on the spine estimated by the intradiscal pressure measured *in vivo* may exceed 2600N [1]. However the ligamentous lumbar spine (spine without muscle) is known to be unstable when subjected to compressive loads of 88 N [2]. It is generally accepted that the ligamentous spine itself is unstable but can be stabilized by the muscle forces(MFs) *in vivo*. Recent experimental study have shown that the ligamentous cervical and lumbar spines can withstand a compressive physiologic load up to 250N and 1200N, respectively, without buckling of the spine while maintaining its flexibility when the compressive force is applied along the spinal curvature (i.e., follower load) [3, 4]. The investigators of these studies postulated that the follower load would be a physiological load on the spine *in vivo*. Furthermore, Han et al. conducted an analytical study using an optimization model incorporating 232 muscles associated with the lumbar spine and demonstrated that there could be numerous combinations of spinal MFs creating a compressive follower load(CFL) in the lumbar spine in various sagittal postures [5]. They also investigated the effects of increasing external compressive force and flexion moment applied on the lumbar spine and found that the back muscles could create a CFL in the spine even under a considerable amount of external loads. These studies suggested that the follower load could be a physiological spinal load and spinal muscles might be controlled to create CFLs in the spine by the central nervous system *in vivo*.

However, *in vitro* experimental studies had their limitations mainly because it was practically impossible to simulate the spinal muscles in the tests. Han et al's study

showed that there existed static equilibriums of spinal joint forces, spinal MFs and external loads in which the directions of the spinal joint forces followed the spinal curvature without the confirmation of the deformations of the spine in relation to the stability of the spine.

Further studies required for more comprehensive tests of the hypothesis that the spinal muscles are controlled to create a follower load in the lumbar spine *in vivo* in order to maintain its stability and flexibility would include analytical studies using 3-D finite element (FE) models incorporating all spinal muscles attached to the spinal column and further experimental studies guided by the FE model predictions. For this purpose, computational studies were performed in this study. The specific aims of this study are:

Aim 1: to develop a 3-D FE model of the lumbar spine incorporating the 232 spinal muscle fascicles and the upper body attached to the L1 vertebral through the T12-L1 joint with the validation of the lumbar spine behavior with *in vitro* experimental data reported in the literature;

Aim 2: to improve the currently available optimization model of the follower load for the perfect synchronization of boundary conditions of the optimization and FE models;

Aim 3: to perform the parametric studies in order to investigate the effect of the variations in follower load path (FLP) and maximum muscle force capacity (MFC); and

Aim 4: to find the patterns of recruiting spinal muscles over the sagittal posture changes (i.e., from full extension to full flexion, from neutral to flexion)

CHAPTER 2

BACKROUND AND SIGNIFINCE

2.1 The anatomy of a spine

A spine is a long and multi segmental column spanning from occiput to sacrum. Its biomechanical roles are 1) to support the upper body and transfer the moment and load to lower extremities during various daily activities and tasks to lower extremities 2) to allow upper motion such as flexion, extension, lateral bending and axial rotation, and 3) protect the spinal cord, nerve roots and internal organs. The understanding of the normal spine anatomy is critical to the planning and executing of various biomechanical experiments and simulations. Human spine (see Figure 2-1) is composed of a series of bones called vertebrae stacked on another. The spine is divided into four main regions; cervical, thoracic, lumbar and sacrum from superior to inferior.

2.1.1 Spinal planes and curves

In order to understand and describe the anatomy more easily, biomechanical engineers refer to a specific body plane. A body plane is imaginary two-dimensional flat surface that is used to define a particular area of anatomy. There are three spinal planes (see Figure 2-2) ; frontal (coronal) plane, median(sagittal) plane and transverse(axial) plane. Coronal plane divides the front and back halves of the entire body and sagittal plane divides the left and right sides of the entire body, while transverse plane divides top and bottom halves of the body at the waist.

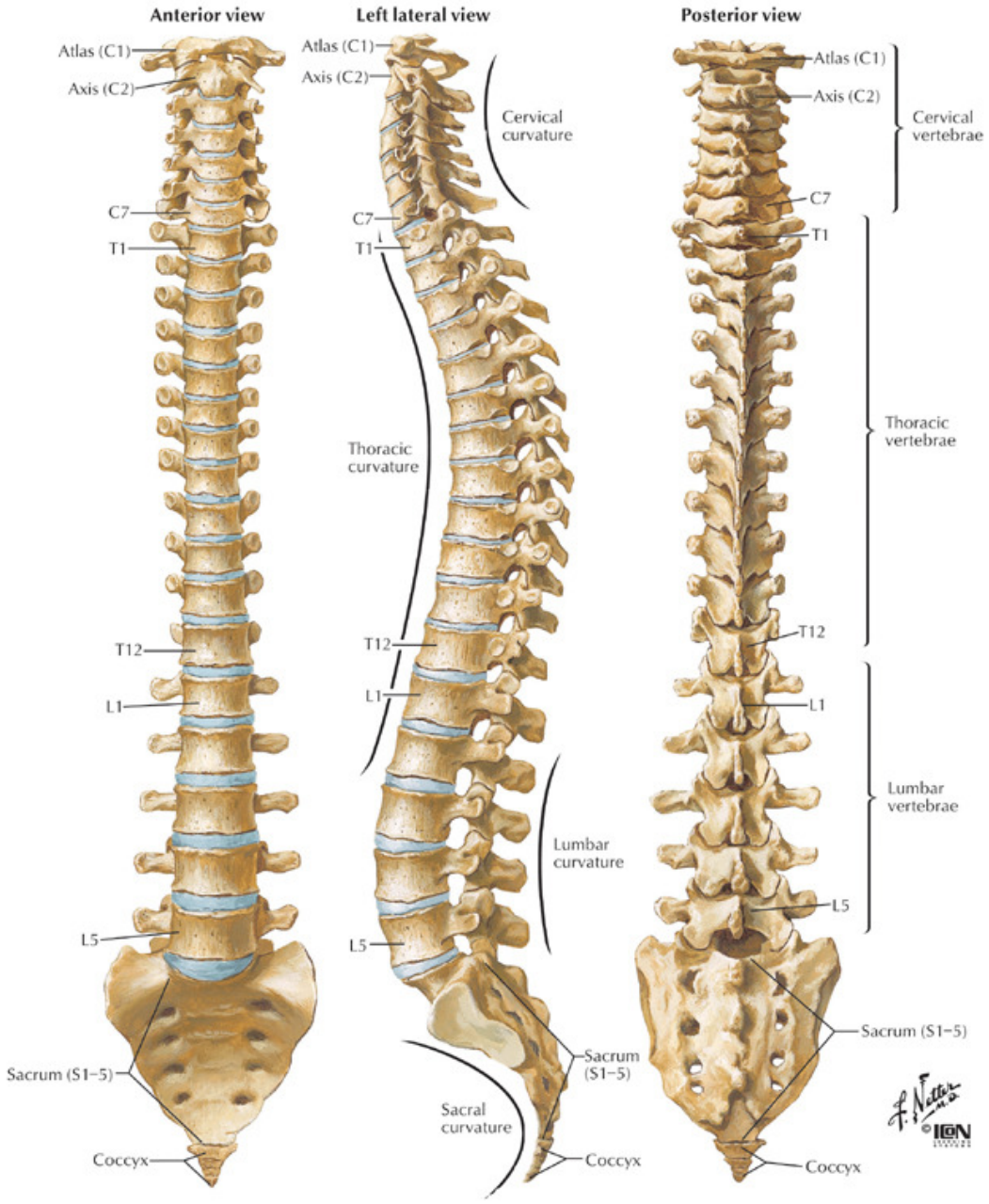

Figure 2-1 The entire human spine in anterior, lateral and posterior view

Source : http://www.backpain-guide.com

On the other hand, when viewed from the side, a human spine has distinct curves called lordosis and kyphosis. A kyphotic curve is a convex curve toward the back of the spine, while a lordotic curve is concave toward the back of the spine.

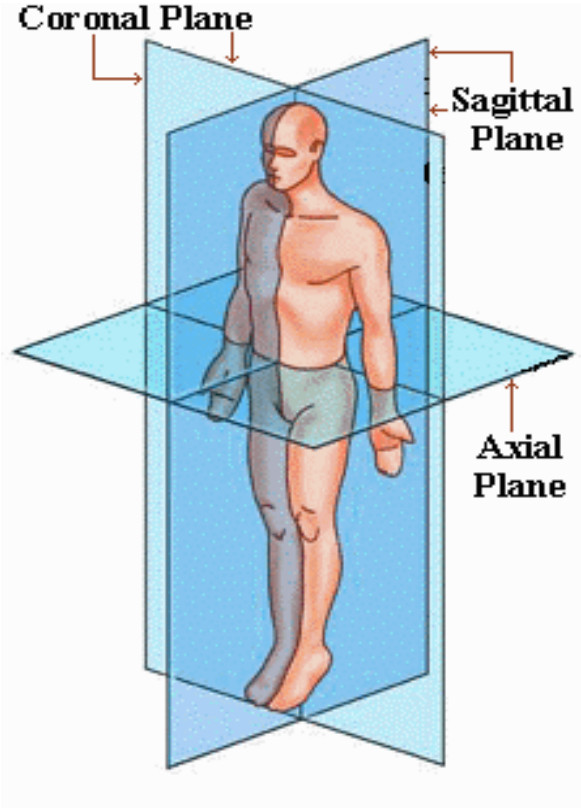

Figure 2-2 The spinal planes

Source : http://www. www.spineuniverse.com

2.1.2 Region of the spine

The cervical spine is made up of seven cervical vertebrae (C1-C7) and has cervical lordosis. The main function of the cervical spine is to support the head and allow a wide range of motion of the head weighing 10 to 12 pounds. The cervical spine has the

greatest range of motion, partly because two specialized vertebrae (C1 and C2) work together (see Figure 2-3) to allow extensive moments of the head and neck. The first cervical vertebra is called the atlas and is unique in shape. It has ring-shaped articulation with two large protrusions on the sides to support the weight of head. The second cervical vertebra is called axis and its shape is also significantly different from other vertebrae. It has a bony protrusion, called dens or odontoids on its superior surface that matches articular facet of atlas.

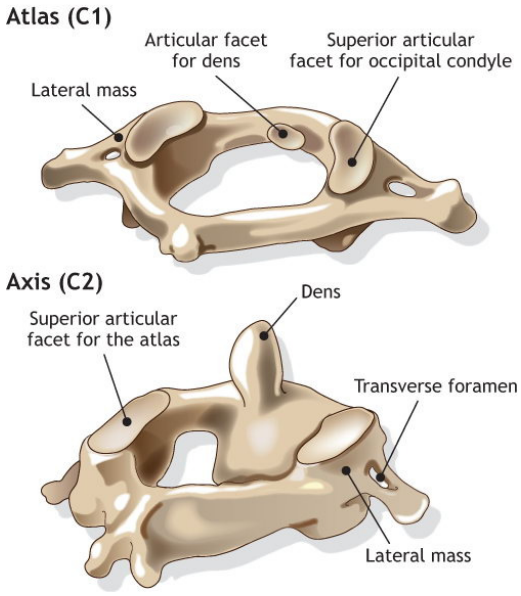

Figure 2-3 The anatomy of atlas (C1) and axis (C2) on cervical spine

Source : http://www. apatech.com

The main function of **thoracic spine** is to protect the organs of the chest such as heart and lungs. The thoracic spine is composed of 12 vertebrae (T1-T12) with a pair of ribs attached to both sides, which construct the cage-shaped structure increasing the chest strength. They are located between the cervical spine and lumbar spine and increase in size as one proceeds down the spine, Thus T1 is the smallest, while T12 is the largest among 12 thoracic vertebrae. The thoracic spine has a kyphosis or "C" curve and is less mobile than cervical and lumbar spine due to the thoracic cage.

The lumbar spine has five lumbar vertebrae (L1-L5) and has lumbar lordosis like the cervical spine. The lumbar vertebrae, the largest vertebrae, are the weight-bearing portion of the spine. The lumbar spine which sits atop sacrum transmits the body weight to the base of the sacrum. The facet joints in the lumbar spine are oriented more sagittally to resist axial rotation and lumbosacral facet is oriented more coronally to resist antero-posterior translation.

The sacrum, formed by five vertebrae (S1-S5) and fused together into a solid unit, is usually non-identifiable disc spaces between the sacral segments. The sacral spine has kyphosis like thoracic spine and acts as the bridge between lumbar spine and pelvic girdle which supports the body weight from the vertebral column and protects the lower organs, including the urinary bladder and the reproductive organs. At the end of the spinal column is the **coccyx** or tailbone.

2.1.3 Spinal motion segment

Spinal motion segment or functional spinal unit (FSU) is the smallest physiological motion unit of a spine to exhibit biomechanical characteristics similar to those of the entire spine [6]. It consists of two adjacent inferior and superior vertebrae, the shared disc along with the annulus fibrosis and all the encasing ligaments, the facet

joints and the capsules around the facet joints. Basically a motion segment is everything that connects two vertebrae. (see Figure 2-4)

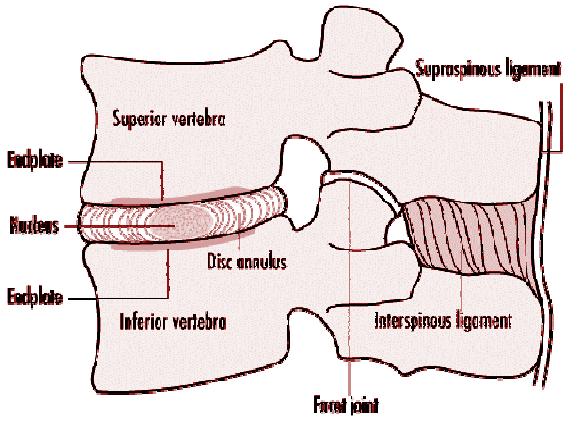

Figure 2-4 Lateral view of spinal motion segment

Source : http:// www.ilo.org

The lumbar vertebra is a bony structure (Figure 2-5) which transmits the upper body weight. It is made of vertebral body, posterior elements and pedicle connecting the posterior elements to the vertebral body. The vertebral body is the largest part in vertebra and cylindrical in shape with flat top and bottom surfaces. Cortical bone which has high elastic modulus surrounds an internal space filled with a web of cancellous bone. This structure is strong enough to support body weight.

The pedicles is a very strong connecting bridge, directed backward from the upper part of vertebral body. It also transmits the resistive forces of facet joints to vertebral body. It is located 1 mm below the tip of the inferior articular process and the posterior-most prominence of the superior process vertically. Sometimes, it is used as a

portal of entrance into the vertebral body for fixation of pedicle screw or placement of bone cement.

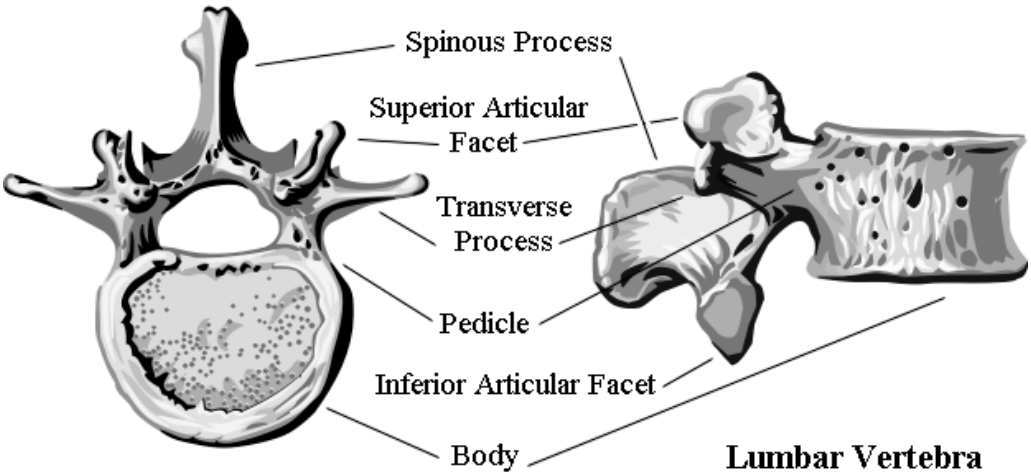

Figure 2-5 The anatomy of lumbar vertebra

Source : http://www. fpnotebook.com

The posterior elements are made of the processes and the lamina which connects the spinous and transverse processes. The processes are divided into three types; transverse process, spinous process and articular process (facet joint). The transverse and spinous processes serve as attachment for ligaments and tendons. On the other hand, facet joint constrains excessive displacement of vertebra by the locking mechanism. Especially facet joints in the lumbar spine are oriented more sagittally resisting axial rotation

The intervertebral disc (IVD) is a fibrocartilaginous soft tissue serving as shock absorber in spinal motion segment. It also confers flexibility on the spine by allowing limited bending and twisting movements between vertebral bodies. IVD is composed of

an annulus fibrosus, nucleus pulposus and endplates. The annulus fibrosus is a strong multi-layered radial tire-like structure made up of lamellae and encloses the nucleus pulposus. Both annulus fibrosus and nucleus pulposus consist of water, collagen fiber, and proteoglycans, however the amount of fluid is the greatest in the nucleus pulposus. While, the endplates separate the vertebral bone from the disc and prevent the highly hydrated nucleus pulposus from bulging into the adjacent vertebra. It also absorbs the hydrostatic pressure resulting from mechanical loading of the spine.

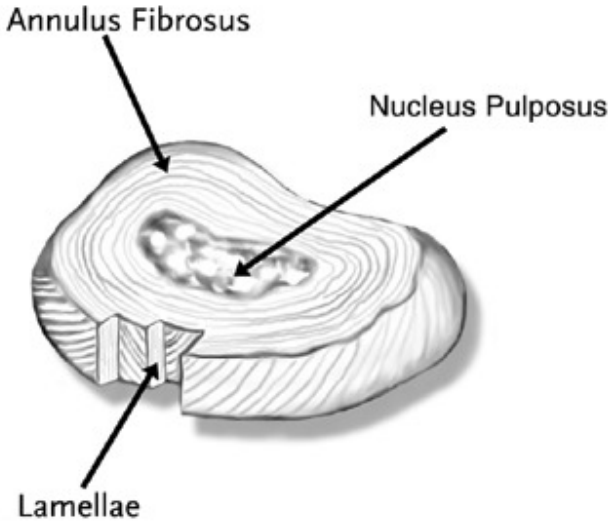

Figure 2-6 The anatomy of IVD

Source : http://www.indyspinemd.com

The ligaments are fibrous connective tissues linking two or more bones, cartilages. Ligaments stabilize the spinal motion segment and protect injuries by restraining the excessive movement such as hyper -flexion or hyper-extension of the

vertebra. Based on the attachment site and their functions, the ligaments are divided into several parts such as anterior longitudinal ligament and the posterior longitudinal ligament (primary stabilizer), ligamentum flavum (strongest), interspinous ligaments, the supraspinous ligament and the capsular ligamentsas shown in Figure 2-7

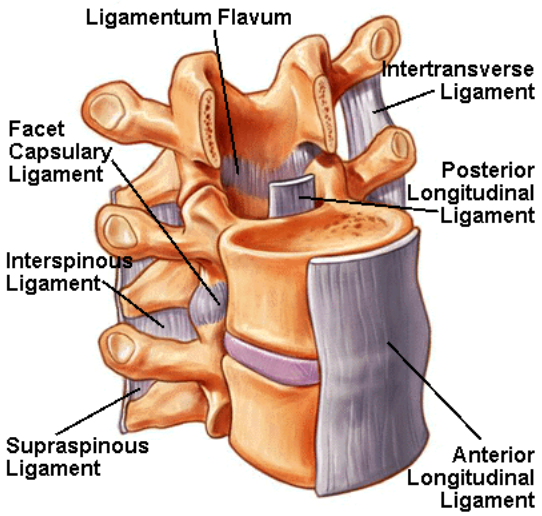

Figure 2-7 Ligaments in a motion segment

Source : http://www. spineuniverse.com

2.1.4 Spinal muscles

Back muscles

The musculature in a spine plays important roles in stabilizing the spine, supporting upper body weight and external load as well as creating the movement of the upper body. There are three groups of muscles in the back; superficial, intermediate and deep.

The latissimusdorsi is the superficial muscle (see Figure 2-8), which arises from vertebral spines from T7 to the sacrum, posterior third of the iliac crest, lower 3 or 4ribs or sometimes from the inferior angle of the scapula. It inserts on the floor of the intertubercular groove. The function of the latissimusdorsi is known to extend the arm and rotates it medially. It is innervated by the thoracodorsal nerve (C7, C8) from the posterior cord of the brachial plexux.

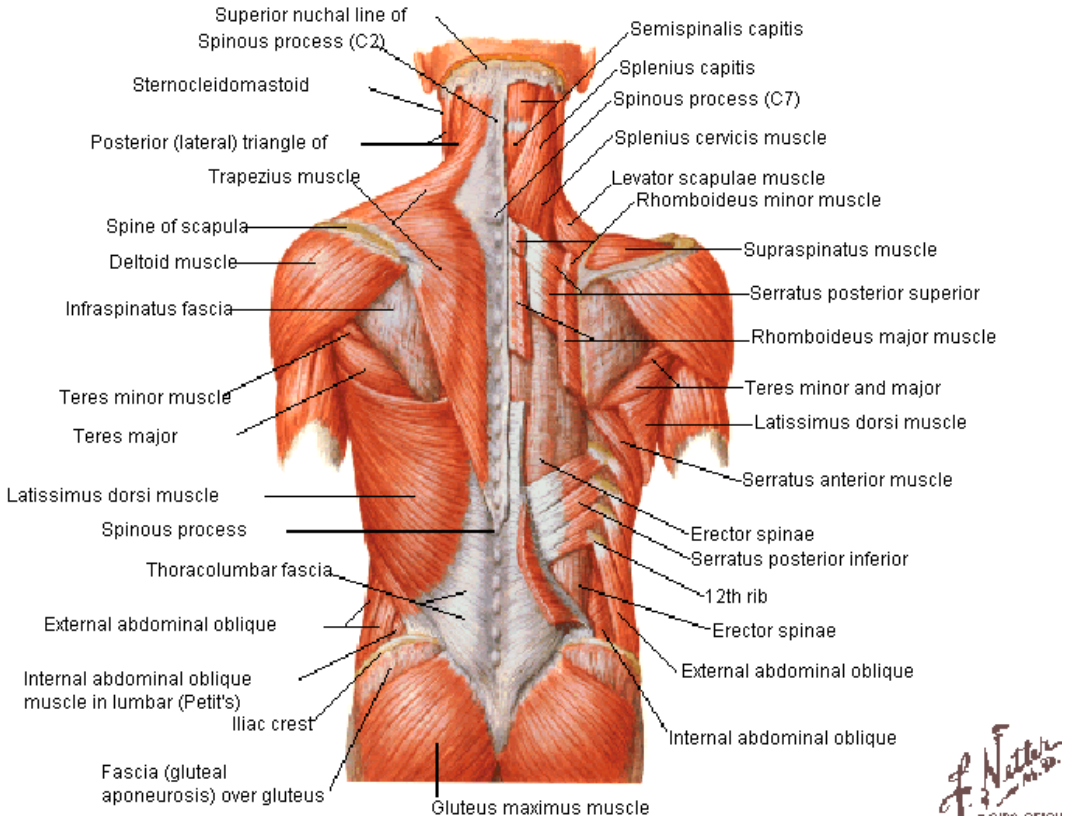

Figure 2-8 The anatomy of muscle of back (superficial layers)

Source : http://www2.ma.psu.edu

The serratus posterior superior and inferior is an intermediate group (see Figure 2-9). The serratus posterior superior arises from the ligamentum nuchae, spines of vertebrae C7 and T1 to T3 and inserts on second rib to fifth rib. It elevates the upper ribs and is innervated by the branches of the ventral primary rami of spinal nerves or intercostals nerves. The serratus posterior inferior arises from the thoracolumbar fascia, spines of vertebrae T11-T12 and L1-L2. It inserts on ribs 9-12 and role of the serratus posterior inferior pulls down lower ribs. It is innervated by the branch of the ventral primary rami of spinal nerves T9-T12.

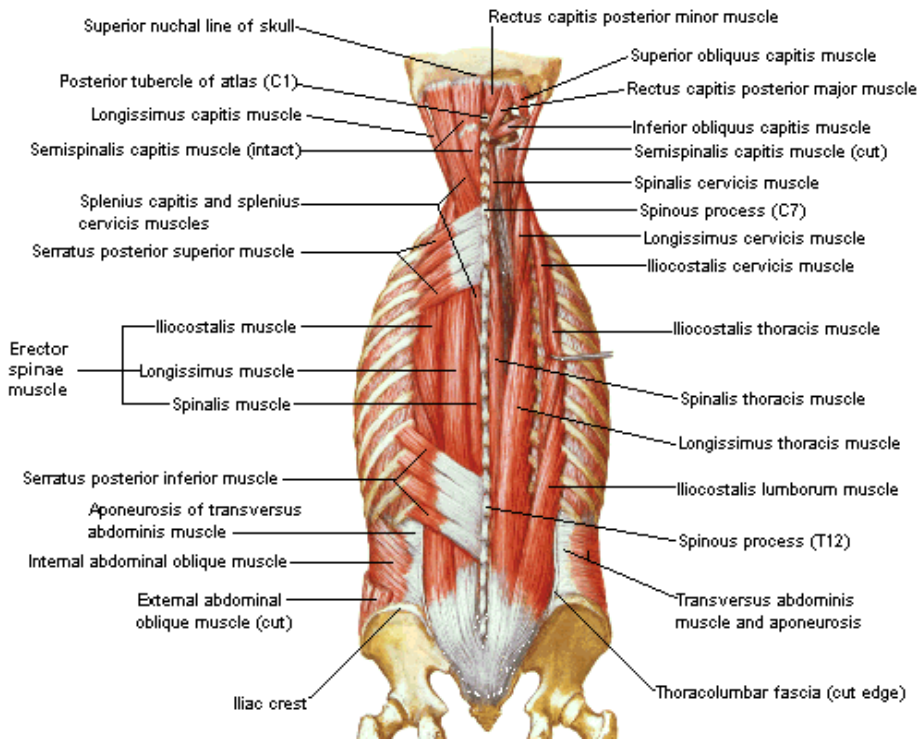

Figure 2-9 The anatomy of muscles of back (intermediate layers)

Source : http://www2.ma.psu.edu

The intrinsic muscles are concerned with movement of upper body. In the intermediate layer of intrinsic deep muscles (see Figure 2-10), the erector spinal muscles lie within a facial compartment between the posterior and middle layer of the thoracolumbar region.

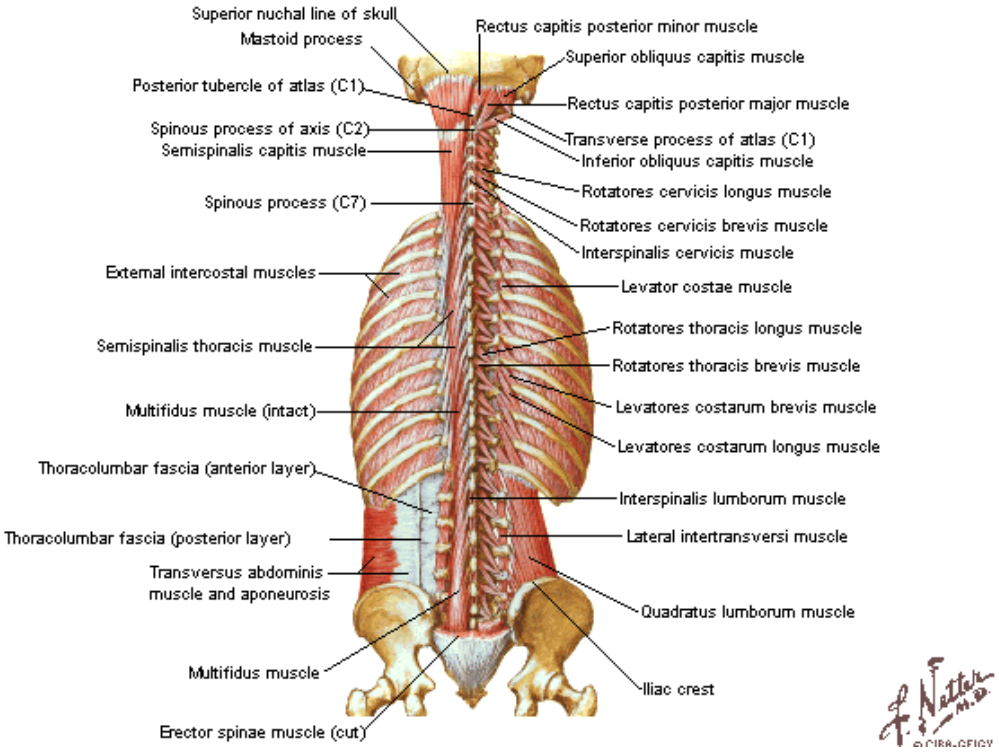

Figure 2-10 The anatomy of muscles of back (deep layers)

Source : http://www2.ma.psu.edu

The erector spinae is divided into three subgroup; iliocostalis which arises from iliac crest and sacrum and inserts on angle of the ribs, longissimus which arises from

transverse process at inferior vertebral levels and inserts on transverse process at superior vertebral levels and mastoid process, and spinalis which arise from spinous processes at inferior vertebral levels and inserts on transverse process at superior vertebral levels and mastoid process. The iliocostalis and the spinalis extend and laterally bend the trunk and neck, while the longissimus extends and laterally bends the trunk, neck and head.

Several short muscles such as semi spinalis, multifidus are found between thee transverse process and spinous process in the deepest layer of intrinsic back muscles. This group of muscles provides rotational, extensional and lateral bending movements between adjacent vertebrae. They also extend the head and neck.

The rotatores, the interspinales and the intertransversarii are also known as short back muscles passing from one vertebra to the next vertebra above (see Figure 2-11).

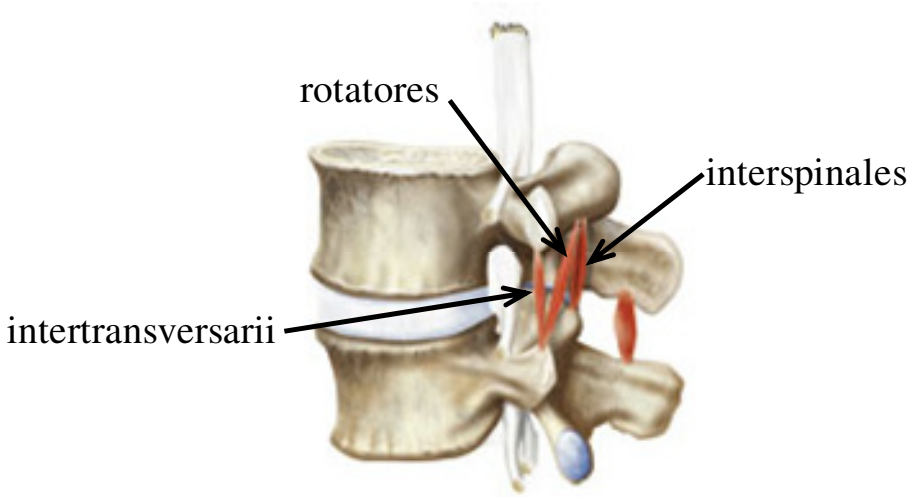

Figure 2-11 Lumbar vertebrae L4 and L5 and short intrinsic muscles(the rotatores, the interspinales and the intertransversarii

Source : http://www. medical-artist.com

The rotatores which arises from transverse process and is attached to junction of lamina and transverse process or spinous process of vertebra or 2 segments superior to vertebra of origin is deep short back muscles. It may stabilize vertebrae and assist local extension and rotation of spinal column.

The intertransversarii is also deep short back muscle, which arises from transverse processes of cervical or lumbar vertebrae and inserts on transverse processes of adjacent vertebrae. The function of the intertransversarii is to assist lateral bending of the spinal column. It also stabilizes the spinal column bilaterally.

The interspinales arises from superior surfaces of spinous processes of cervical and lumbar vertebrae and inserts on inferior surfaces of spinous processes of vertebrae superior to vertebrae of origin. The role of the interspinales is to aid extension and rotation of vertebral column [7].

Abdominal muscles

The psoas major (see Figure 2-12) is a long muscle located on the side of the lumbar region of the spinal column and brim of the lesser pelvis. It arises from bodies and transverse processes of lumbar vertebrae and inserts on the lesser trochanter of femur via iliopsoas tendon. It flexes and laterally bends the lumbar vertebral column. It is innervated by the branches of the ventral primary rami of the spinal nerves L2-L4.

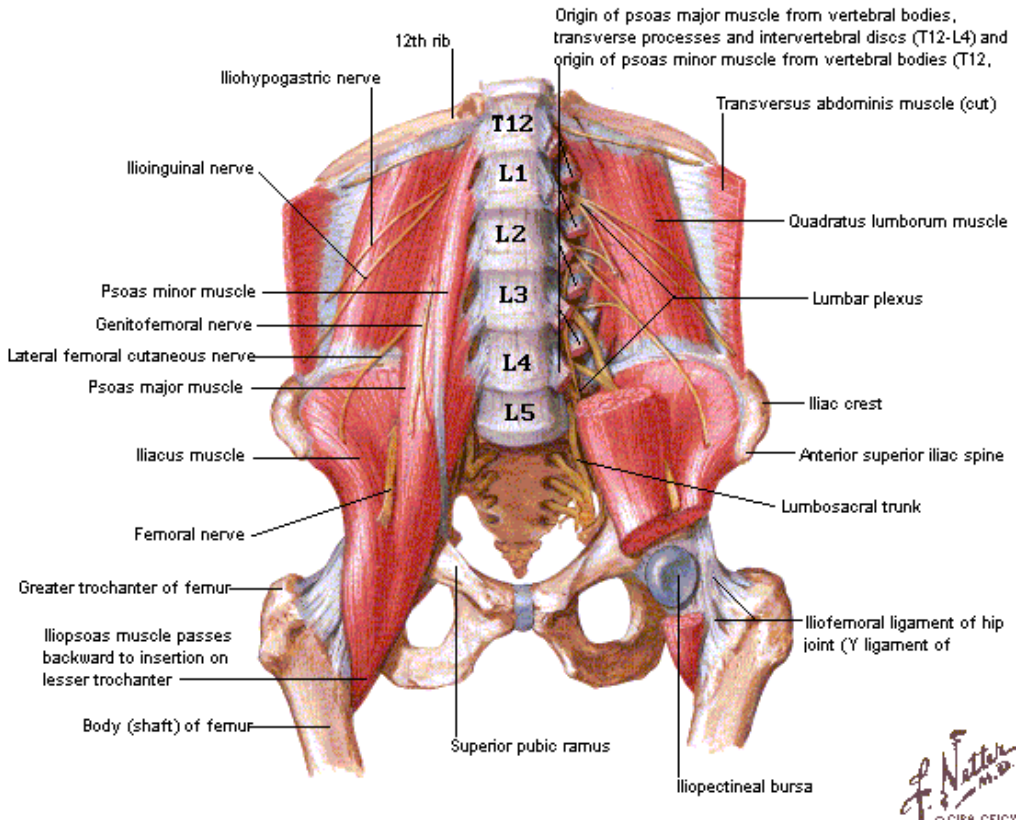

Figure 2-12 The anatomy of abdominal muscles

Source : http://www2.ma.psu.edu

The quadratus lumborum arises from posterior part of the iliac crest and the iliolumbar ligament and inserts on transverse processes of lumbar vertebrae 1-4 and the 12^{th} rib. It laterally bends the trunk and fixes the 12^{th} rib. It is innervated by subcostal nerve and ventral primary rami of spinal nerves L1-L4.

The external abdominal oblique muscle is the largest superficial muscle and lies most superficially in the lateral anterior abdomen. It arises from lower 8 ribs and inserts on linea area, pubic crest and tubercle, anterior superior iliac spine and anterior half of

iliac crest. It flexes and laterally bends the trunk. It is innervated by intercostals nerves 7-11, subcostal, iliohypogatric and ilioinguinal nerves.

The internal abdominal oblique muscle (see Figure 2-13) is the intermediate abdominal muscle and its fiber runs perpendicular to the external abdominal oblique muscle. It begins in the thoracolumbar fascia, anterior 2/3 of the iliac crest, lateral 2/3 of the inguinal ligament and inserts on the lower 3 or 4 ribs, linea alba and pubic crest. It flexes and laterally bends the trunk. It is innervated by the intercostals nerves 7-11, subcostal iliohypogastric and ilioinguinal nerves.

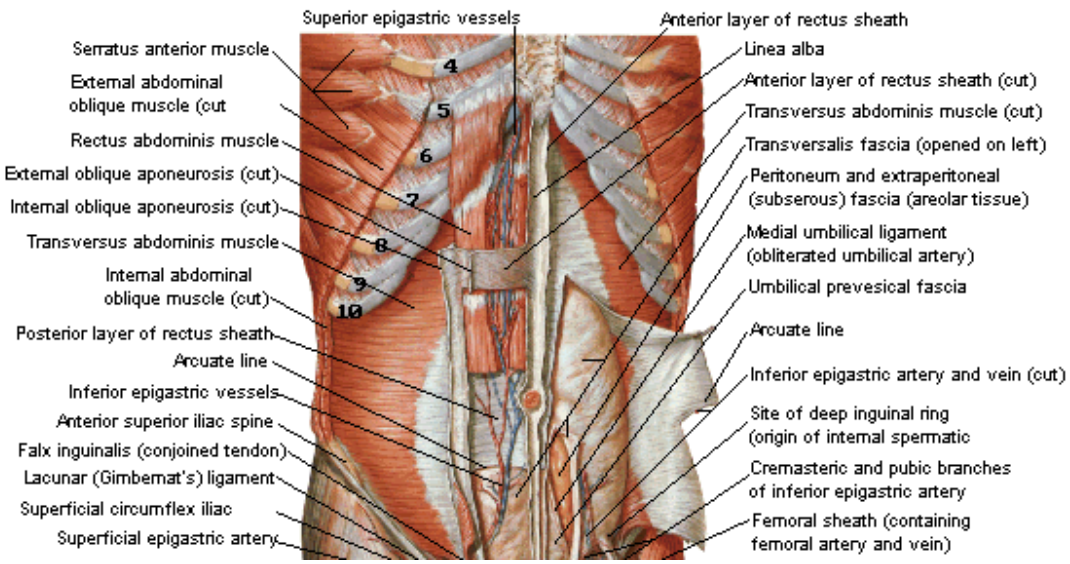

Figure 2-13 The anatomy of abdominal muscles (deep layers)

Source : http://www2.ma.psu.edu

The rectus abdominis muscle also known as six packs is a paired muscle running vertically on each side of the anterior wall of the human abdomen. It arises from pubis

and the pubic symphysis and inserts on the xiphoid process of the sternum and costal cartilages 5-7. It flexes the trunk and is innervated by the intercostal nerves 7-11 and subcostal nerve.

2.2 *In vivo* loads on the lumbar spine

One of the major biomechanical functions of the spine is to support the upper body weight and external loads. Due to the bipedal nature of the human, the compressive load has been considered a crucial component of the spinal loads while the spine can be subjected to complex 3-D loads during normal activities. The biomechanical loads applied on the spine have been known to play a significant role in causing various spinal disorders and the major focus of numerous biomechanical studies of the spine.

2.2.1 Measurement of *in vivo* compressive loads on the spine

The *in vivo* biomechanical loads in the lumbar spine are extremely difficult to measure experimentally, but the compressive components of the spinal loads were estimated from the *in vivo* measurement of the intradiscal pressure in the L3-L4 disc [8, 9]. Nachemson found that the estimated compressive load in the spine of a subject of 70 Kg weight can vary depending upon the posture and activities (500 N in a quiet standing posture, 1000 N in forward bending 40 deg; and 2100 N in forward bending 20 deg with 20 Kg weight). The results that Wilke et al. found are also very similar to those in Nachemson's study [9]. The results of these studies are valuable but largely limited the understanding of spinal loads *in vivo* because only compressive loads on IVD were measured in a specific spinal level. Furthermore, no estimation of MFs was investigated in these studies.

2.2.2 Estimation of *in vivo* spinal loads and MFs

Because of the practical limitations in direct *in vivo* measurement, the *in vivo* spinal loads and muscle forces (MFs) have been estimated using a variety of indirect methods. The typical method is to use an analytical model of the spine system (spinal column, spinal muscles, and the trunk)in which the spinal column is simulated as either a link of elastic beams or a comprehensive finite element (FE) structure. However, the spine system is indeterminate because of the number of unknown forces exceeding the number of equality constraints. Thus the equilibrium equations in these models were solved by reducing the number of unknowns based upon on various assumptions (i.e., neglecting some muscles, grouping some muscles, or a priori relations between the muscles) in the earlier studies. In recent studies, however, optimization methods have been used in solving the equilibrium equations by minimizing (or maximizing) some cost functions constrained with other constraints.

For example, Bean and Schultz et al. investigated the compressive load on L5/S1 level using a linear optimization muscle model incorporating 10 muscles [10]. They predicted a compression load of 870 N applied at the L5/S1 level when minimizing the compression load, and 1100 N when minimizing muscle intensity. Stokes et al. [11] predicted the compressive forces at the L5-S1 level in response to maximum bending effort made in the neutral standing posture using a 3-D lumbar spine model in which the intervertebral joints were simulated by linear beam elements. A total of 132 spinal muscles were also simulated in this model. The predicted compressive and shear forces were 1359 N and 458N, respectively, in response to an extension effort of 63 Nm and 770 N and 482 N, respectively, in response to a flexion effort of 23 Nm. The results of these studies were valuable, but the optimization approach inherently lacks the biological sensitivity to various possible muscle recruitments and co-contraction patterns. EMG-

assisted models in which the measured electromyography (EMG) data of selected muscles were used to assist in the portioning of the total moment of forces acting about a joint into the individual contributions made by the many anatomical structures that can produces forces and moments [12]. Furthermore, new methods incorporating the optimization and EMG method have developed to minimize the variations in gains while satisfying the moment equations of equilibrium in different planes [13, 14] and used in assessing the spinal loads and MFs during various activities. Regardless of the methods, the findings of these studies clearly showed that the magnitude of forces in the lumbar spine can reach thousands of Newtons [15, 16] while it varies depending upon the type of activities as well as the amount of external loads to handle. For example, El-rich et al. predicted a large compression forces about 2000 N in lower lumbar levels when a weight of 380 N was held in front. Cholewicki et al. [15] predicted that the compression force in the L4-L5 level can be greater than 4000 N while bending the trunk in flexion, extension and lateral bending. The compressive force in the lumbar spine predicted during power lifting was about 18000 N [16].

As such, the lumbar spine can experience large compressive loads *in vivo* without buckling while still preserving the flexibility required for everyday tasks[17]. In contrast, the isolated ligamentous lumbar spine was shown to buckle when subjected to a vertical compressive load of only 88 N, whereas the single motion segment was found stiff and strong enough to support the large compressive load without failure. Such an inherently unstable lumbar spinal column is known to be stabilized by the spinal muscles. Yet, the results of spinal MFs failed to provide the stabilizing roles of those MFs.

2.3 Spinal stability

The term, "spinal instability" originates from Kuntsson's radiologic observation of retrodisplacement of a vertebra during flexion and its relationship to low back pain in 1944 [18]. The early definition of instability focused on translation in the sagittal plane (spondylo- or retro-listhetic deformities) and has been represented by a segment that induces either hypermobile or catastrophic conditions [18-21]. However, the observation of instability in asymptomatic subjects raised a question whether the detected instability is the source of pain. Frymoyer and Selby [22] defined spinal instability as a symptomatic condition in which a physiologic load causes abnormally large deformations of the intervertebral joint. Kirkaldy-Willis and Farfan [23] defined "clinical instability" as pain resulting from the unstable motion segment. White and Panjabi [24] defined clinical instability as "the loss of the ability of the spine under physiologic loads to maintain relationships between the vertebrae in such a way that there is neither damage nor subsequent irritation to the spinal cord or nerve roots, in addition, there is no development of incapacitating deformity or pain due to structural changes." As such, spinal (or clinical) instability has been used as a clinical entity in the diagnosis of spinal disorders. Clinical instability, however, remains controversial. For example, there is no real consensus on its definition although it is most widely agreed that the loss of the normal pattern of spinal motion causes pain and/or neurologic dysfunction. Most importantly, it is poorly understood how the normal spine maintains its stability while keeping flexibility, which is crucial for determining the loss of the normal pattern of spinal motion.

The stabilizing system of the spine may be divided into 3 subsystems: 1) the spinal column and 2) the surrounding muscles, well coordinated by 3) the motor control unit, [25] and efforts had been made to evaluate the stabilizing effect of MFs.

Biomechanical investigators introduced analytical models of the spinal column and muscles, assuming that the model system is conservative. They quantify the potential energy (V) of the system for each joint degree of freedom and predicted the mechanical stability of the system in terms of "stability index" determined as the value of the smallest eigenvalue of the Hessian matrix (second derivative of V with respect to the generalized coordinates) [16, 26-29]. The underlying theory is that a conservative mechanical system must be stable when the system is in mechanical equilibrium and the Hessian matrix is positive-definite (i.e., the smallest eigenvalue of the Hessian matrix is greater than zero.). In all of these studies, the stability index was found positive regardless of postures and trunk movements, indicating that the lumbar spine is stable *in vivo* with the spinal MFs.

However, the previous studies failed to provide the knowledge of an physiological algorithm to control the muscle activations for the *in vivo* maintenance of the stability and flexibility of the spine because of following reasons. (1) Numerous intrinsic short segmental muscles, such as rotatores, intertransversari, and interspinales are known to exist and play a significant role in maintaining the stability of the whole lumbar spine [16], but they were not simulated in the spine models of the previously mentioned studies. (2) MFs predicted in the previous studies can be one solution out of numerous possible solution sets determined to satisfy the equilibrium equations of motion. Different MFs were predicted from the same optimization problem in varying the cost function, demonstrating the need for more constraints that may be used in determining more physiological spinal MFs. Because of the absence of these intrinsic muscles, the spinal musculature worked as guy wires spanning a bending mast in the previous studies. Such guy wire action may increase the stability of the spinal column sufficiently to support the physiological loads on the spine but with a significant loss in the column flexibility as

observed in Wilke et al's study [30]. They found 93% and 85% decreases in flexion and flexion range of motions with five pairs of guy wires simulating constant MFs (80 N per pair) attached to the ligamentous lumbar spine. There could be another combination of MFs to stabilize the ligamentous spine while allowing its flexibility needed for normal *in vivo* upper body movements.

2.4 Follower load in the spine

The concept of a follower load was initially introduced by Timoshenko and Gere and Bazant [31, 32]. In the studies of column buckling, they showed that the critical load (or buckling load) of a column can increase when the column is subject to an axial compressive force whose direction is adjusted to a direction which is always normal to the cross section at the end of beam (or along the tangential line of the deflection curve) as shown in Figure 2-14 and named such force the follower force [32].

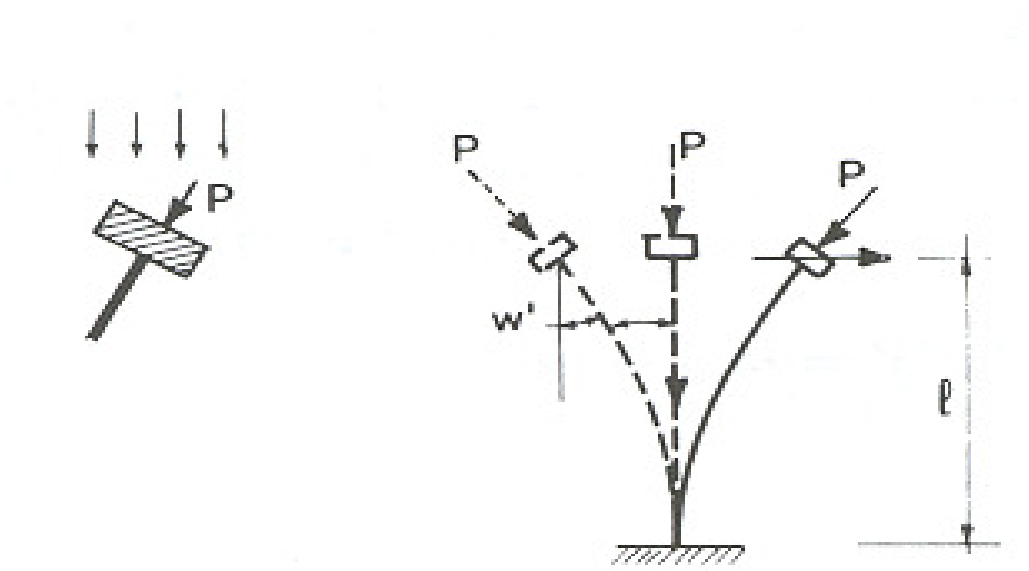

Figure 2-14 Column loaded by a constant follower force [31]

In the field of spine biomechanics research, the loading configuration concept that compressive forces travel along the curvature in the lumbar spine was first proposed by Aspden [33]. Then, Patwardhan et al. developed an experimental method to apply a

compressive follower load (CFL) on the ligamentous spine as shown in Figure 2-15 and conducted biomechanical experiments to study the effect of the follower load on the stability and flexibility of the spinal column. Results of their studies showed that the ligamentous cervical and lumbar spine can withstand a compressive physiologic load up to 250N and 1200N, respectively, without buckling of the spine while maintaining its flexibility well [3]. They predicted similar mechanical behaviors of the spinal column using an analytical model of the spinal column assisted by five MFs (one force vector as a resultant of MFs acting on each vertebra). Based upon the analytical and experimental findings, they postulated that the follower load could be a physiologic normal load on the lumbar spine with no internal joint moments and shear forces [4, 34]. Since the follower load was introduced by Patwardhan et al., it has been adopted in several experiments in conjunction with other loading conditions, and its successful application simulated high physiological compressive loads on the ligamentous spine without buckling during various *in vitro* biomechanical tests of the spine [35-40]. These successful applications led to the hypothesis that the spine may indeed be subjected to the CFL *in vivo*, in order to maintain its stability while at the same time maintaining its flexibility.

As an analytical trial, Kim and Kim [41] developed and used a 3-D FE lumbar spine model including 117 pairs of spinal muscles to prove the hypothesis. However, they failed in finding a perfect follower load (i.e., no joint moments and shear forces) and called their model a modified follower load model because they had to allow various degrees of shear forces in joints to obtain the solution convergence.

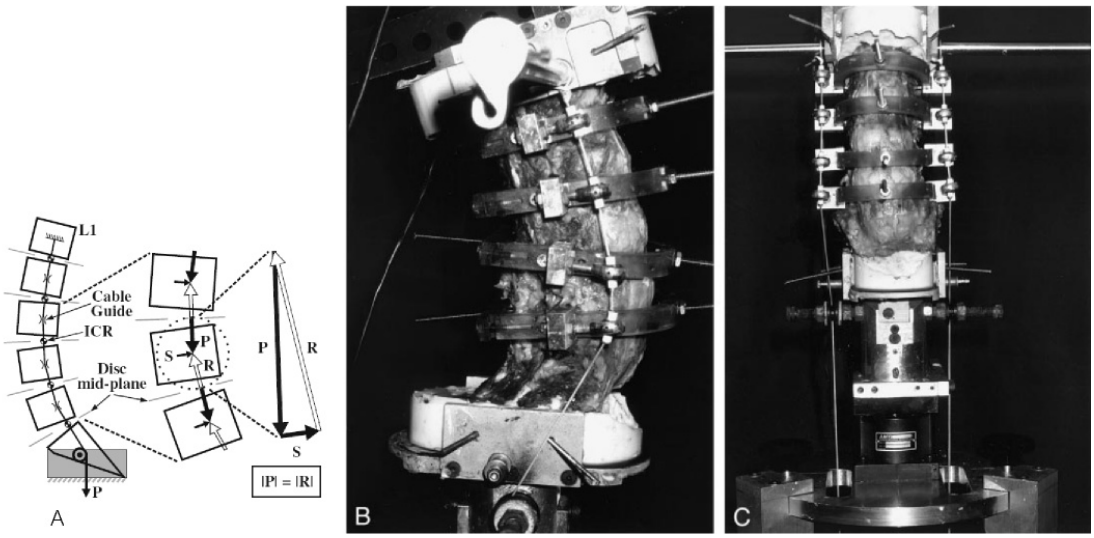

Figure 2-15 Schematic diagram of CFL on the lumbar spine [4, 34]

In contrast, Han et al. recently introduced an optimization model of the lumbar spine system incorporating 232 spinal muscles and demonstrated the existence of possible combinations of MFs creating CFLs in the lumbar spine in various sagittal postures (neutral, fully flexed, and fully extended) within the physiologically possible maximum muscle force capacity (MFC) defined as the maximum force that can be created per unit physiological cross-section area of a muscle. Han [5] also showed that a perfect follower load can be created by the spinal muscles even when an additional external load (weight and moment) is applied to the spine up to fairly high amount of loads (more than 1000 N in vertical external weight, for example). The importance of biomechanical roles of intrinsic short segmental muscles (such as interspinales, intertransversari, and rotatores) in creating CFLs in the spine was also found in Han's study. These results indicate that spinal muscles are most likely to stabilize the lumbar spine *via* a follower load mechanism in the spine and the CFLs may be the normal

physiological loads in the spine. However, the major drawback of Han et al.'s studies is no confirmation of the stability and flexibility of the lumbar spine under the CFLs creating MFs and upper body weight. A finite element model of the spinal system in connection with the optimization model needs to be developed to investigate the static and dynamic deformation of the spinal column under CFLs for comprehensive understandings of the spinal biomechanics.

2.5 Future directions for the studies of the spinal system

As reviewed previously, the ligamentous lumbar spine is an inherently unstable column but can be stabilized by spinal MFs. The results of the studies of spinal muscles using mathematical models in combination with *in vivo* experiments on human subjects undergoing various tasks indicated that the stability index was high (large stability safety margin) in the tasks that required large muscular effort but low in the tasks that demanded very little muscle activity, demonstrating the stabilizing roles of the spinal muscles acting as guy wires. However, these studies have not provided an insight into the possible mechanism for the control of spinal muscle force configuration due to following limitations: (1) no consideration of the flexibility of the spine although the guy wires can increase the stiffness of the structure significantly; and (2) exclusion of numerous spinal muscles (mostly those directly attached to the vertebrae). In fact, the stiffness of a guy wire assisted structure (i.e., the spine with active MFs) can increase too high to allow a physiological motion efficiently. In contrast, the results of the follower load mechanism in the lumbar spine clearly demonstrated a great possibility that the spinal muscles are controlled to create CFLs in the spine *in vivo* to maintain its stability and flexibility simultaneously. While numerous studies required to support the hypothesis, one of the eminent needs is to create a FE model of the spinal system in conjunction with the current optimization model with perfect matches of boundary and loading conditions between the models not only for the studies of the stability and flexibility of the lumbar spine under CFLs but also for the better understanding of the main algorithm for controlling the spinal MFs.

CHAPTER 3

METHODS

3.1 Development a 3-D FE model of the spinal system

A 3-D finite element (FE) model of the spinal system in the neutral standing posture consisting of the eight rigid bodies including trunk (ribcage and T12), lumbar spine (five vertebrae, discs and ligaments), sacrum-pelvis, and spinal muscles was developed as shown in Figure 3-1.

The trunk was considered to be connected to the L1 vertebra through the T12-L1 intervertebral joint. The geometry and shapes of vertebrae and the disc height were obtained from previous CT scan measurements done by Zhou et al [42]. The lordosis of the spine was set to 50 degrees (Cobb's angle measured between the top of L1 and the sacrum) and each vertebra was located in a position appropriate to make a whole lumbar spinal column with a balanced shape. Bony structures in the 3-D FE model were assumed rigid and modeled using shell elements with extremely high elastic modulus.

The intervertebral joint consisting of the intervertebral disc (IVD) and two facet joints is modeled as shown in Figure 3-2 to allow the segmental motions. The IVDs with anterior longitudinal and posterior longitudinal ligaments were considered as a deformable body to allow the segmental motions. The height of the IVD was assumed to be about 10 mm in all levels to represent the static state deformed by the body weight and MFs according to the reported *in vivo* data ranging from 5mm to 16mm in L3-L4 and L5-S1 levels measured from the radiographs of the lumbar spine in the quiet standing posture [42]. The material property of the disc was regarded as non-linear isotropic material and its nonlinearity was defined using stress versus strain relationships of a spinal motion segment experimentally determined in the previous studies [43, 44]. The facet joint was

modeled using a nonlinear compression-tension spring element to mimic the kinetic characteristics of the apophyseal joint (bony contact and capsular ligament) as shown in Figure 3-2.

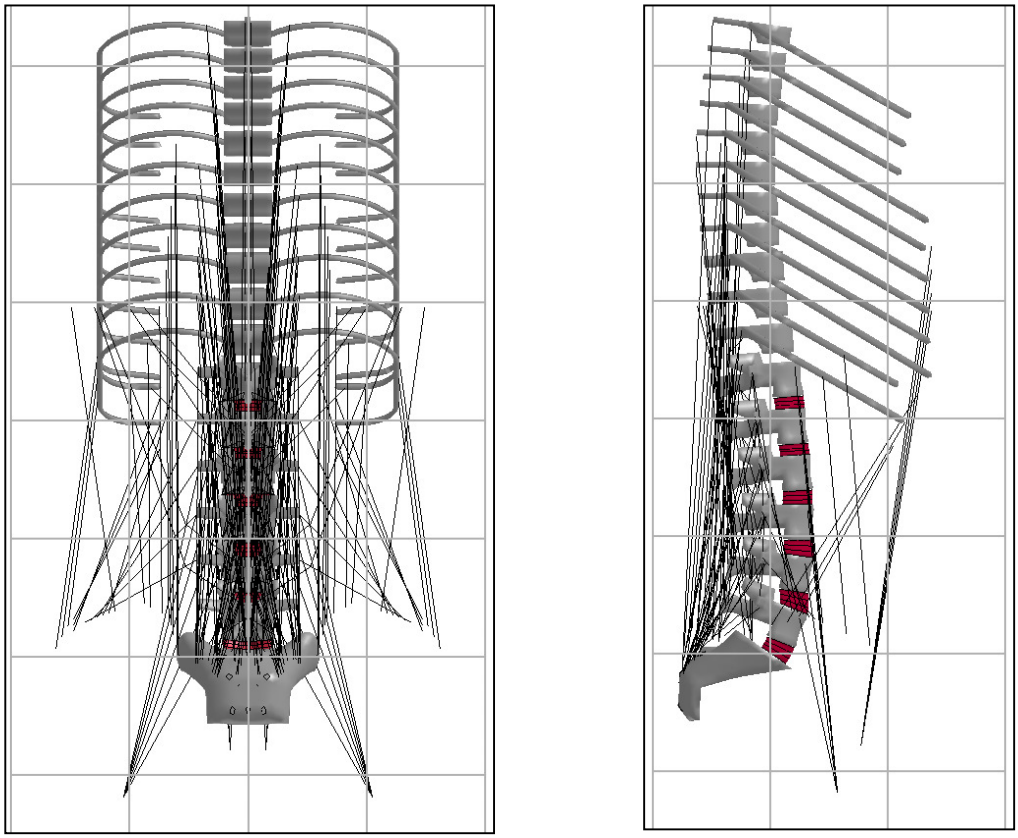

Figure 3-1 The 3-D Finite element model of the spinal system

Ligaments were regarded as passive elements of the spinal stabilizing system limiting the excessive movement of each vertebra. All the spinal ligaments except for the anterior longitudinal (ALL), posterior longitudinal ligament (PLL), and capsular ligament were modeled using a tension spring element because they are known to exert the

resisting force only when elongated. While the effect of ALL and PLL was incorporated in the disc material properties and capsular ligaments in the facet spring, the mechanical roles of the remaining spinal ligaments were simulated by using one tension spring element located between the spinous processes as shown in Figure 3-2.

A total of 232 muscle fascicles including 4 serratus posterior inferior, 14 latissimusdorsi, 6 external oblique, 6 internal oblique, 48 longissimus, 24 iliocostalis, 12 psoas major, 10 quadratuslumbarum, 8 rectus abdominis, 6 spinalisthoracis, 40 multifidi, 12 interspinales, 20 intertransversarii, and 22 rotatores identified in the anatomy literature [45-55] were simulated in the model. Origin and insertion points of all the muscle fascicles were determined according to the literature. Although the pelvis was not shown in Figure 3-1, muscle attachment points on the pelvic bone were determined appropriately based upon the CT image of the pelvis. Many of the long muscles (spanning 3 or more motion segments) were forced to pass through several nodes rigidly attached to various vertebrae in order to simulate their wrapping over the spine during various spinal motions. All the muscle fascicles were modeled using 1-D discrete elements to simulate the spinal MFs. Types and material characteristics of the elements used in the FE model of the spinal system are summarized in Table 3-1.

Table 3-1 Finite element model - Parts Summary

Parts	Type	Material type
Vertebrae	Shell element	rigid
Discs	Solid element	Nonlinear (see 3.1.2)
Rib cage	Shell element	rigid
Muscle	Discrete (spring) element	Nonlinear
Ligaments	Discrete (spring) element	Nonlinear (see 3.1.3)

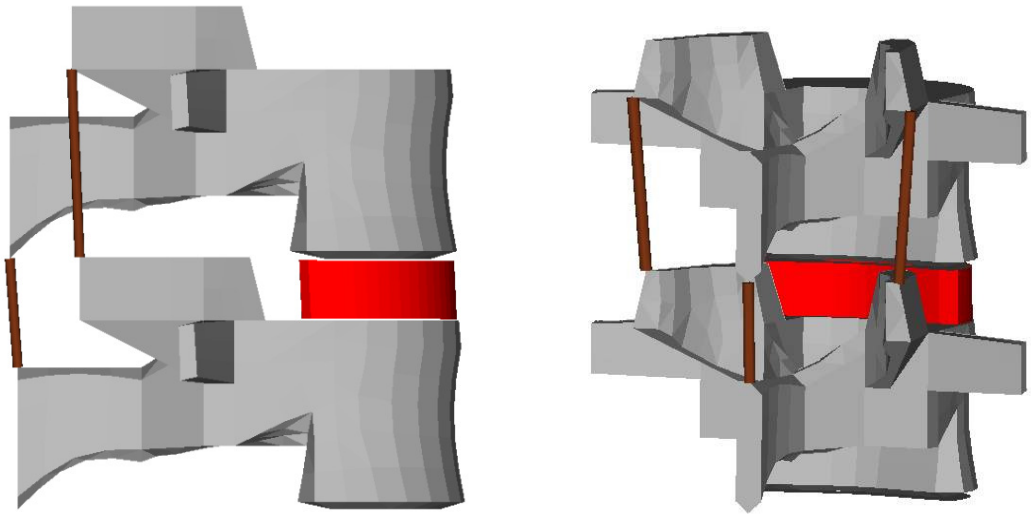

a) Side view of FSU (L3-L4) b) Real iso view of FSU (L3-L4)

Figure 3-2 Functional spinal unit (FSU) in the 3-D FE model is composed of two adjacent vertebral bodies and intervertebral joints (Disc, ligaments and apophyseal joint)

Following loading and boundary conditions were always assumed in all FE computations in this study: 1) The weight of the upper body of 350N [41, 56] was assumed to be located at the center of gravity (CG) of the trunk determined according to the literature so that the trunk produces a flexion moment of 3.5 Nm [41] about the geometrical center (GC) of T12 vertebra body when the spine is in a upright standing posture. 2) The MFs calculated from the optimization models for various cases were added to the FE model as case specific loading conditions. 3) The sacrum and pelvis were considered stationary whereas the trunk and all the lumbar vertebrae were allowed to move freely in the space.

The 3-D FE model of the spinal system was executed using a commercial software package, LS-Dyna (Livermore Software Technology, Livermore CA USA).

3.1.1 Determination of the material properties of the IVD

In order to determine the mechanical properties of the disc elements, the endplate-disc-endplate unit was isolated from the model and modified to simulate the in-vitro compression tests performed by Brown et al [43]. For this purpose, the disc was modified to have a uniform height of 12 mm (Figure 3-3) according to the literature [44], and the superior endplate was subjected to an increasing compressive load while the inferior endplate was fixed. The displacement of the superior endplate in response to the applied compressive load was predicted to obtain a load-displacement curve. It was possible to determine the mechanical properties of the disc element (non-linear, isotropic properties as in Table 3-2) with which the model can result in a load-displacement curve in almost perfect agreement with that obtained in the in-vitro test [43] as shown in Figure 3-4.

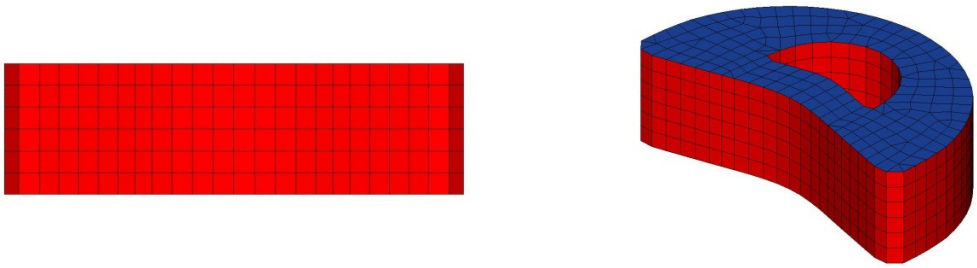

a) Rear view of IVD

b) Iso view of IVD

Figure 3-3 IVD FE model (thickness of 12 mm)

Table 3-2 Stress (GPa) vs. strain relationship of the IVD

strain	Stress (GPa)
0.000000	0.000000
0.041667	0.000771
0.059524	0.001541
0.075397	0.002312
0.088294	0.003082
0.101191	0.003853
0.115079	0.004624
0.126984	0.005394
0.005000	0.001080

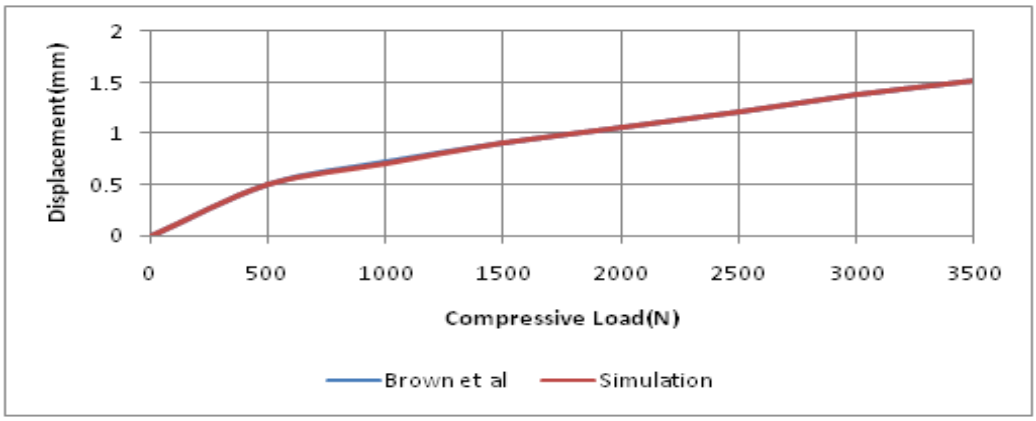

Figure 3-4 Comparison of compressive load vs. axial displacement between experiment and simulation.

3.1.2 Determination of the load-displacement behavior of the spring elements used for the simulation of facet joints and ligaments

In order to determine the range of motion (ROM) of L5-S1 motion segment, the vertebral body (L5)-disc-vertebral body (S1) unit with spring element was isolated from the model and modified to simulate the in-vitro mechanical tests performed by Adams et al [57, 58]. A massless rigid bar was attached to the top of L5 vertebral body (Figure 3-5) and a vertical force (F) was applied to the end of the rigid bar to apply a bending moment

to the upper vertebral body (L5) with a negligible compressive force. The rotation of the L5 in response to the applied moment was predicted to obtain a moment-rotation angle curve in cases with varying stiffness characteristics of the spring elements while the material properties of the disc elements were fixed as those determined in section 3.1.1. It was possible to determine the characteristics of the ligament-joint elements (non-linear, compression-tension and tension spring properties as in Table 3-3) with which the model predictions can result in the predicted flexion and extension ROMs to those measured in the in-vitro tests [57, 58] as shown in Figure 3-6.

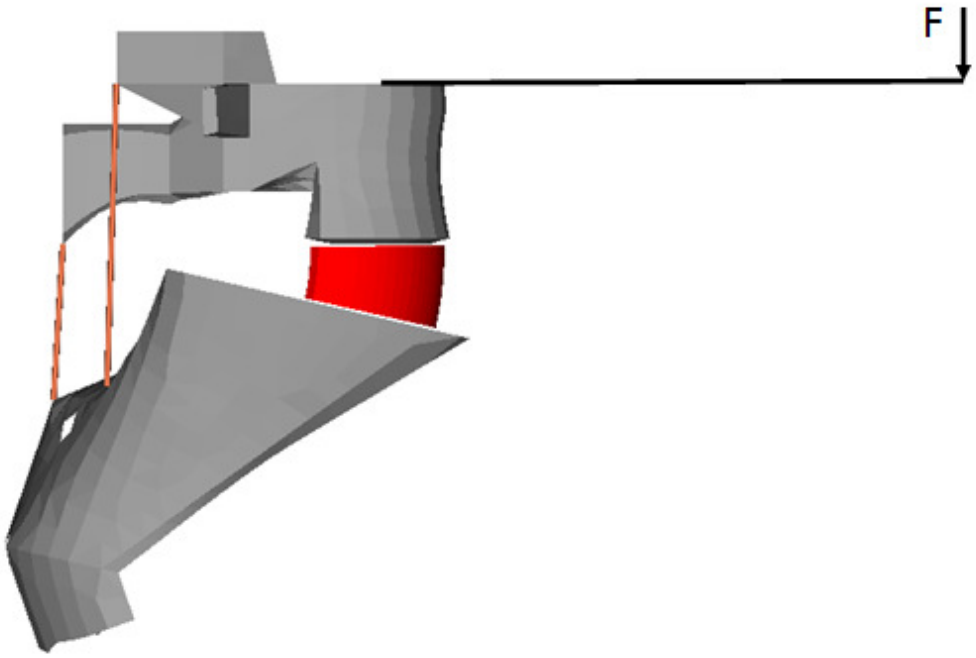

Figure 3-5 Schematic diagram to simulate the ROM of L5-S1 (Flexion)

Table 3-3 Characteristic disp. vs. load definition of apophyseal joint-ligament spring element

Compression (Apophyseal joint)	
Disp. (mm)	Force (KN)
-25.0	-1.021
-5.0	-1.021
-3.0	-0.020
-1.5	-0.015
0.0	0.000

Tension (Ligament)	
Disp. (mm)	Force (KN)
0.0	0.000
7.0	0.015
15.0	1.020
25.0	1.021

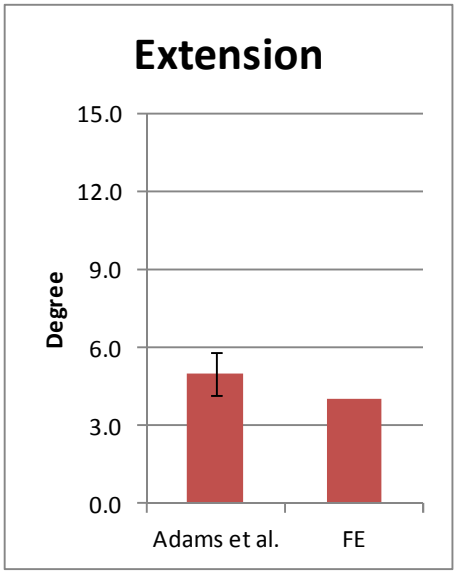

a) ROM of L5-S1 at 21.3 ±9.0 Nm

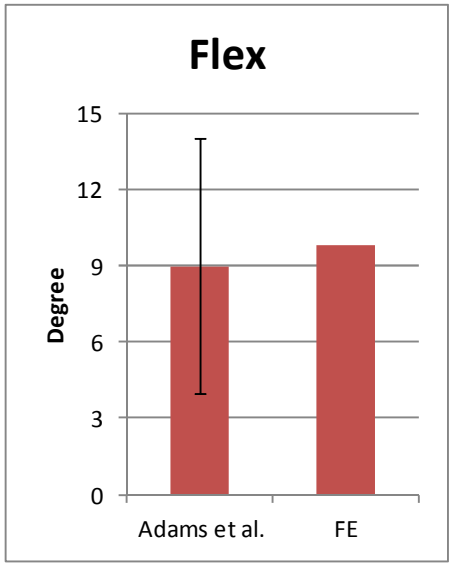

b) ROM of L5-S1 at 50.9 ±26.7 Nm

Figure 3-6 ROM of L5-S1 in flexion and extension (The Rom of L5-S1 in flexion was 9±5 (Adams et al.) and 9.8 (FE), while the Rom of L5-S1 in extension was 5.0±0.8 (Adams et al.) and 4.0 (FE) respectively)

3.2 Improvement of optimization model with follower load constraint

Since musculo-skeletal system of human spine was indeterminate, an optimization technique has been recruited as a standard tool to calculate muscle forces (MFs). An optimization formulation for determining the MFs producing compressive follower loads (CFLs) in the lumbar spine was developed in our laboratory [5, 59]. Mathematical formulation to find MFs creating CFLs in the lumbar spine is:

$$min(f) = \sum_{l=1}^{6} \left\| F_l^{jt} \right\| + \sum_{l=1}^{6} \left\| M_l^{jt} \right\| \tag{1.1}$$

Subject to

$$\sum_{k=1}^{n} \vec{F}_{k,l}^{m} + \sum_{k=1}^{n\prime} \vec{F}_{k,l}^{ext} + \vec{F}_l^{jt} + \vec{F}_{l+1}^{jt} = 0 \quad (l = 1, \dots, 6) \tag{1.2}$$

$$\sum_{k=1}^{n} \vec{r}_{k,l}^{m} \times \vec{F}_{k,l}^{m} + \sum_{k=1}^{n'6} \vec{r}_{k,l}^{ext} \times \vec{F}_{k,l}^{ext} + \vec{r}_l^{jt} \times \vec{F}_l^{jt} + \vec{r}_{l+1}^{jt} \times \vec{F}_{l+1}^{jt} + \vec{M}_l^{jt} = 0 \quad (l = 1, \dots, 6) \tag{1.3}$$

$$\vec{F}_{l+1}^{jt} // (\vec{r}_{l+1}^{jt} - \vec{r}_l^{jt}) \qquad (l = 1, \dots, 6) \tag{1.4}$$

$$-30 \le \eta \le 15 \qquad (l = 1, \dots, 6) \tag{1.5}$$

$$0 \le \left\| \vec{F}_k^m \right\| \le F_{max}^m \qquad (k = 1, \dots, 232) \tag{1.6}$$

F_l^{jt} and M_l^{jt} in (1.1) are compressive follower load (CFL) and moment at *l-th* intervertebral joint force and joint moment, while $\vec{F}_{k,l}^{m}$ and $\vec{F}_{k,l}^{ext}$ in (1.2) are muscle force and external force affecting *I-th* vertebra. $\vec{r}_{k,l}^{m}$ is the normal vector from the center of the *l-th* vertebra body to the muscle force, while $\vec{r}_l^{jt}$ and $\vec{r}_{k,l}^{ext}$ are the normal vector from the center of the *l-th* vertebral body to the *l-th* CFL and to the external force respectively. Equation (1.4) is the constraint for CFL that resultant force just above in *l-th* level have to run parallel to the curvature of the spinal column. η in equation (1.5) is the distance

between the GC of vertebral body and compressive follower load path (FLP) and $\vec{F}_k^m$ and F_{max}^m in equation (1.6) is the MFs to be determined and the maximum muscle force of each muscle, respectively.

The cost function of optimization problem (1.1) was the summation of CFL and joint reaction moment at each level shown in Figure 3-7. It was the representation of mechanical burden in the spine based on the idea that the minimum mechanical burden exerted in the intervertebral joints induced the least chance of mechanical injury. Such a cost function was selected for this study because it would be physiological if the exerted burden can be minimized during normal activities.

The above formulation was made to find the MFs that create the CFL in the lumbar spine while minimizing the total joint reaction forces and moments. Since there could be numerous curves following the lumbar curvature within the anatomic range of the intervertebral joint, the location of the FLP for minimum CFLs was determined as an anterior or posterior shift from the base spinal curve connecting GCs of the vertebral bodies (η in equation (1.5)). The maximum muscle force (F_{max}^m) for each muscle (1.7) was determined by the multiplication of the physiological cross-section area (PCSA) of each muscle and its maximum force capacity (MFC) defined as a maximum muscle force generated per PCSA in each muscle fascicle. PCSAs and MFCs were determined according to the values reported in the literature. For example, PCSAs of superficial muscles were taken from previous studies [54, 60, 61]. Due to the lack of information of the PCSAs of internal, short muscles in the literature, however, they were assumed to be 1 cm^2 [59]. The MFCs of all muscles were assumed to be 0.45 MPa since the MFC of spinal muscles was known to vary between 0.1 to 1.0 MPa in previous studies [54, 59, 62-67].

$$F^{m}_{max,k} = PCSA_k * MFC \qquad (k = 1, \dots, 232) \tag{1.7}$$

The modification of the above formulation made in this study was that the inputs of spinal geometry (the locations and orientation of the vertebrae, muscle attachment points, and the CG of the upper body) were replaced by those used in the 3-D FE model of the spinal system to make the geometrical inputs in both models exactly same.

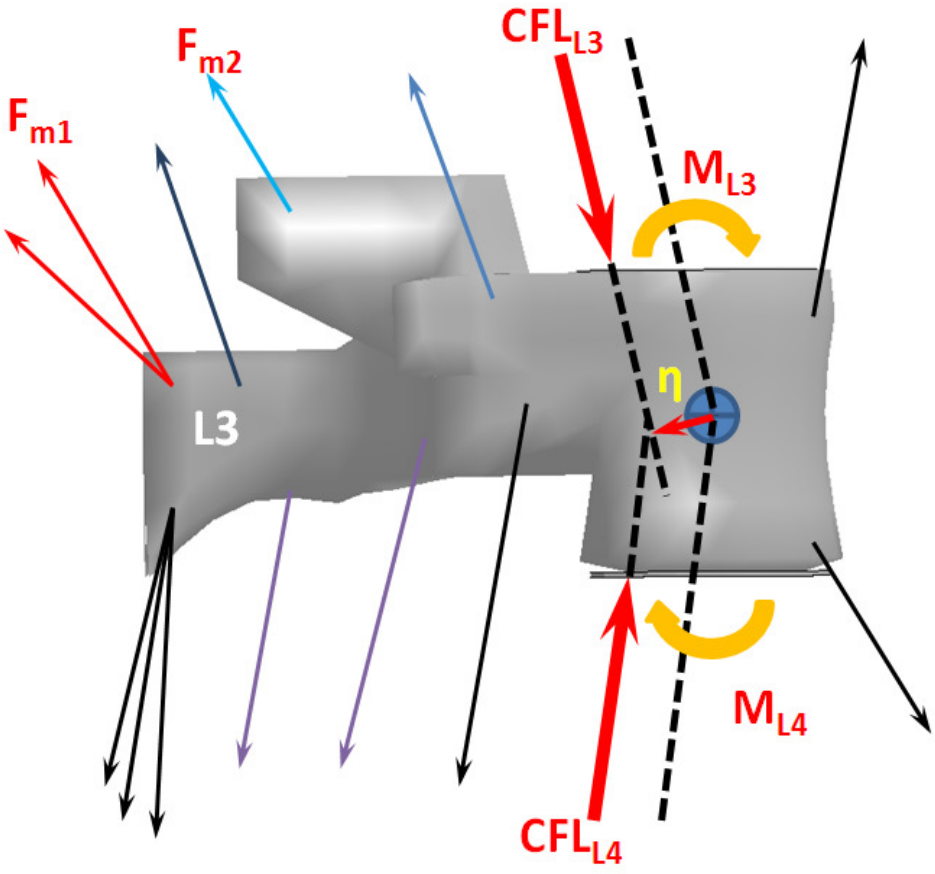

Figure 3-7 Free body diagrams at L3 vertebra in case of CFLs

CHAPTER 4

EXPERIMENTAL VALIDATION OF THE 3-D FE MODEL OF THE LUMBAR SPINE

4.1 ROMs of the lumbar spine under no compression pre-load

The 3-D FE model of the spinal system was completed by assigning the material properties of the intervertebral discs (IVDs), facet joints and ligaments determined in the previous sections 3.1.1 and 3.1.2. However, the lumbar spine model needs an experimental validation because the geometry of individual segments in the lumbar spine model was different from that of the motion segment model used in the previous section and the same material properties of the intervertebral joint were used in all levels. For the experimental validation, the lumbar (L1-S1) spinal model composed of 6 vertebrae (S1-L1), 5 IVDs and 15 spring elements for ligament- apophyseal joint was isolated from the 3-D FE model of the spinal system. Then, to apply flexion-extension moments with negligible compressive force, a long massless rigid bar was attached to the top of L1 vertebra body while the sacrum of the FE model was fixed as shown in Figure 4-1.

The rotation of the L1 vertebra in response to the applied moment was predicted to obtain the range of motion (ROM) of L1-S1 in response to a certain moment in previous studies (21.3Nm in extension and 49.4Nm in flexion) [57, 58, 68]. The predicted ROMs fell within one standard deviation of the results in previous studies as shown Figure 4-2. The ROM of L1-S1 predicted by FE model was 48.8° in flexion and 28.2° in extension, whereas the accumulated ROM from L5-S1 to L1-L2 was 52°±16° [58] in flexion and 23.6°±6.1° in extension [57]. Meanwhile the *in vivo* ROMs were 53.0° ± 10.2° and 23.4° ± 8.3° in flexion and extension reported in the literature respectively [68].

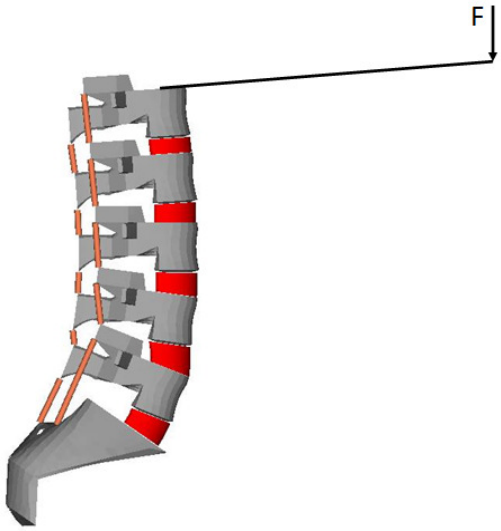

Figure 4-1 Schematic diagram to simulate the ROM of L1-S1 (Flexion)

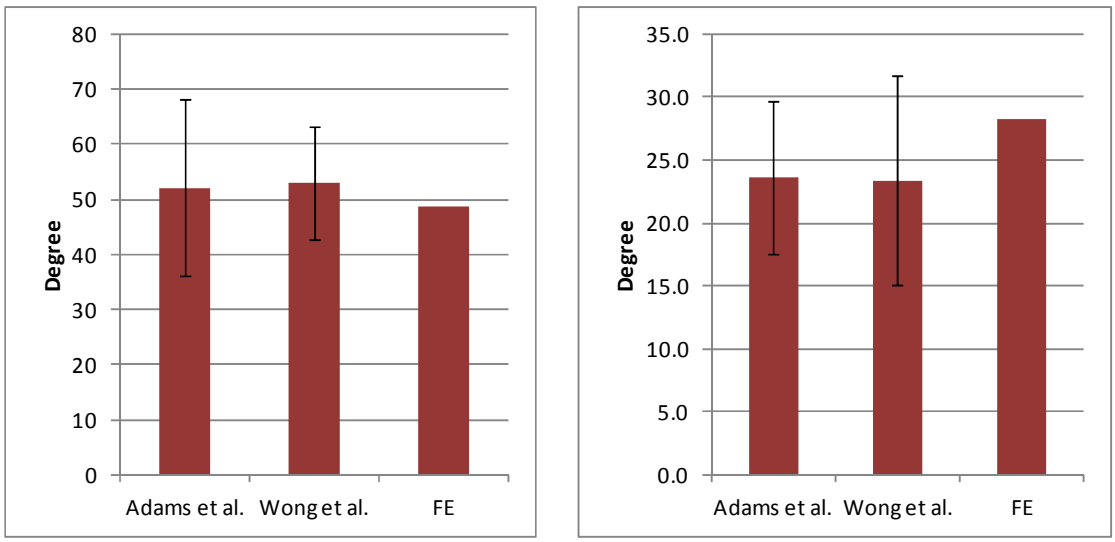

a) ROM of L1-S1 in flexion at 43.98Nm

b) ROM of L1-S1 in Extension at 21.3Nm

Figure 4-2 ROM of L1-S1 in flexion was at 52±16° (Adams et al), 53±10.2° (Wong et al) and 48.8° (FE) at 43.98Nm, while ROM of L1-S1 in extension was 23.6±6.1° (Adams et al), 23.4±8.4° (Wong et al) and 28.2° (FE) at 21.3 Nm respectively

4.2 ROMs of the lumbar spine under physiological pre-load (follower load)

It is well known that the lumbar spine becomes unstable under a compressive force much less than the physiological compressive load, but Patwardhan et al. were able to test ROMs of whole lumbar spine under a physiological compressive load which was applied using a wire following the spinal curvature as shown in Figure 4-3 A [4]. In order to use the ROM results of their testing for an experimental validation, the 3-D FE model of the lumbar spine was isolated for the model of the spinal system and modified to simulate the follower pre-load as shown in Figure 4-3 B [4].

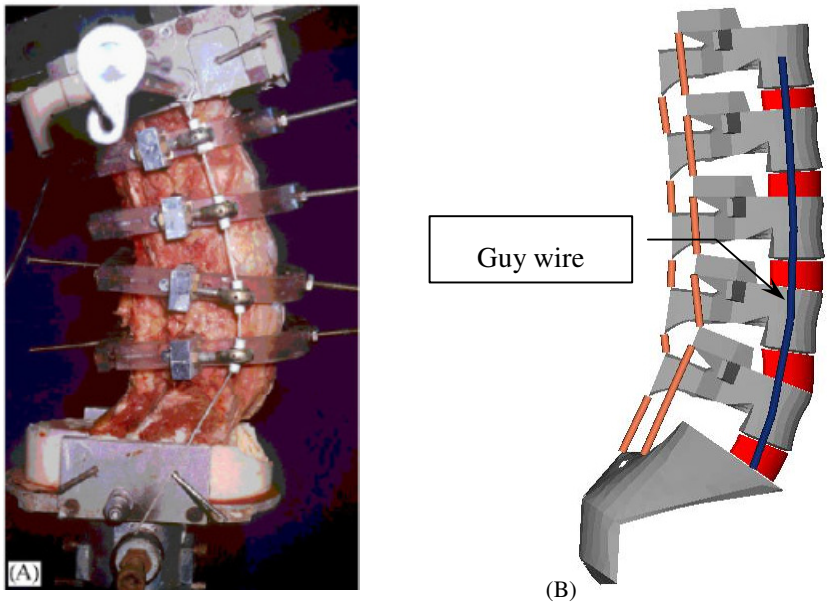

Figure 4-3 A schematic diagram of the lumbar spine subjected to a CFL-lateral view ((A)Experiment [4] and (B)FE)

Figure 4-4 shows the predicted flexion-extension ROMs under no compressive preload in comparison with experimental results [37]. The model prediction and experimental results showed a good agreement not only in the total spinal motion but also

in the segmental motions at all levels except at the L2-3 level where a small over prediction was found.

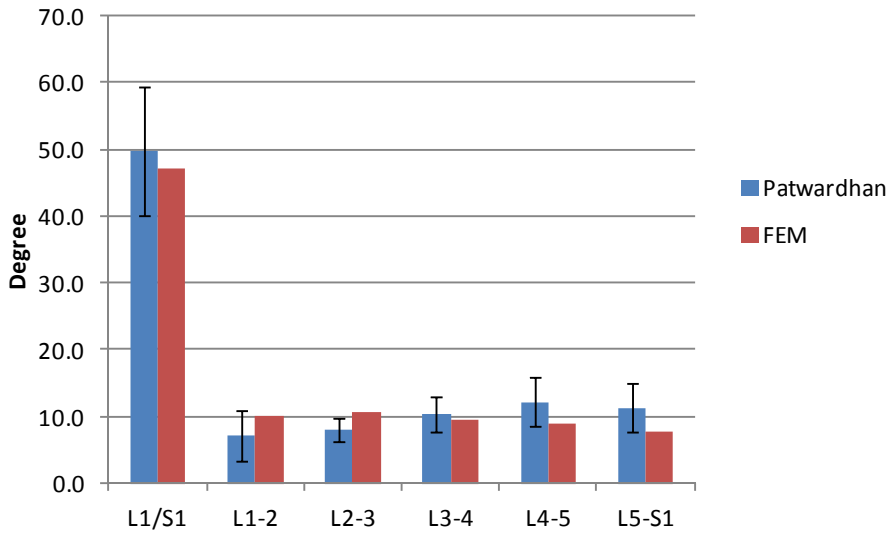

Figure 4-4 In-vitro and finite element total segmental flexion-extension ROM without preload. Mean flexion-extension ROM of L1 with regard to S1 predicted by the FEM (47.1°)demonstrated good agreement with the experimental results from previous study conducted by Patwarden et.al (49.7±9.7°)

When the follower preload of 800 N was applied through the cables, the ROMs in response to the flexion (8 Nm) and extension (6 Nm) moments showed a decrease from those under no-preload not only in the in-vitro experiment [69] but also in our model predictions as shown in Figure 4-6 (blue bars from the experiment and brown bars from the model predictions).

These agreements were encouraging, but the material properties used in the FE model, particularly those for the elements of the IVDs needed to be modified because of the following reasons: (1) The FE-model of the spinal system was developed to simulate an in-vivo condition, in which the application of follower pre-load using a cable system is not feasible. (2) It is well known that the spinal motion segment is stiffer in an *in-vivo* situation (loaded by the body weight and muscle forces (MFs)) than in an in-vitro case where there is no pre-compressive load [70]. Thus, it was necessary to assign a stiffer stress-strain relationship to the disc elements in the FE model of the spinal system in order to develop an FE model simulating the in-vivo spine. For this purpose, the stress-strain relationship shown in Table 4-1 and Figure 4-5 (blue line) was determined from the portion of the previous stress-strain relationship (stresses and strains resulting from the compressive pre-load greater than 800 N) assuming that the physiological compressive load in a quiet standing posture is about 800 N according to the previous studies [1, 37, 59]. When the FE model of the lumbar spine with stiffer intervertebral disc (IVD) was subjected to the flexion-extension moments under no follower pre-load (zero-cable force), the predicted flexion-extension ROMs (green bars in Figure 4-6) also showed reasonably good agreement with experimental results (obtained from the in-vitro lumbar spine under a 800 N follower pre-load) not only in the total spinal ROM but also in the segment ROMs. Such a good agreement indicates that the FE model with stiffened disc properties represents the in-vivo lumbar spine reasonably well.

Explicit code was used in solving multi-segmented spine FE model due to the limitation of implicit code for material definition to solve flexion and extension simulation of initially stiffened-disc model. In explicit code, tensile stiffness of the IVD was assumed to be that of annulus fibrous of the disc or 45 MPa based on the previous study of IVDs [71].

Table 4-1 Stress vs. strain relationship on stiffened IVD

Strain	Stress (N/mm^2)
0	0
0.0007706	0.041667
0.0015412	0.059524
0.0023118	0.075397
0.0030824	0.088294
0.003853	0.101191
0.0046236	0.115079
0.0053942	0.126984

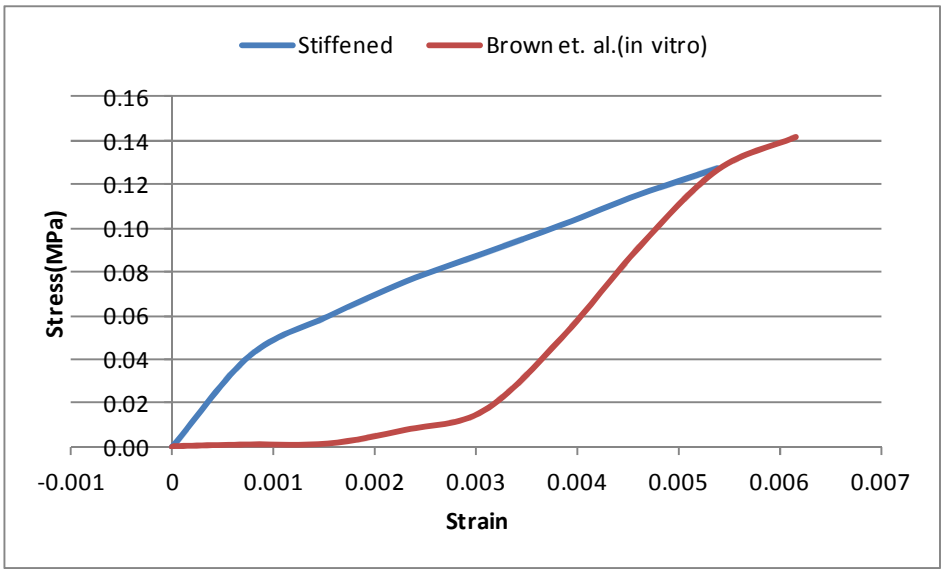

Figure 4-5 Stress vs. strain relationship of IVD (Brown et al. and Stiffened disc respectively)

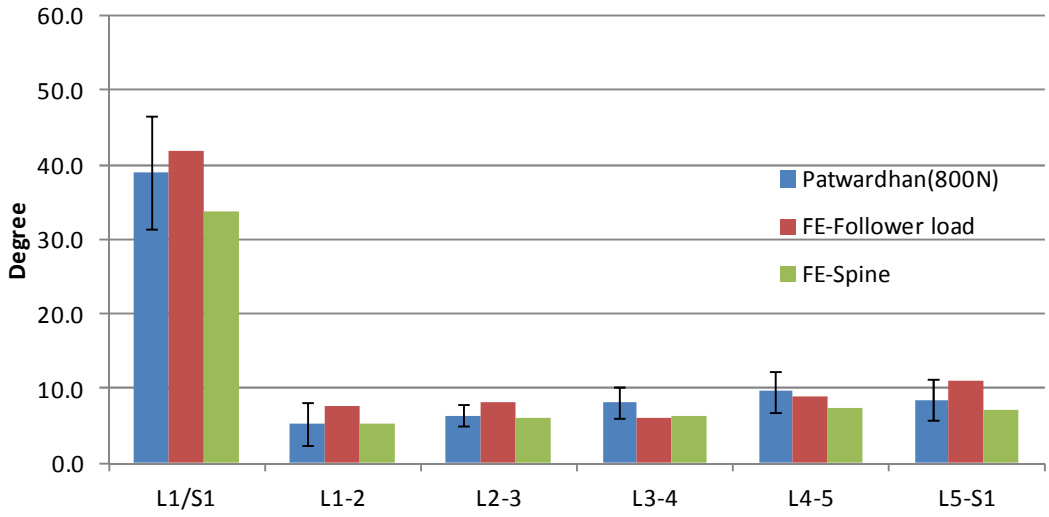

Figure 4-6 In-vitro and finite element total segmental flexion-extension ROM with preload. The L1-S1 flexion-extension predicted be FEM with an 800N of follower load(41.8°) was in good agreement with the results in vitro (39.0±7.6°), whereas the ROM of the stiffened disc was 33.7° and it also fell within one standard deviation.

The application of flexion-extension moments on the model was simulated using the same method in section 4.1 (Figure 4-1). In fact, the same method was used to apply the flexion-extension moments on the L1 vertebra in Patwardhan's study [4]. The location of the cables in the FE model was determined by the approximation of the center of rotation of each motion segment. Flexion and extension moments were on T12 by varying transverse forces applied on the rod on T12, which was long enough to minimize the effects of compressive load when compared to compressive follower load (CFL) so that almost pure moment application can be achieved. The application of flexion and extension moments of greater than 8 and 6 Nm was simulated in the model, but the ROMs predicted in response to 8 Nm flexion and 6 Nm flexion moments were used for a comparison with those measured in Patwardhan et al's studies[4].

CHAPTER 5

RESULTS OF THE 3-D FE MODEL IN NEUTRAL POSTURE

5.1 Optimum solutions for MFs in a neutral standing posture for CFL and non-CFL cases

From the modified models, optimum solutions of muscle forces (MFs), compressive follower loads (CFLs) (compressive loads in the spine in case of follower load), joint reaction moments, and the location of follower load path (FLP) for the spine in a quiet standing posture were computed using a commercial non-linear optimum solver (Lingo) for the spinal system in various conditions. The solutions are listed in Table 5-1.

Table 5-1 Recruited muscles in the neutral posture with MFC45 N/cm^2 under follower load (FLP:-11.38 mm)

Level	Superficial muscles	N	Internal muscles	N
Th-L1	LatissimusDorsi_L1_RibHum	22.4	Rotatores_L1_T12	45.0
	LatissimusDorsi_L2_RibHum	58.9		
L1-L2			Interspinales_L2_L1	0.3
			Rotatores_L2_L1	45.0
			Rotatores_L3_L1	6.3
L2-L3			Interspinales_L3_L2	41.1
			Rotatores_L3_L2	42.7
L3-L4			Interspinales_L4_L3	35.6
			Intertransversarii_L4_L3	33.9
L4-L5	Longissimus_Sa_L4	79.9	Interspinales_L5_L4	9.0
			Intertransversarii_L5_L4	45.0

Then, the MFs obtained from the above optimization models were applied as external loads in the FE model of the spinal system. When no MFs were simulated, the model predictions showed that the lumbar spine buckles in flexion by the trunk weigh (350 N) as shown in Figure 5-1 (a). In contrast, when the MFs predicted from the optimization models (listed in Table 5-1) were added, the lumbar spine was able to support the trunk weight with some deformation resulting in the posterior sway of the

trunk but without buckling as shown in Figure 5-1 (b). The magnitude of the posterior sway of the trunk CG was 63 mm posteriorly in the CFL case.

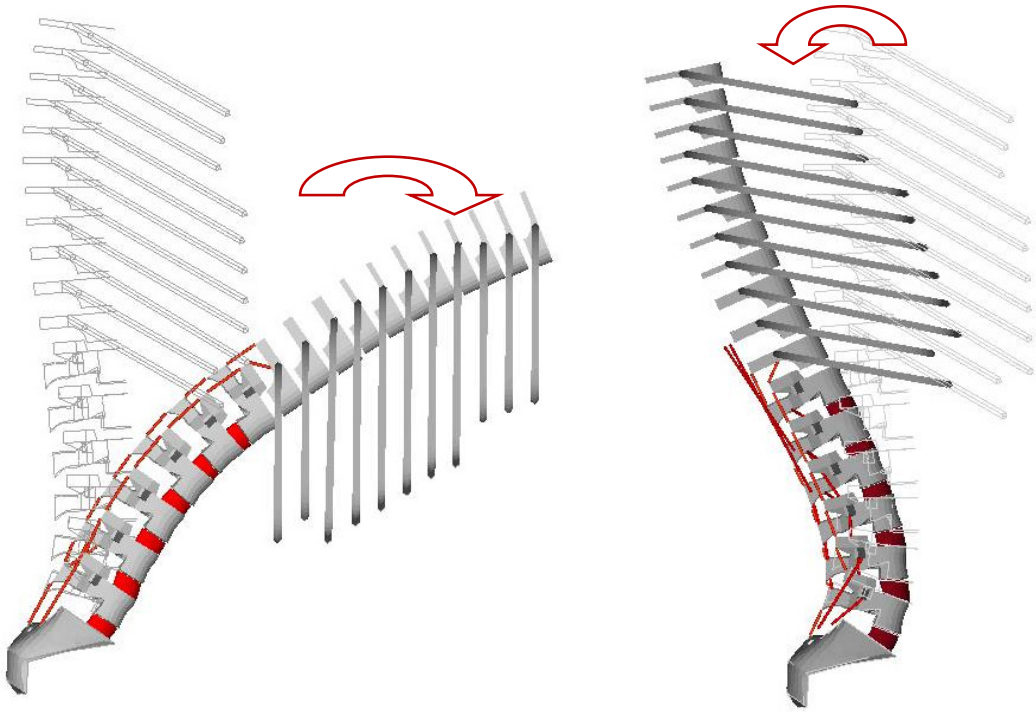

a) FE model of ligamentous spine under 350N on trunk CG

b) Muscles stabilize the upper body under CFLs (FLP=-11.38mm)

Figure 5-1 CFL of the spine can support the upper body in a neutral standing posture.

5.2 Parametric studies of FLP variation and MFC variation in a neutral standing posture

The results in section 5.1 clearly demonstrate the importance of the MFs in the stabilization of the lumbar spine. However, about 63 mm sway seems to be too large considering the control of the trunk position in-vivo in a standing situation. This mandated us to conduct a parametric study to investigate the effect of FLP variations on the MFs. In addition, another parametric study examined the effects of muscle force

capacity (MFC) variations because the MFs are likely to vary depending upon the MFC variations

5.2.1 The effects of the variations in FLP

In order to simulate the FLP variation, η in the optimization model was varied from the optimum FLP (η = -11.38 mm) to FLPs at η = -5 mm, 0 mm, and 5 mm. The optimization problem was solved for each η value. In all FLP variation cases, the optimum solutions were feasible. MFs required to create CFLs for each FLP are listed in Table 5-1. In the cases of FLP at η =-11.38mm, a total of 28 muscles need to be recruited to create CFLs in a neutral standing posture. As the FLP position moved away from the FLP at η = -11.38 mm, it was predicted that not only all 28 but also additional muscles need to be activated in order to create CFLs in the lumbar spine. The needs for recruiting more muscles resulted in the increases in CFLs in all levels as shown in Figure 5-2.

The changes in CFLs in the cases of FLP at η = -5 mm and 0 mm were substantial whereas , in the case of FLP at η = 5 mm, predicted CFLs were greater than 1,000 N which would be too high to be a physiological compressive loads in the lumbar spine during quiet standing. Therefore, the case of FLP at η = 5 mm was considered not physiological and removed from further FE analyses.

Table 5-2 Recruited muscles in FLP variation

Recruited muscle pattern	Activated muscles		FLPs			
Opt -11.38 / -5 / 0 / 5			Opt -11.38	-5	0	5
TR-L1	LatissimusDorsi_L1_RibHum	L	22.4	83.6	106.5	135.4
	LatissimusDorsi_L2_RibHum	L	58.9	4.0	3.4	55.4
	LatissimusDorsi_L4_lr	L	0.0	11.0	0.0	0.0
	LatissimusDorsi_L4_lr	L	0.0	11.0	0.0	0.0
	ExternalOb_Pel_Rib10	L	0.0	0.0	7.5	93.2
	RecAbdominis_Pel_Rib7	L	0.0	25.6	47.3	67.4
	Rotatores_L1_T12	S	45.0	45.0	45.0	45.0
	Rotatores_L2_T12	S	0.0	21.6	45.0	45.0
L1-L2	Multifidus_L4_L1_F4	L	0.0	0.0	39.1	59.3
	Interspinales_L2_L1	S	0.3	19.8	6.6	0.0
	Intertransversarii_L2_L1_La	S	0.0	0.0	0.0	21.3
	Rotatores_L2_L1	S	45.0	45.0	45.0	45.0
	Rotatores_L3_L1	S	6.3	45.0	45.0	45.0
L2-L3	Interspinales_L3_L2	S	41.1	33.1	30.8	45.0
	Intertransversarii_L3_L2_La	S	0.0	0.0	0.0	35.1
	Intertransversarii_L3_L2_Me	S	0.0	0.0	0.0	20.1
	Rotatores_L3_L2	S	42.7	23.6	27.8	45.0
L3-L4	Longissimus_Sa_L3	L	0.0	0.0	0.0	27.3
	Interspinales_L4_L3	S	35.6	45.0	32.8	45.0
	Intertransversarii_L4_L3_La	S	0.0	0.0	0.0	45.0
	Intertransversarii_L4_L3_Me	S	33.9	20.7	45.0	45.0
L4-L5	Longissimus_Sa_L4	S	79.9	82.7	91.4	138.3
	Interspinales_L5_L4	S	9.0	6.9	18.3	17.5
	Intertransversarii_L5_L4_La	S	0.0	0.0	0.0	45.0
	Intertransversarii_L5_L4_Me	S	45.0	45.0	45.0	45.0
L5-Sa	Longissimus_Sa_L5	S	68.5	75.6	84.3	127.2

(Note: Long muscle: L, Short muscle: S, unit: N)

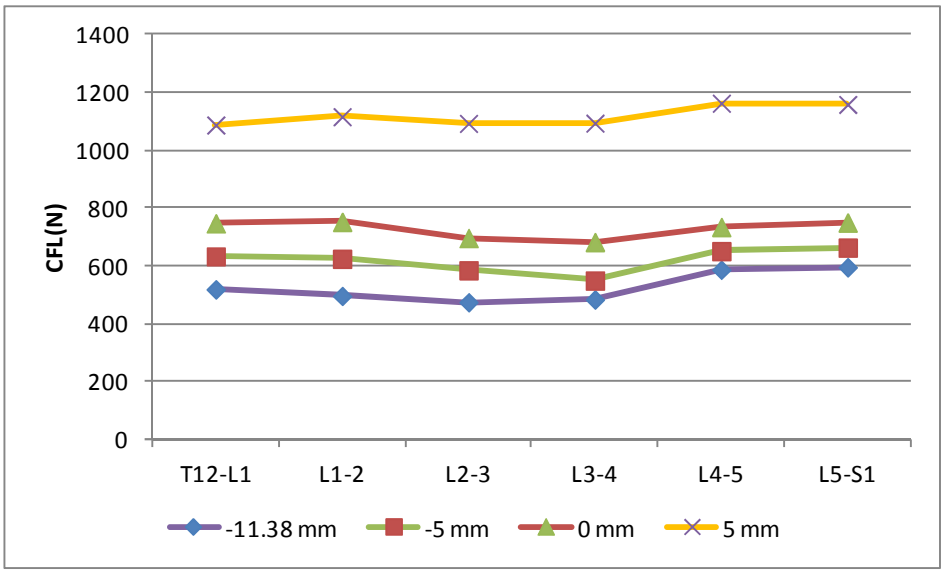

Figure 5-2 Reaction forces at different lumbar level under various FLP (η = opt., -5 mm, 0 mm and 5mm shift).

The MFs predicted from the above parametric study were applied to the FE model of the spinal system as external forces, and the FE analyses were conducted to predict the spinal deformation under different MFs. Figure 5-3 shows the predicted deformations in terms of lumbar lordosis change resulting from the changes in MFs in response to FLP variations from η = -11.38 mm to η = 0 mm). Interestingly, MFs to create CFLs along FLP at η = 0 mm produced so small deformation to result in almost no change in the lumbar lordosis even though the predicted CFLs were greater than those in the other two cases. This phenomenon indicates that the lumbar spine can be stabilized most effectively when the FLP is following the spinal curve formed by connecting the geometric centers (GCs) of the vertebral bodies.

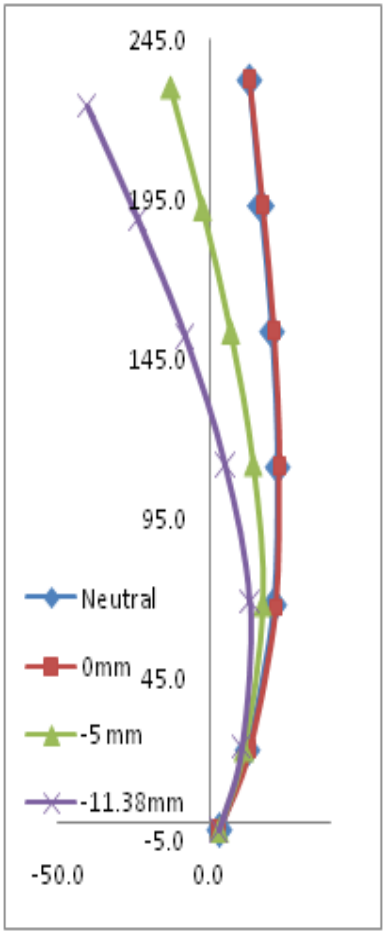

Figure 5-3 Changes in lordosis in a neutral posture under MFC 45N/cm^2

5.3.2 Effect of MFC variations

MFC is an indicator to represent the strength (or healthiness) of muscle. Since each individual may have different MFCs, the effects of MFC variations on the CFLs were investigated using the optimization model. The CFLs in all lumbar levels predicted in the cases of various MFC values are shown in Figure 5-4. It is clearly shown that CFLs at all lumbar levels decreased with increasing MFCs, indicating that the lumbar spine can experience less compressive loads with healthier muscles. Such decreases in

CFLs with increasing MFCs resulted from the fact that the number of muscles recruited to produce CFLs decreased with greater MFCs as listed in Table 5-3. Interestingly, Figure 5-4 demonstrated that the minimum CFL was predicted in the L3-L4 intervertebral joint not in the T12-L1 joint regardless of MFC variations, even though it is generally considered that the compressive force in the lumbar spine reaches a minimum at L1-L2 and maximum at L5-sacrum. These model predictions in this study may explain why the human feels pain in the low back as well as in the thoracolumbar junction during a long quiet standing.

Table 5-3 Spinal muscles recruited to create CFLs in cases of various MFCs

Level	Activated muscles		MFC45	MFC50	MFC60	MFC70	MFC80	MFC90
TR-L1	LatissimusDorsi_L1_RibHum	L	106.5	96.4	104.6	86.6	41.7	32.2
	LatissimusDorsi_L2_RibHum	L	3.4	0.0	0.0	30.9	76.2	76.7
	LatissimusDorsi_L3_lr	L	0.0	0.0	0.0	0.0	0.0	6.3
	LatissimusDorsi_L4_lr	L	0.0	4.5	11.7	7.4	0.0	0.0
	ExternalOb_Pel_Rib10	L	7.5	0.0	0.0	0.0	0.0	0.0
	RecAbdominis_Pel_Rib7	L	47.3	49.8	48.6	47.6	46.9	46.9
	Rotatores_L1_T12	S	45.0	50.0	60.0	70.0	79.0	82.6
	Rotatores_L2_T12	S	45.0	50.0	20.3	0.0	0.0	0.0
L1-L2	Multifidus_L4_L1_F4	L	39.1	4.1	0.0	0.0	0.0	0.0
	Interspinales_L2_L1	S	6.6	21.9	21.9	13.6	0.0	0.0
	Rotatores_L2_L1	S	45.0	50.0	60.0	70.0	80.0	90.0
	Rotatores_L3_L1	S	45.0	50.0	60.0	50.2	19.5	5.5
L2-L3	Interspinales_L3_L2	S	30.8	42.1	33.7	38.8	52.5	50.9
	Rotatores_L3_L2	S	27.8	43.9	30.8	42.1	78.0	90.0
L3-L4	Interspinales_L4_L3	S	32.8	50.0	60.0	67.4	72.6	69.2
	Intertransversarii_L4_L3_Me	S	45.0	29.9	7.3	0.0	0.0	0.0
	Rotatores_L4_L3	S	0.0	23.8	5.0	1.8	6.3	5.1
L4-L5	Longissimus_Sa_L4	S	91.4	84.9	82.1	79.8	78.1	78.1
	Interspinales_L5_L4	S	18.3	12.1	2.8	0.0	0.0	0.0
	Intertransversarii_L5_L4_Me	S	45.0	50.0	60.0	70.0	77.8	77.8
L5-Sa	Longissimus_Sa_L5	S	84.3	82.7	83.8	84.7	85.4	85.4

Note: Long muscle: L, Short muscle: S, unit: N

It is also interesting to note the significant roles of latissimus dorsi and intrinsic short muscles at the upper levels (T12-L1 and L1-L2) in creating CFLs in the lumbar spine. The lumbar spine is a vertical column and the spinal load needs to be properly directed from the top level to the bottom level in order to create CFLs. The forces in short intrinsic muscles at the upper levels (for example, rotatores T12-L1 and L1-L2) were found to increase with increasing MFCs, which indicates the crucial role of intrinsic short muscles in creating CFLs. At the lower levels (L4-l5 and L5-Sa), in contrast, there were less variations in CFLs as well as in the muscle recruitment patterns because the short muscles required for creating CFL in the lower level were not intrinsic short muscles but the short fascicles of a long muscle, the longissimus.

Although the longissimus is a long superficial muscle, the model predictions in this study demonstrate that only the short fascicle across the L5-Sa level needs to be activated to stabilize the lumbar spine during a quiet standing by creating CFLs.

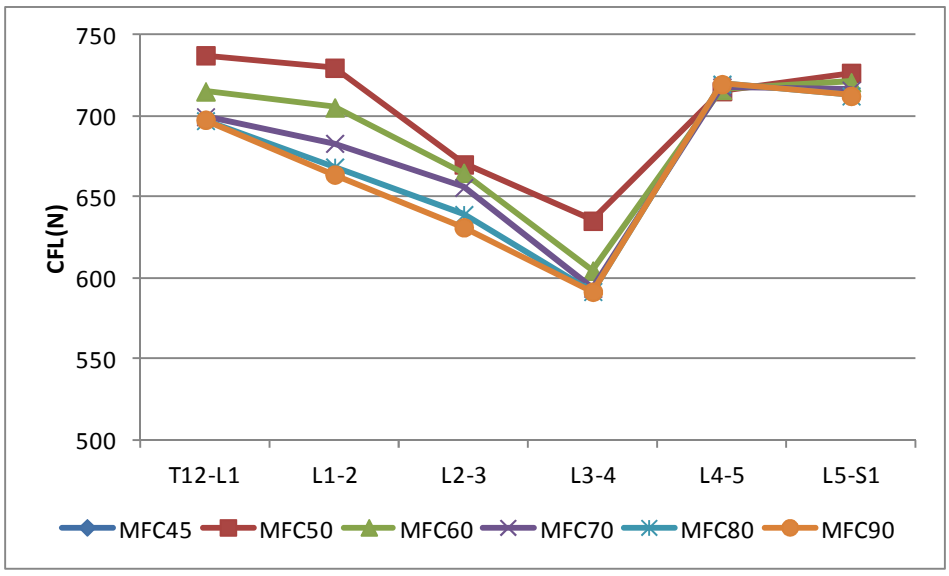

Figure 5-4 CFLs at different levels in various MFC.

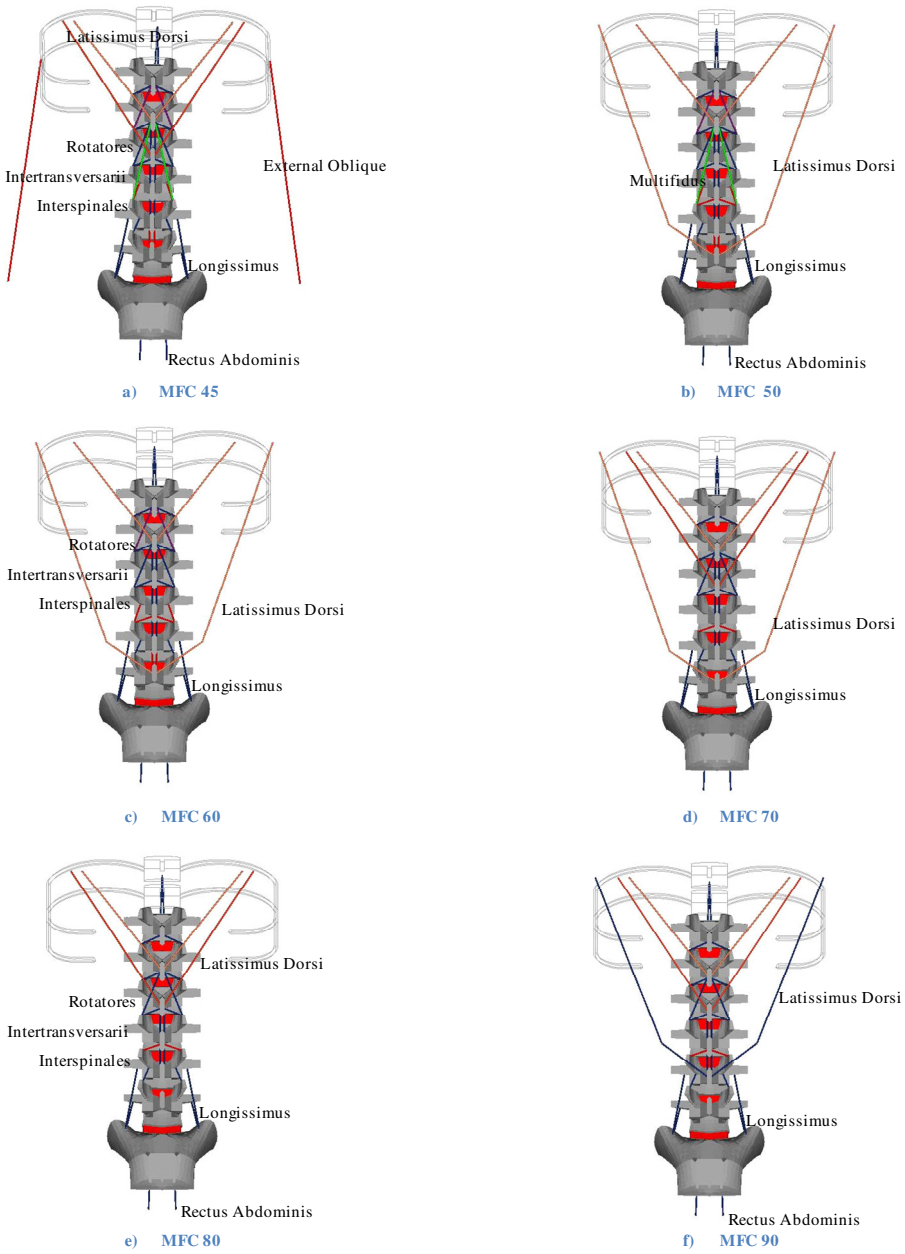

Figure 5-5 Recruited muscles for neutral standing posture in response to MFC variations

The MFs predicted in response to the MFC variations from the optimization models were applied as external forces to the FE model of the spinal system in order to investigate the corresponding changes in the deformation of the lumbar spine. For a clearer look, the deformation of the lumbar spine was demonstrated schematically in Figure 5-6 where the dots indicate the GCs of the vertebral bodies in the sagittal plane and the curves connecting the dots the lordotic curve of the lumbar spine. In all cases, MFs creating CFLs were found to produce very small deformation in the lumbar spine with almost no change in the spinal curvature.

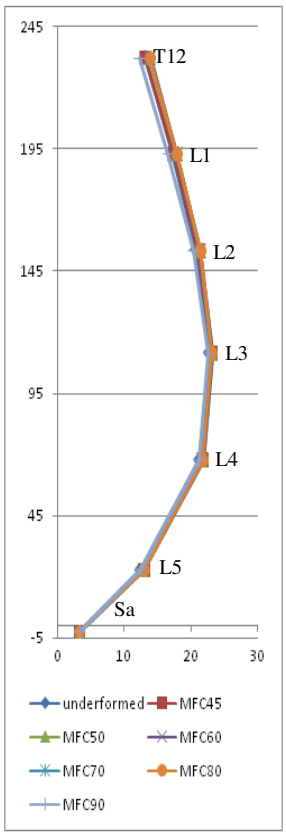

Figure 5-6 Deformation of lumbar spine under various muscle force capacities.

5.4 Comparison of CFLs predicted from the optimization model with those from the 3-D FE model of the spinal system

The FE model predictions showed that the MFs predicted from the optimization model, though small, resulted in the deformation of the lumbar spine. The differences in the CFLs in the FE model from those in the optimization were investigated with all model predictions in previous sections.

For example, Figure 5-7 shows the muscles activated to produce the CFLs along the base curve (FLP = 0 mm) in the case of MFC= 45 N/cm^2) in a neutral standing posture. When these MFs were applied to the FE model, the FE predictions of CFLs demonstrated an almost perfect match for the spinal curve before loading (as expected from the minimal changes in the lordosis in section 5.3.1) as shown in Figure 5-8. The magnitude of CFLs obtained from the FE analyses showed an outstanding agreement with those predicted from the optimization model as listed in Table 5-4.

Table 5-4 Direction of reaction forces at different levels (The differences are less than 1 % at all levels (Degrees from horizontal axis))

	Optimization(°)	3-D FE(°)	%difference
CFL-Trunk	84.17	83.95	-0.27
CFL-L1	84.95	84.77	-0.21
CFL-L2	87.28	87.14	-0.16
CFL-L3	88.03	88.15	0.13
CFL-L4	78.91	78.78	-0.17
CFL-L5	70.49	70.43	-0.08

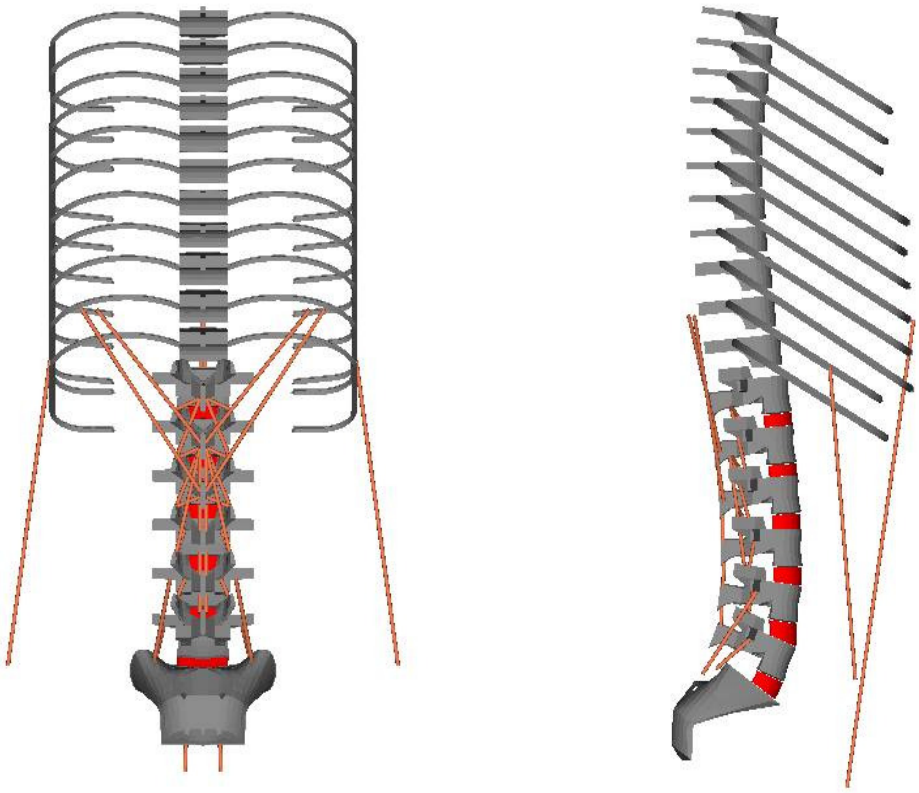

Figure 5-7 Muscle force combination for MFC45 N/cm^2 Neutral posture under follower load constraints (Simulation result)

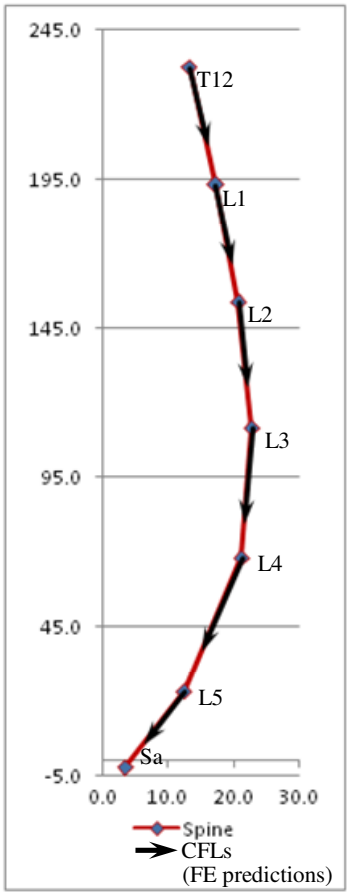

Figure 5-8 Direction of reaction force at different level. Predicted reaction forces run parallel to the curvature of the spine

CHAPTER 6

FE MODEL PREDICTIONS IN CASE OF VARIOUS SAGITTAL POSTURES

Previous results clearly showed that optimum compressive follower loads (CFLs) could be produced in a quiet standing posture in the sagittal plane at muscle force capacity (MFC) 45N/cm^2 along an follower load path (FLP) at various positions. It was also shown that MFs creating CFLs along an FLP in the vicinity of the base spinal curve ($\eta = 0$ mm) produce a stable deformation of the lumbar spine whereas MFs creating the smallest CFLs an unstable deformation of the lumbar spine. Similar results were found in the optimization and FE model predictions with increasing MFC values (i.e., simulation of the spinal system with stronger muscles). However, the stability of the whole lumbar spine under CFL creating MFs and the upper body was not investigated in cases of flexed or extended spines.

In this section, the stability of the lumbar spine in various sagittal postures were investigated using the same computational methods in order to show that the spinal muscles can create CFLs in the lumbar spine in all sagittal postures. The geometrical information of the flexed and extended lumbar spines as shown in Figure 6-1 was obtained from the FE model by applying the bending moment on the L1 vertebra without any muscle forces (MFs). The FE model predictions of the lumbar spine shape corresponding to two extended and three flexed postures in Figure 6-1 were used as inputs to formulate the corresponding optimization models.

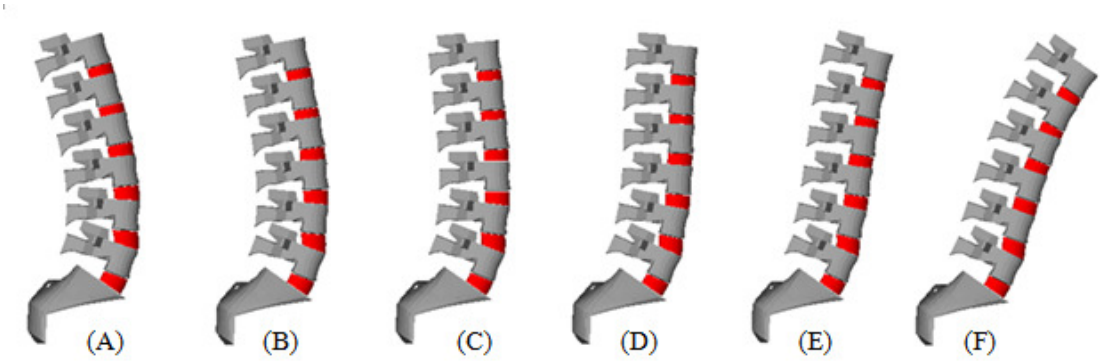

Figure 6-1 Schematic of 3D FE models of the spine in (A) 10° extension, (B) 5° extension, (C) neutral, (D) 10° flexion (E) 20° flexion, and (F) 40° flexion postures

6.1 Stability of the spine in various sagittal postures

6.1.1 CFLs in flexion 10° (MFC = 45 N/cm^2)

The optimization model predicted the minimum CFLs along the FLP at η = -0.65 mm in the lumbar spine flexed by 10° when MFC was assumed 45 N/cm^2. The predicted CFLs ranged from 503 N at T12-L1 to 665 N at L5-Sac joint. A total of 37 back muscles (20 long and intermediate muscles and 17 muscles short intrinsic muscles) were recruited to produce the minimum CFLs. However, the FE model predictions showed that these MFs were not able to produce a stable deformation of the lumbar spine in the flexed posture.

Further analyses demonstrated that MFs creating the CFLs along the FLP at η = -1.3 mm in the lumbar spine in flexion 10° were found to produce a stable deformation of the lumbar spine (small enough to result in the trunk center of gravity (CG) sway less than 10 mm from the before-loading posture). The predicted CFLs were 500 N at T12-L1, 499 N at L1-L2, 511 N at L2-L3, 570 N at L3-L4, 656 N at L4-L5 and 670 N at L5-Sac joint and magnitude of CFLs between the case of minimum CFLs and the case of the

most stabilized were compared in Figure 6-2. Among the total 35 muscles activated to stabilize the lumbar spine, 19 long and intermediate muscles and 16 short and intrinsic muscles were recruited as shown in Figure 6-3. The recruited muscles were stabilized the lumbar spine within 2 mm sway of the GC's of the upper body.

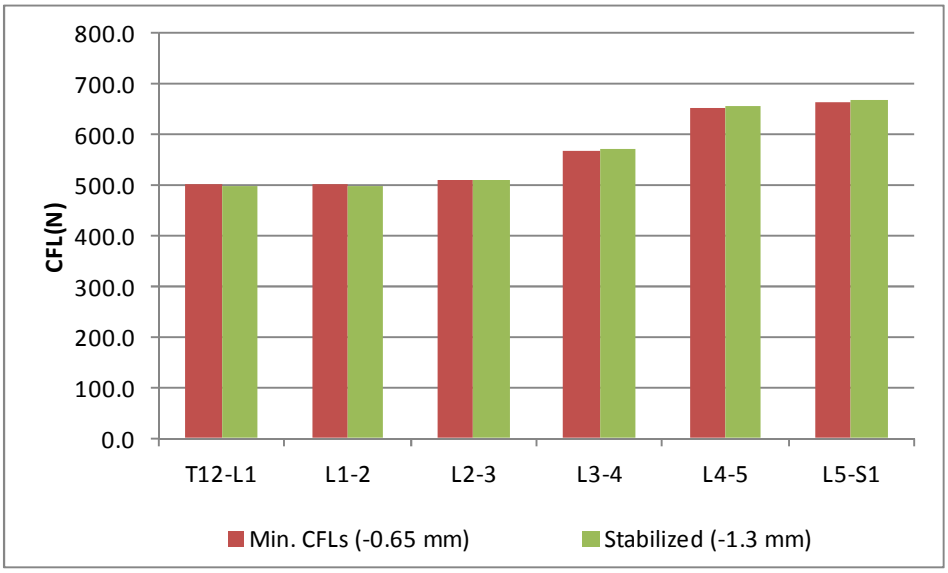

Figure 6-2 CFL on different levels in flexion 10°

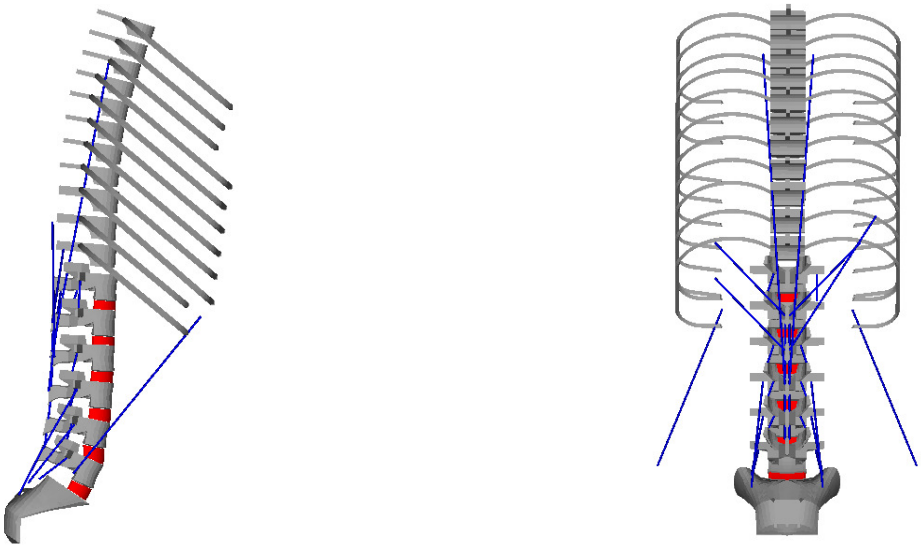

A) Lateral view of muscle recruitment B) Lateral view of muscle recruitment

Figure 6-3 Muscles to produce follower load on the spine in Flexion 10° (sway of trunk CG : 2.0 mm under MFC 45 N/cm^2)

6.1.2 CFLs in flexion 20° (MFC = 45 N/cm^2)

In flexion 20°, the minimum CFLs ran FLP at η = 15 mm (anterior margins of the vertebral bodies). Predicted CFLs ranged from 557 N at L2-L3 to 649 N L5-Sac joint as shown in Figure 6-4. the number of activated long and intermediate muscles were 17 out of 178, which were mostly internal oblique and various longissimus fascicles, while 17 out of 54 short intrinsic muscles were activated to create minimum CFLs. FE analysis, however showed that the application of these MFs produces an unstable deformation of the lumbar spine.

While, the predicted CFLs were 620 N at T12-L1, 624 N at L1-L2, 623 N at L2-L3, 667 N at L3-L4, 729 N at L4-L5 and 778 N at L5-Sac joint and magnitude of CFLs between the case of minimum CFLs. Figure 6-4 shows the CFLs at all lumbar levels

predicted from both cases along the FLP at η = 15 mm (minimum case) and along the FLP at η = 0 mm (stabilized case).

MFs that produce a stable deformation in the lumbar spine were those creating CFLs along the FLP at η = 0 mm (base spinal curve). The sway of trunk GC less than 3 mm was predicted in response to the application of these MFs and the upper body weight from the FE analysis. The recruited muscles in this case included 17 long and intermediate muscles (internal oblique and longissimus fascicles) and 15 short and intrinsic muscles as shown in Figure 6-5.

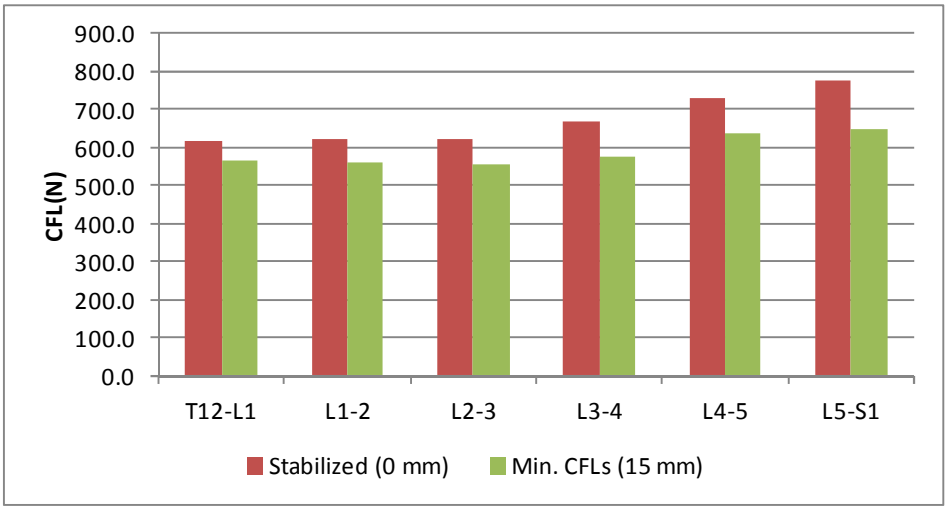

Figure 6-4 CFL on different levels in flexion 20°

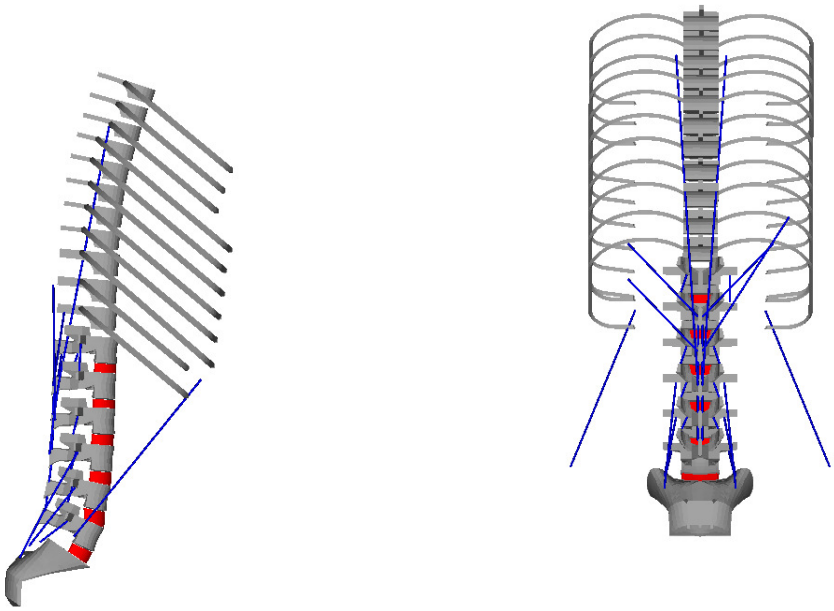

A) Lateral view of muscle recruitment B) Lateral view of muscle recruitment

Figure 6-5 Muscles to produce follower load on the spine in flexion 20° (sway of trunk CG : 1.8 mm under MFC 45 N/cm^2)

6.1.3 CFLs in flexion 40° (MFC = 45 N/cm^2)

The optimization model predicted the minimum CFLs along FLP at η = 15.0 mm in the lumbar spine flexed by 40°. The predicted CFLs ranged from 860 N at L2-L2 to 892 N at L5-Sac joint as shown in Figure 6-6. Activated back muscles included 21 long muscles (Longissimus, Serratus, Quadratus lumborum and internal oblique) and 18 intrinsic muscles (interspinales, intertransversari and rotatores). However, these MFs creating the minimum CFLs were found to produce an unstable deformation of the lumbar spine in the FE analysis as predicted in the case of flexion 20°.

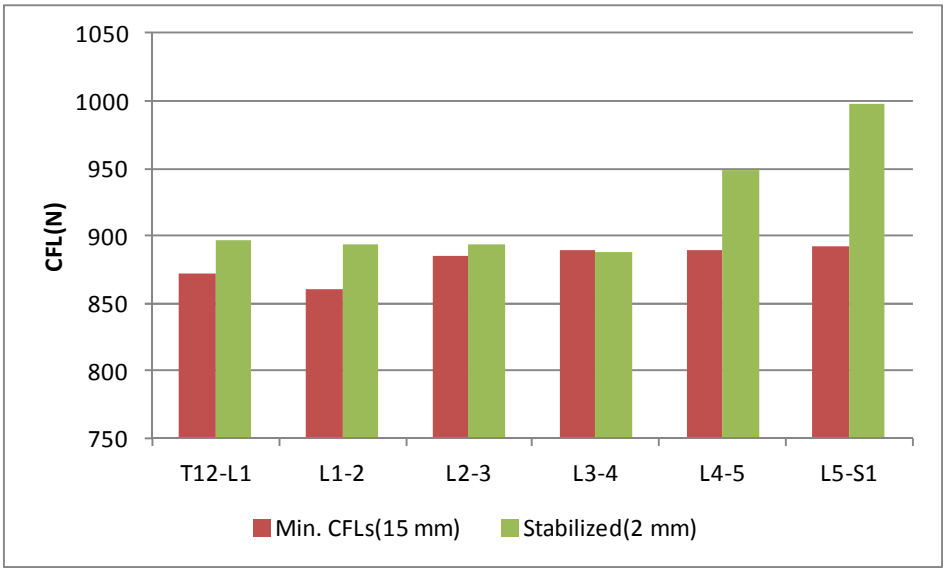

Figure 6-6 CFL on different levels in flexion 40°

The MFs producing a stable deformation of the lumbar spine were found when they created the CFLs along the FLP at $\eta = 2.0$ mm. The predicted CFLs in this stable deformation case were 896 N at T12-L1, 893 N at L1-L2, 893 N at L2-L3, 887 N at L3-L4, 949 N at L4-L5 and 997 N at L5-Sac joint as shown in Figure 6-6 in comparison with the minimum CFLs in all lumbar levels. 22 long and intermediate muscles and 20 short and intrinsic muscles produced a stable deformation (less than 2 mm sway of the trunk CG) are shown in Figure 6-7.

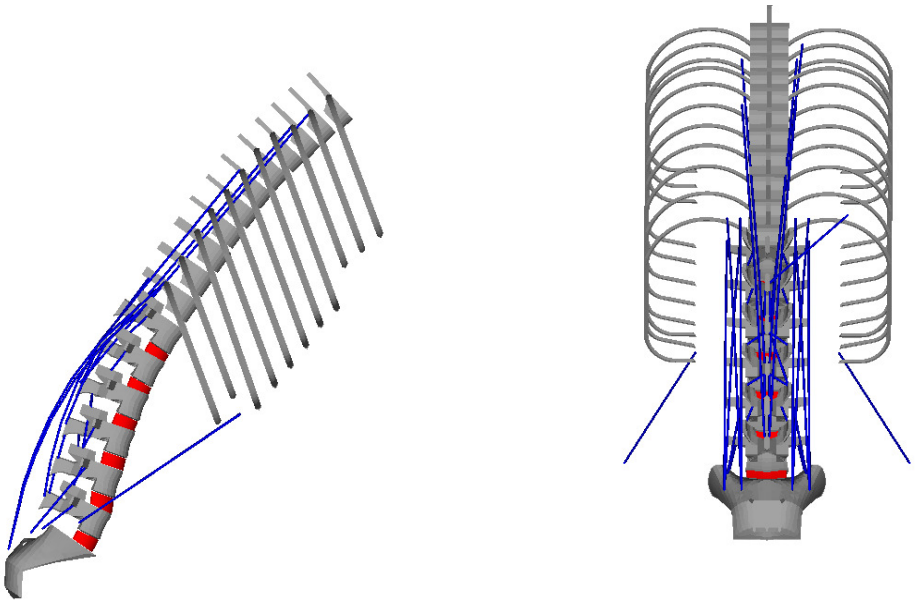

A) Lateral view of muscle recruitment B) Lateral view of muscle recruitment

Figure 6-7 Muscles to produce follower load on the spine in flexion 40° (sway of trunk CG : 1.1 mm under MFC 45 N/cm^2)

6.1.4 CFLs in extended 5° and 10° (MFC = 45 N/cm^2)

The optimization model predicted the minimum CFLs along FLP at η = -23.1 mm in the lumbar spine extended by 5°. The predicted CFLs in this stable deformation case were 685 N at T12-L1, 658 N at L1-L2, 561 N at L2-L3, 479 N at L3-L4, 609 N at L4-L5 and 616 N at L5-Sac joint. Activated back muscles included 22 long muscles (Latissimus dorsi, multifidus, and longissimus) and 18 intrinsic muscles (interspinales, intertransversari and rotatores).

On the other hand, minimum CFLs predicted by the optimization model along FLP was located at η = -30.0 mm in the lumbar spine extended by 10°. The predicted CFLs in this stable deformation case were 1086 N at T12-L1, 1083 N at L1-L2, 858 N at

L2-L3, 767 N at L3-L4, 823 N at L4-L5 and 901 N at L5-Sac joint. Activated back muscles included 51 long muscles (Latissimus dorsi, external oblique, multifidus, and longissimus) and 20 intrinsic muscles (interspinales, intertransversari and rotatores). However, in case of both extended 5° and 10° , these MFs creating the minimum CFLs were found to produce an unstable deformation of the lumbar spine in the FE analysis regardless FLP variation.

6.2 Stability under the lowest MFC in various postures

Another aspect that should be investigated was the effect of variations in MFC values on the MFs and CFLs in the spine in various sagittal postures. In this section, the effects of MFC variations from 10 to 45 N/cm^2 were investigated for the cases of neutral standing and flexed posture to determine the lowest MFC under which condition CFL-creating MFs can produce the stable deformation of the spine. In cases of extended postures, in contrast, the effect of MFC values greater than 45 N/cm^2 was investigated because the spinal muscles with MFC of 45 N/cm^2 were found able to create CFLs but not to produce the stable deformation of the lumbar spine.

6.2.1 Stability in neutral standing posture

When MFC was 30 N/cm^2, the minimum CFLs were found to be created along the FLP at η = -11.38 mm in a neutral standing posture. The predicted CFLs ranged from 488N at L3-L4 to 601N at L5-Sac joint as shown in Figure 6-8. The spinal muscles needed to create such CFLs including 14 long and intermediate muscles (only latissimus dorsi and longissimus), and 22 short and intrinsic muscles (intertransversarii, rotatores and interspinales).

As found in the previous case under MFC = 45 N/cm^2, the spinal muscles with MFC of 30 N/cm^2 were able to produce a stable deformation of the lumbar spine when

they created CFLs along the FLP at η = 0 mm. The predicted CFLs in such a case were 1031 N at T12-L1, 1068 N at L1-L2, 1033 N at L2-L3, 1078 N at L3-L4, 1157 N at L4-L5 and 1178 N at L5-Sac joint as shown in Figure 6-8 (green bars).

In contrast to the corresponding case with MFC = 45 N/cm^2, 56 muscles out of 232 muscles had to be recruited to support the upper body in a stable manner. The activated muscles were 24 long and intermediate muscles and 32 short and intrinsic muscles as shown in Figure 6-9. Such recruitment of more muscles were found to dramatically increase the CFLs at all lumbar levels not only from those predicted in case of MFC = 45 N/cm2 but also from the minimum CFL case as shown in Figure 6-8. It was also interesting that, even though stable, the sway of trunk CG was greater in case of MFC = 30 N/cm^2 than in the case of MFC = 45 N/cm^2 (4.5 mm vs. 0.7 mm). These results indicate that the weakness in back muscles may increase the spinal loads significantly and make the stability control more difficult.

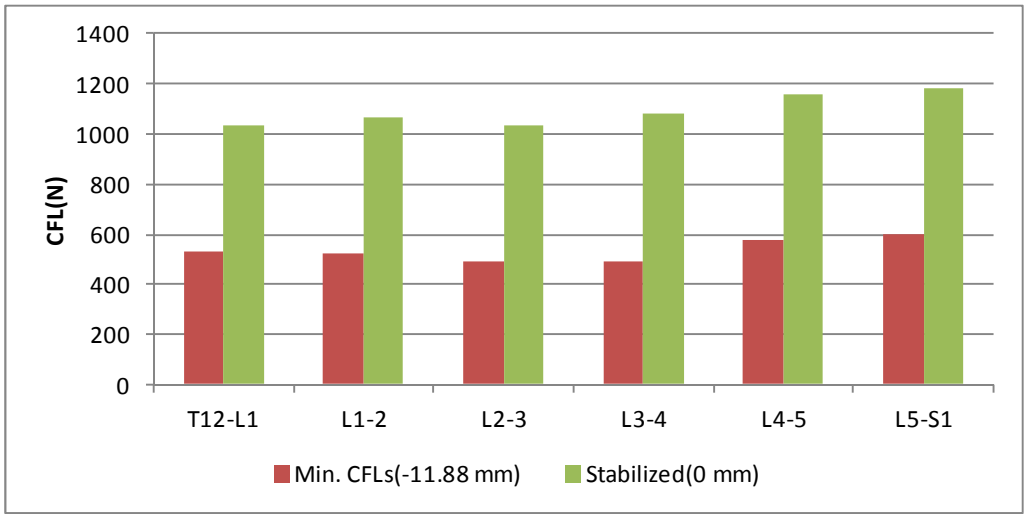

Figure 6-8 CFL on different levels in neutral posture under MFC 30 N/cm^2

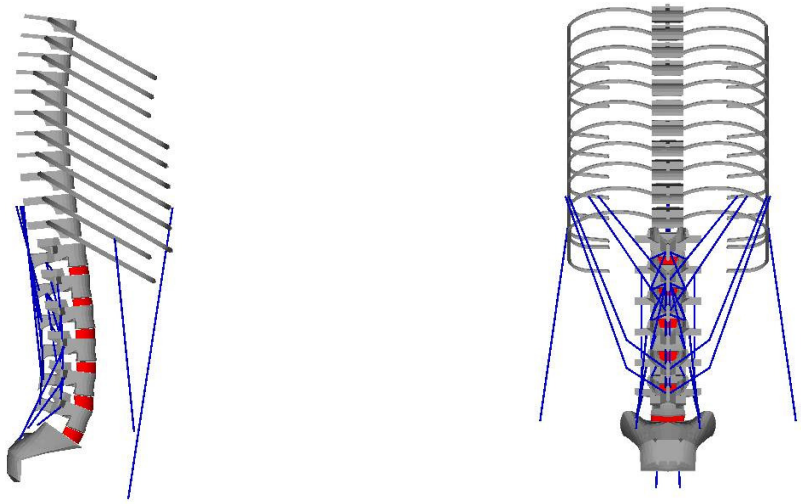

A) Lateral view of muscle recruitment C) Lateral view of muscle recruitment

Figure 6-9 Muscles to produce follower load on the spine in neutral posture (sway of trunk CG : 4.5 mm under MFC 30 N/cm^2)

6.2.2 Stability in flexed 10°

When MFC was 10 N/cm^2, the minimum CFLs were found to be created along the FLP at η = -3.8 mm in flexion 10°. The predicted CFLs ranged from 553N at L2-L3 to 686N at L5-Sac joint as shown in Figure 6-10. The spinal muscles needed to create such CFLs include 29 long and intermediate muscles (latissimus dorsi, external oblique, internal oblique, longissimus, iliocostalis, and multifidus), and 19 short and intrinsic muscles (intertransversarii, rotatores and interspinales).

The spinal muscles with MFC of 10 N/cm^2 were able to produce a stable deformation of the lumbar spine when they created CFLs along the FLP at η = -1.3 mm. The predicted CFLs in such a case were 554 N at T12-L1, 556 N at L1-L2, 553 N at L2-L3, 581 N at L3-L4, 650 N at L4-L5 and 686 N at L5-Sac joint as shown in Figure 6-10 (green bars).

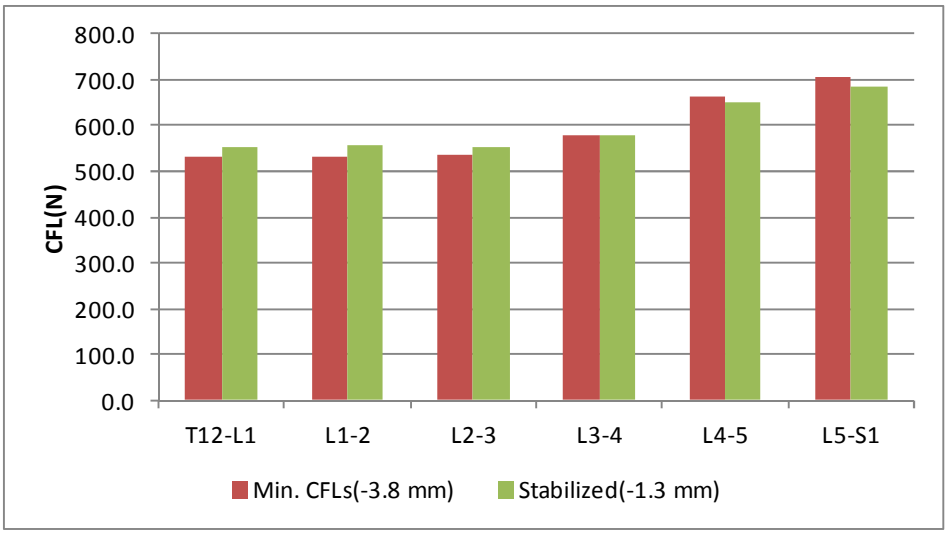

Figure 6-10 CFL on different levels in flexion 10° under MFC 10 N/cm^2

A total of 48 muscles out of 232 muscles were recruited to support the upper body in a stable manner. The activated muscles were 26 long and intermediate muscles and 22 short and intrinsic muscles as shown in Figure 6-11. The sway of trunk CG in flexion 10° was 4.3 mm in the case of MFC = 10 N/cm^2.

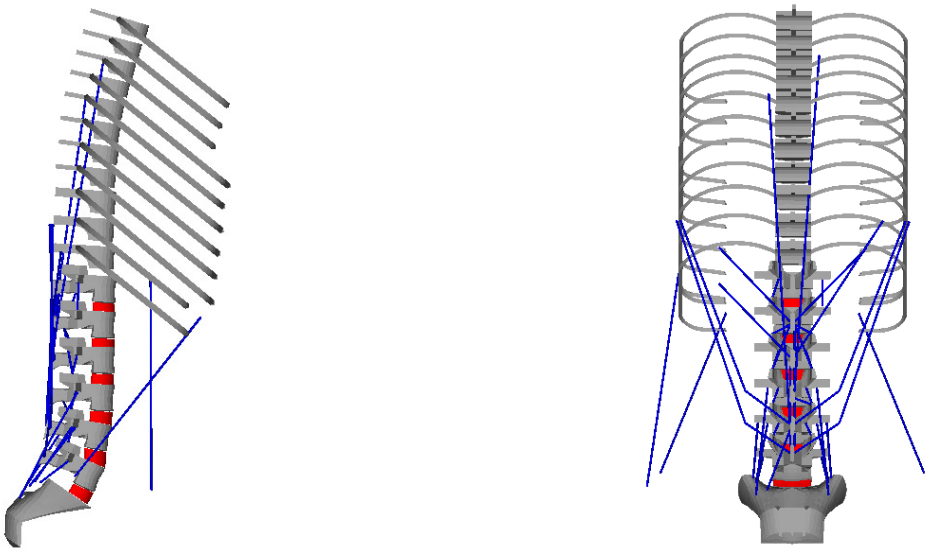

A) Lateral view of muscle recruitment B) Lateral view of muscle recruitment

Figure 6-11 Muscles to produce follower load on the spine in flexion 10° (sway of trunk CG : 4.3 mm under MFC 10 N/cm^2)

6.2.3 Stability in flexed 20°

When MFC was 10 N/cm^2, the minimum CFLs were found to be created along the FLP at η = 15.0 mm in flexion 20°. The predicted CFLs ranged from 592N at T12-L1 to 658 N at L5-Sac joint as shown in Figure 6-12. The spinal muscles needed to create such CFLs include 24 long and intermediate muscles (serratus, latissimus dorsi, internal oblique, longissimus, and multifidus), and 25 short and intrinsic muscles (intertransversarii, rotatores and interspinales).

The spinal muscles with MFC of 10 N/cm^2 were able to produce a stable deformation of the lumbar spine when they created CFLs along the FLP at η = 0.0 mm. The predicted CFLs in such a case were 644 N at T12-L1, 641 N at L1-L2, 641 N at L2-

L3, 671 N at L3-L4, 751 N at L4-L5 and 785 N at L5-Sac joint as shown in Figure 6-12 (green bars).

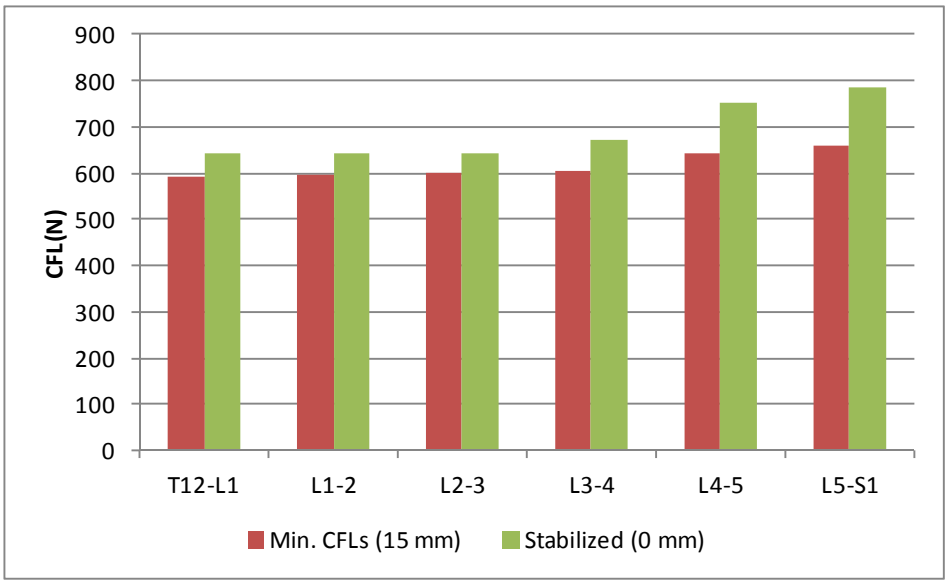

Figure 6-12 CFL on different levels in flexion 20° under MFC 10 N/cm^2

54 muscles in total out of 232 muscles were recruited to support the upper body in a stable manner. The activated muscles were 31 long and intermediate muscles and 23 short and intrinsic muscles as shown in Figure 6-13. The sway of trunk CG in flexion 20° was 2.6 mm in the case of MFC = 10 N/cm^2.

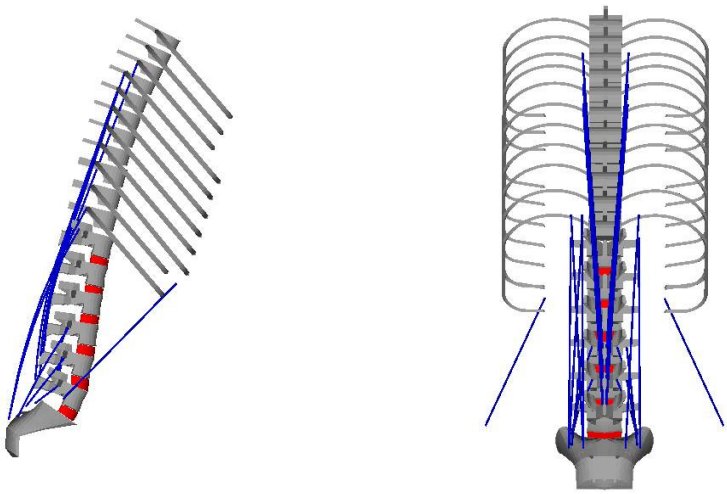

A) Lateral view of muscle recruitment B) Lateral view of muscle recruitment

Figure 6-13 Muscles to produce follower load on the spine in flexion 20° (sway of trunk CG : 2.6 mm under MFC 10 N/cm^2)

6.2.4 Stability in flexed 40°

The minimum CFLs were found to be created along the FLP at η = 15.0 mm in flexion 40°, when MFC was 10 N/cm^2 . The predicted CFLs ranged from 929N at T12-L1 to 1104 N at L5-Sac joint as shown in Figure 6-14. The spinal muscles needed to create such CFLs include 48 long and intermediate muscles and 23 short and intrinsic muscles.

As found in the previous case under MFC = 45 N/cm^2 , the spinal muscles with MFC of 10 N/cm^2 were able to produce a stable deformation of the lumbar spine when they created CFLs along the FLP at η = 2.0 mm. The predicted CFLs in such a case were 978 N at T12-L1, 996 N at L1-L2, 1012 N at L2-L3, 1010 N at L3-L4, 1072 N at L4-L5 and 1113 N at L5-Sac joint as shown in Figure 6-14 (green bars).

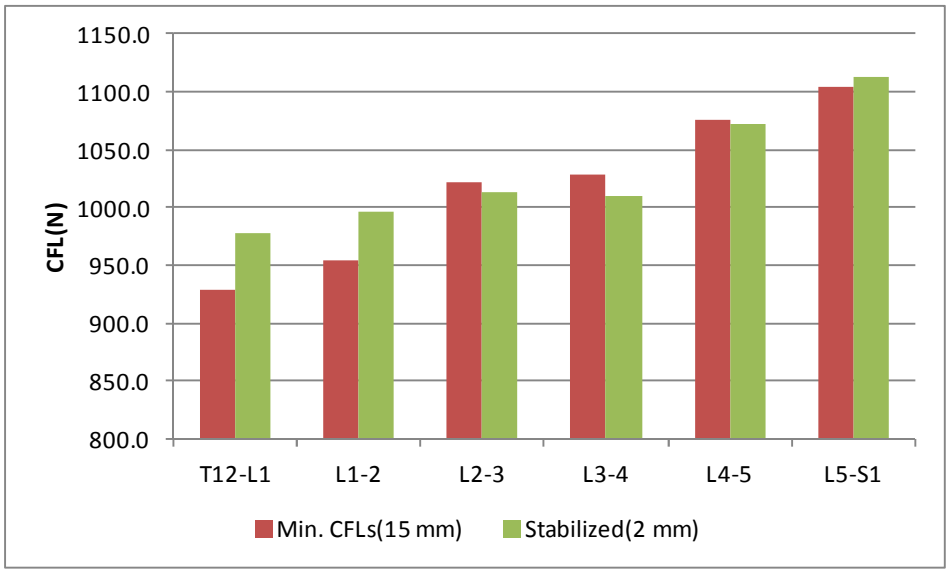

Figure 6-14 CFLs at different levels in flexion 40° under MFC 10 N/cm^2

In contrast to a corresponding case with MFC = 45 N/cm^2, 83 muscles out of 232 muscles had to be recruited to support the upper body in a stable manner. The activated muscles were 52 long and intermediate muscles and 31 short and intrinsic muscles were recruited as shown in Figure 6-15. The recruited muscles were able to stabilize the lumbar spine within 2 mm sway of the trunk CG.

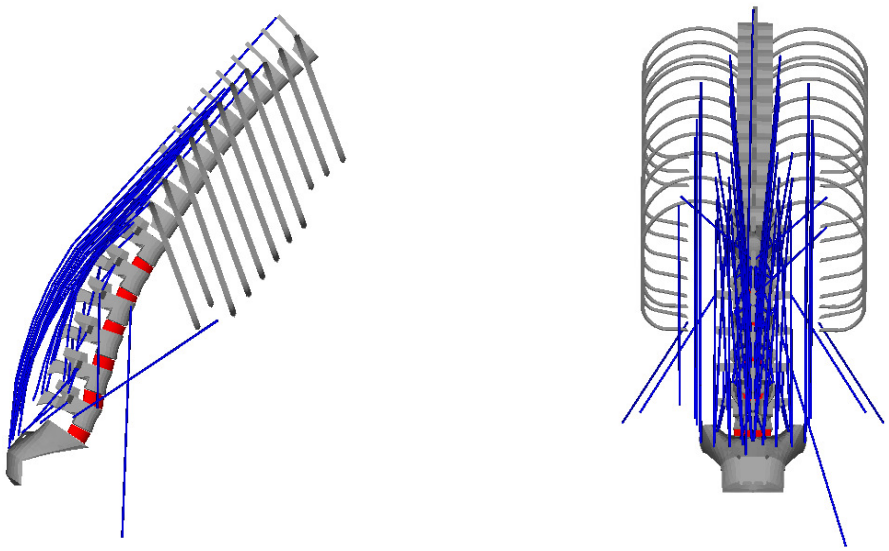

A) Lateral view of muscle recruitment B) Lateral view of muscle recruitment

Figure 6-15 Muscles to produce follower load on the spine in flexion 40° (sway of trunk CG : 1.5 mm under MFC 10 N/cm^2)

6.2.5 Stability in extension 5°

Through numerous trials, it was possible to determine the MFC of 70 N/cm^2. under the MFC 70 N/cm^2, the optimum solutions of MFs produced the stable deformation of the lumbar spine extended by 5°. In this case of MFC = 70 N/cm^2, the minimum CFLs were found along the FLP at η = -18.09 mm by the activation of 32 muscles (11 long and intermediate muscles of latissimus dorsi and longissimus and 21 short intrinsic muscles of intertransversarii, rotatores and interspinales).

The predicted minimum CFLs ranged from 397N at L3-L4 to 705 N at L5-Sac joint as shown in Figure 6-16. MFs creating these CFLs, however, were found to produce an unstable deformation of the lumbar spine.

In contrast, the spinal muscles with MFC of 70 N/cm^2 were able to produce a stable deformation of the lumbar spine in 5° extension when they created CFLs along the FLP at η = -1.0 mm. The predicted CFLs in this case were 1257 N at T12-L1, 1315 N at L1-L2, 1223 N at L2-L3, 1224 N at L3-L4, 1301 N at L4-L5 and 1334 N at L5-Sac joint as shown in Figure 6-16 (green bars). The spinal muscles activated in this case include 17 long and intermediate muscles and 31 short and intrinsic muscles, and these muscles are shown in Figure 6-17. The stable deformation of the extended lumbar spine was found to result in the 4.8 mm sway of the trunk GC.

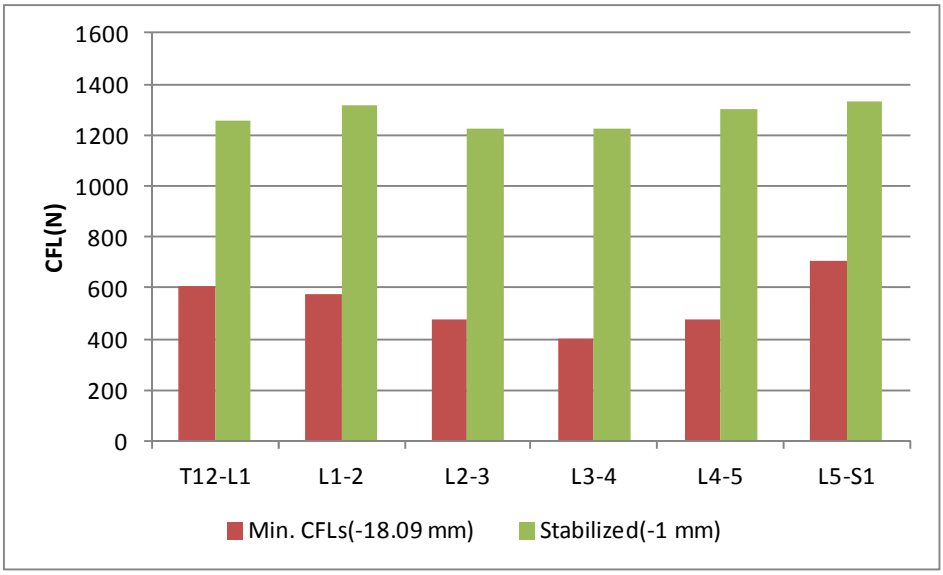

Figure 6-16 CFL on different levels in extension 5° under MFC 70 N/cm^2

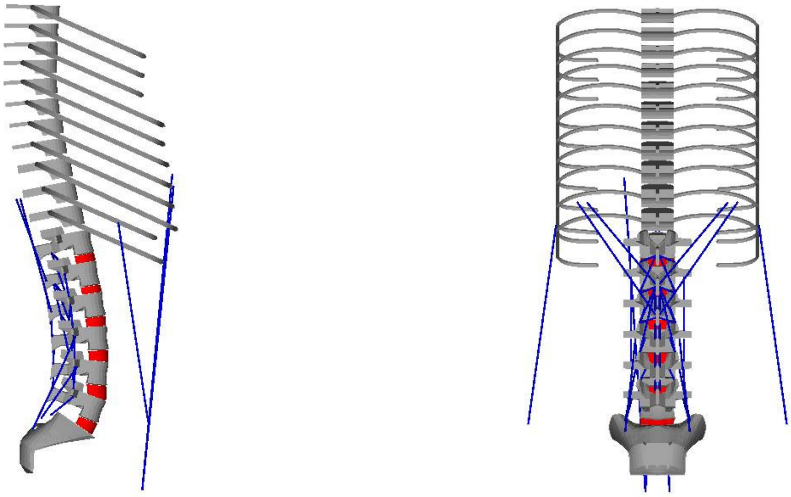

A) Lateral view of muscle recruitment B) Lateral view of muscle recruitment

Figure 6-17 Muscles to produce follower load on the spine in extension 5° (sway of trunk CG : 4.8 mm under MFC 45 N/cm^2)

CHAPTER 7
DISCUSSION

The basic biomechanical functions of the spine are to support the body weight and external loads without buckling (stability) and to allow upper body movement (flexibility). In general, it is challenging to design a mechanism that maintains both functions since higher stability restraints flexibility. However, it is widely accepted that the mechanically contradicting functions of the spine are achieved *in vivo* by the spinal muscles. The spinal muscles stabilize the ligamentous spinal column which is inherently unstable due to its long and flexible features. As the lumbar spine is the only linkage which connect the upper body and sacrum, the kinematics of lumbar spine is likely to be one of the major contributors to normal spinal functions [72].

In numerous biomechanical studies [2, 12, 15, 73-78], the stabilizing roles of spinal muscles have been investigated analytically and experimentally. For example, biomechanical investigators developed analytical models of the spinal column and muscles to determine the stability index of the spine based upon the underlying theory that a conservative mechanical system must be stable when the system is in mechanical equilibrium and its stability index is greater than zero. Stability index is a sophisticated way to quantify the stability of the human spinal system based on "the hypothesis that the lumbar spine normally is stabilized in response to small disturbances from the maximum effort state by the stiffness of the spinal musculature" [27]. In all of these studies, the stability index was found to be positive regardless of the trunk postures and movements,

indicating that the lumbar spine is stable with the spinal muscle forces (MFs) in any of the investigated conditions. However, the major drawback of these previous studies was that their results did not improve our understandings of how the activities of spinal muscles are controlled for the maintenance of the spinal stability *in vivo.* Another limitation of these studies was that they had no incorporation of the activities of numerous intrinsic short segmental muscles, such as rotatores, intertransversari, and interspinales, which are known to exist and play a significant role in maintaining the stability of the whole lumbar spine [16].

Meanwhile, Patwardhan et al. [4, 34] recently reported interesting results of *in vitro* biomechanical tests of the lumbar spine under a compressive follower load (CFL) that turns its direction so as to always remain tangential to the deflection curve (lumbar lordosis). Their experimental results showed that the ligamentous lumbar spine can sustain a large compressive load without buckling while maintaining its flexibility reasonably well, when the compressive load is applied in a follower force pattern. Other investigators [79, 80] also have successfully used the follower load in simulating a high physiological compressive load on the ligamentous spine without buckling during various *in vitro* biomechanical tests of the spine. These experimental results suggest that the spine may be subjected to the CFL *in vivo* to maintain its stability while maintaining flexibility.

Computational studies of the CFLs also have been reported to investigate if the follower load can be created in the spine by human spinal musculature. Patwardhan et al. [81] conducted an analytical study using a continuum model of the spine and showed that

trunk muscles may co-activate to generate a follower load. However, they simulated the spinal muscles as 5 different hypothetical muscle architecture, and their results were not sufficient to figure out the contribution of individual muscles making the follower load.

Another disadvantage of Patwardhan et al's study was that they investigated the spinal stability in the coronal plane although the stabilization of the spine would be more challenging in the sagittal plane than in the coronal plane because of the lordosis and more concentration of spinal muscles in the posterior aspect of the spine. Kim and Kim [82] also recently investigated using a finite element model of the spine with the spinal muscles in greater detail including short intrinsic muscles the feasibility of the follower load creation in the spine in a standing posture but failed to create the follower load using spinal MFs in the sagittal plane. On the other hand, using an optimization of the lumbar spinal system incorporating 232 spinal forces including short intrinsic muscles, Han et al. [83, 84] showed that there could be numerous combinations of spinal MFs creating a CFL in the lumbar spine in various sagittal postures. They also investigated the effect of increasing external compressive force and flexion moment applied on the lumbar spine and found that the back muscles could create CFLs in the lumbar spine while supporting not only the upper body weight but also a considerable amount of external loads [5, 85].

The results of the above studies clearly suggested that the CFL could be a physiological spinal load and spinal muscles may be controlled to create CFLs in the spine by the central nervous system *in vivo* in order to maintain the spinal stability. Complete tests of this hypothesis are extremely challenging due to the practical limitations in experimental studies of spinal muscles. However, one of the logical steps

of such tests would be to study the deformation of the lumbar spine resulting from the spinal MFs creating CFLs in the lumbar spine in relation to the spinal stability using a finite element (FE) technique. In this study, a 3-D FE and optimization models of the lumbar spine, sacrum, the trunk (upper body connected to the L1 through T12-L1), and 232 spinal muscles attached to the appropriate bony elements were developed and used interactively for this purpose.

7.1 Validation of the 3-D FE model and synchronization of the optimization with the FE model

The validation of the computational models and methods was essential to the reliability of the model predictions. Although complete experimental validation of these computational studies were not practical, it was possible to validate and the FE model predictions and the optimization formulation at least in part in the following ways.

The validity of the FE model was confirmed by comparing the FE model predictions with various experimental results.. For example, the comparison of FE model predictions with in-vitro range of motions (ROMs) of ligamentous lumbar spine without physiological preload during flexion and extension (section 4.2) showed an excellent agreement not only in the ROMs of the lumbar spine but also in the segmental ROMs in all lumbar levels.

The validity of the 3-D FE model of the multi-segment lumbar spine (S1-L1) under physiological load was also confirmed by using flexion-extension ROMs of the lumbar spine under physiological preload (CFL of 800 N) in measured in the previous

study [37]. The ROMs predicted from the FE model simulating the in vitro flexibility tests under the follower load demonstrated a good agreement with those measured in the experiment as presented in 4.2. Figure 4-6 showed the predicted FE results of flexion and extension range of motion (ROM) of the lumbar spine compared with *in vitro* experiment. The ROM with preload (39.0°) was only 20% smaller than the ROM without preload (49.7°) in the previous study and this was predicted from FE model (47.1° and 41.8° respectively). Especially, the ROMs of stiffened intervertebral disc (IVD) for 3-D *in vivo* FE model fell within one standard deviation at all levels, and the total flexion-extension ROM (33.7 @ S1-L1) also fell within one standard deviation. As such, the 3-D FE model developed in this study may be reliably used not only for simulating the spinal system in vivo and but also studying the follower load mechanism in the spinal system. Another possible way to validate the current 3-D FE model was to compare the model predictions of compressive follower loads (CFLs) with the corresponding spinal compressive load measured in previous *in vivo*, *ex vivo* and *in vitro* experiments [1, 8, 80, 86, 87]. For example, while standing at ease, the compressive load at the L3-L4 joint predicted from the FE model (compressive follower load (CFL) along the follower load path (FLP) at η = 0 mm) was 682.7N, whereas the range from in vitro and in vivo experiments ranged from 500N to 800N. Meanwhile, the predicted CFLs on the L3 disc in the flexed spine (667N in 20° flexion and 888 N in 40° flexion) also agreed well with those (600N in 20° flexion and 1000 N in 40° flexion) measured in vivo by Nachemson. Considering the possible variations in the spinal load depending on the changes in muscle strength, muscle orientations with respect to the spinal column, and the spinal lordosis from

individual to individual, , the discrepancy between the CFLs predicted from the 3-D Fe model and measured in previous studies might be ineluctable, and the FE model predictions of this study look physiological.

The validity of the optimization formulation was also investigated by comparing the CFL vectors obtained from the optimization analyses with those predicted from the FE model in response to the application of muscle forces (MFs) obtained from the optimization analysis as presented in section 5.4. The outstanding agreement in those CFLs (less than 1% not only in the magnitudes and the directions) clearly demonstrate that there was no flaw in the optimization formulations because both the optimization and FE solvers used in this study were a commercial software package whose validity has been well known.

7.2 Limitation of current biomechanical study

The major limitation of this study in proving the hypothesis of lumbar spine stabilization by spinal muscles via CFL mechanism was that the lumbar spine only in sagittal postures was investigated in this study while the spine is certainly a dynamic 3-D structure.

As a first step, the lumbar spine in various static postures was investigated in this study because of two reasons. Firstly, the sagittal posture was selected because the maintenance of the stability should be most challenging due to the geometry of human body (more spinal muscles in the posterior side of the spine, trunk weight applied on the anterior side of the spine and the midsagittal symmetry). The study of the spine in a static posture was selected not only because it is much simpler than the dynamic study but also

because the maintenance of the spinal stability in a static posture would be more challenging than that during a motion.

Thus, the results of this study are likely to be physiologically meaningful and sufficient to predict the stabilizing roles of back muscles *via* a follower load mechanism. However, further studies of the spine in 3-D postures during a motion are required, and the studies of muscle activities for stabilizing the lumbar spine in other static postures, such as lateral bending and axial rotation by creating CFLs are the topics of our current investigations using the same computational methods.

Another limitation of the current study was lack of validation of muscle activities for stabilizing the lumbar spine in various postures, such as flexed or extended posture. The solution convergence was checked in every solution case, which suggested that spinal muscles be able to produce the follower load in neutral and every flexed posture under muscle force capacity (MFC) of 45N/cm^2.

However, the muscle activation patterns, the magnitude of muscle force (MF) information *in vivo* were currently impractical to approach and should be further investigated for the improvement and the full validation of the 3-D FE model to support hypothesis that the spine is stabilized *in vivo* through a follower load mechanism created by spinal muscles. This is a common limitation in all analytical and/or experimental studies of spinal muscles. There is an eminent need for the development of new methods to quantify the MFs and diagnose the muscle strength and the contraction patterns.

Finally, it is important to understand that the FE models of this study were formulated and validated to investigate the load-displacement behaviors of the lumbar spine and/or lumbar spinal segments. More realistic detail simulation of the intervertebral discs, facet contacts, ligaments and bones was possible but not made in our models in order to reduce the computational cost. Therefore, only model predictions

related with the load-displacement behavior were valid and presented in this study. Further refined models are required to obtain the reliable information of the stresses and strains in the spine under the physiological loads (upper body weight and CFL creating MFs) predicted in this study.

7.3 Innovative features in current biomechanical study

Despite a few limitations, major contributions of this study to the field of spine research can be found in the following aspects:: 1) modeling of the intrinsic short muscles (rotatores, intertransversari, etc.) which have never been explicitly simulated in the previous studies; 2) FE analyses of the lumbar spine under the upper body weight and CFL creating MFs; and 3) offering a computational tool for improving the current understandings of the follower load mechanism in the spine.

The stabilizing roles of intrinsic short muscles have been suggested by some investigators [16] but never been studied separately. The intrinsic short muscles were simulated for the first time in this optimization and FE studies of the spinal system. The forces in the intrinsic short muscles were found to be crucial for CFL creation by spinal muscles (see Appendix D). If the CFL were the physiological *in vivo* spinal load as postulated by Patwardhan et al. [4, 37], the existence of healthy intrinsic short muscles would be one of the most critical requirements to prevent the occurrence of abnormal loads in the spine. Further studies of the biomechanical effects of these short MFs on the spinal stability are required to improve the current clinical treatment to spinal instability and low back pain. In addition, no FE models of the whole lumbar spine that simulate the

stable standing of the lumbar spine under the upper body weight only by the spinal MFs have been introduced in the literature.

Another innovation of this study would be the introduction of a versatile computational tool for the study of the follower load in the spine. The development of an experimental method to apply a CFL on the ligamentous spine opened the way to test the spine under a physiological compressive load. However, the use of two wires following the spinal curve on the right and left lateral sides of the spine was found to produce a large artifact particularly when the spine is subjected to the lateral bending or axial rotational moment. During such a rotation in the coronal or transverse plane, the wire tensions were found to produce moments of which magnitude cannot be well quantified. Because of this artifact, the flexibility tests of the spine under a physiological CFL have been valid only in flexion and extension motion. Furthermore, a few computational studies of the follower load in the spine in the literature have not been as comprehensive as this study. For example, the spine was simulated as a rigid link system in some FE studies with MFs with the incorporation of the limited number of spinal muscles. An optimization study simulating all intrinsic short muscles showed the possible combination of MFs producing CFLs but provide no further information on the effect of those MFs on the spinal deformation.

The computational models and analysis methods introduced in this study were found useful to obtain excellent insights into the CFLs in the lumbar spine. Although the studies conducted in this study was limited to the studies of CFLs and MFs in the lumbar spine in various static sagittal postures, the current computational approach can be easily

extended to the study of the CFLs in the lumbar spine in other postures, such as lateral bending, axial rotation, and/or combined 3-D bending postures. Furthermore, the FE models used in this study were formulated for both static and dynamic analyses and have great potential to provide a valuable tool for studying the roles of back muscles in controlling the dynamic motion of the upper body in a stable manner.

7.4 Interpretation of results

The feasibility of optimum solutions of MFs, joint reaction forces (CFLs), and FLP location for all studied sagittal postures indicate that it is be possible to create CLFs by using the spinal MFs in the lumbar spine. However, it was also found in the FE analyses that some CFLs can produce the lumbar spine deformation large enough to cause a significant sway of the trunk (> 10 mm) depending upon the location of the CFLs as shown in Figure 5-1.

The stable deformation (resulting in the trunk sway < 10 mm) of the lumbar spine in a neutral or flexed posture was found only by MFs creating CFLs along a FLP in the vicinity (about ± 2 mm) of the base spinal curve (FLP at η =0 mm) established by connecting the GCs of the vertebral bodies when the MFC was 45 N/cm^2. In the extended postures, in contrast, the MFs created CFLs along a FLP located within the range from η = -30 mm to-13 mm in 5° extension and from η = -30 mm to η = -25 mm in 10° extension, and these MFs were found to produce unstable deformation of the extended lumbar spine.

These results suggest that CFLs should be created along an FLP nearby the base spinal curve for the stability of the lumbar spine in a neutral or flexed posture. The maintenance of an extended spine in a stable manner using a CFL mechanism may require stronger back muscles as shown in the parametric study of the effect of MFC variation. This may explain the reason why a human can maintain a flexed posture longer with more comfort than an extended posture.

7.4.1 Variations in FLP location

In this study, a non-linear optimization method was used for the cases that FLP was not fixed. However in the case of fixed FLP, the moment arm in equation (1.3) was set to a certain constant and the non-linear optimization problem became a linear optimization problem. In this case, feasible space was convex and linear equality constraints were mutually independent. It was proven that the solution of such a linear optimization had to be unique with the cost function value of the global minimum.

The FLP is the location of the combined reaction force on each vertebra and its location changed the moment arm of CFLs. The location of FLP or combined reaction forces affected the load distribution on IVD and resulted in changing of stress distribution. The CFLs variation by changing the location of FLP's was shown in Figure 7-1. The predicted CFLs were obtained from the optimization model which was solved from the FLP at η = -30mm to the FLP at η = 10mm in a neutral standing posture under MFC 45N/cm^2. Figure 7-1 also showed that the CFLs increased steeply as the FLP shifted anteriorly from the center of vertebra body and deviated from the physiological range.

The FLP in neutral posture under MFC 45 N/cm^2 was in its optimum at FLP at η = 11.83 mm where the location of combined reaction forces shifted posteriorly parallel to the connected tangent line of the center of each vertebra. Though the CFLs were the lowest among the cases, the sway predicted by 3-D FE model of the center of gravity (CG) of upper body was the largest among cases. On the contrary, the sway of the CG on trunk in the case that the FLP at η = 0 mm was 1.4 mm and the smallest among cases. This result indicates that the lowest cost could not guarantee the maximum stability of the spine and the 3-D FE model could be powerful tool to evaluate the stability of the spine.

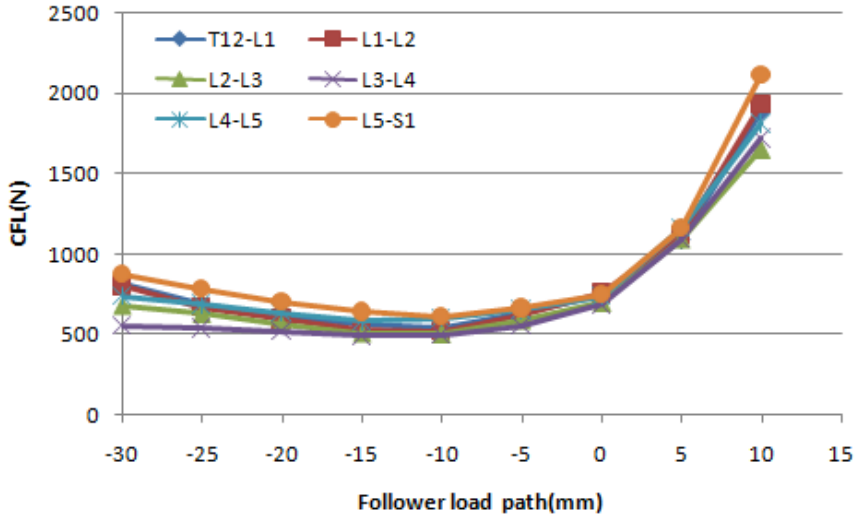

Figure 7-1 Variation in CFLs (N) at each level with respect to the FLP variation from the GCs of each vertebra. Negative x-value indicates the posterior shift from the center of vertebral body.

Meanwhile, to investigate the range of stability region and the relation between η and the sway of trunk CG near η = 0 mm in a neutral standing posture, η in the optimization model varied from 0 mm to ±2 mm at 0.5mm interval. In order to evaluate

the stability of spinal column within a certain range in a neutral standing posture, the sway of the trunk CG body was limited to 10 mm. If the sway of the trunk CG exceeded 10 mm either anteriorly or posteriorly, no further analysis was conducted. Muscles required to create CFLs in the neutral standing posture are listed in Table 7-1. In all cases, the latissimus dorsi (L1-Rib) generated the largest forces and the longissimus (Sa-L4) played critical role to create the CFLs in the lumbar spine.

Table 7-1 Recruited muscles which stabilized the lumbar spine in different FLP

FLP (η)	-1.0 mm	-0.5 mm	0 mm	0.5 mm	1.0 mm	1.5 mm
LatissimusDorsi_L1_RibHum	100.82	106.99	106.55	105.92	105.29	108.05
LatissimusDorsi_L2_RibHum	3.17	0.00	3.45	7.33	11.52	12.57
ExternalOb_Pel_Rib10	0.00	1.55	7.54	13.97	20.80	25.75
RecAbdominis_Pel_Rib7	45.08	47.07	47.33	47.59	47.89	49.10
Rotatores_L1_T12	45.00	45.00	45.00	45.00	45.00	45.00
Rotatores_L2_T12	45.00	45.00	45.00	45.00	45.00	45.00
Multifidus_L4L1_F4	29.40	42.29	39.10	35.37	31.44	28.85
Interspinales_L2_L1	10.00	4.49	6.62	9.06	11.66	0.00
Intertransversarii_L2_L1_La	0.00	0.00	0.00	0.00	0.00	30.20
Rotatores_L2_L1	45.00	45.00	45.00	45.00	45.00	45.00
Rotatores_L3_L1	45.00	45.00	45.00	45.00	45.00	45.00
Interspinales_L3_L2	32.32	26.04	30.83	36.19	41.92	45.00
Intertransversarii_L3_L2_Me	0.00	0.00	0.00	0.00	0.00	1.64
Rotatores_L3_L2	31.79	26.24	27.85	29.75	31.78	35.31
Interspinales_L4_L3	42.51	27.71	32.79	38.68	44.97	45.00
Intertransversarii_L4_L3_La	0.00	0.00	0.00	0.00	0.00	9.00
Intertransversarii_L4_L3_Me	29.25	44.67	45.00	45.00	45.00	45.00
Longissimus_Sa_L4	85.61	87.00	91.39	96.12	101.14	104.91
Interspinales_L5_L4	16.29	16.96	18.30	19.76	21.31	22.61
Intertransversarii_L5_L4_Me	45.00	45.00	45.00	45.00	45.00	45.00
Longissimus_Sa_L5	80.73	81.88	84.31	86.92	89.69	91.97
Number of recruited muscle (pairs)	17	17	18	18	18	20

The range of CFLs increases, as the FLP position moved away from the FLP at η = -1 mm as shown in Figure 7-2. In the case of FLP at η = -2 mm, -1.5 mm, 2 mm, FE model predicted that the sway of trunk CG exceeds 10 mm during standing quietly. Therefore, the cases of FLP at η = -2 mm, -1.5 mm, and 2 mm were considered not stable and removed from further FE analysis. The figure also showed that the predicted lumbar joint force was at its minimum in L3-4 level. It seemed that a number of long muscles were involved to satisfy the moment equilibrium on T12 induced by the trunk weight and it produced large reaction forces on T12-L1 level and L1-L2 level. Meanwhile, in case of lower levels such as L4-L5 level and L5-S1 level, a sudden change of curvature might be the main reason of activation of the longissimus and it generated the larger joint reaction forces.

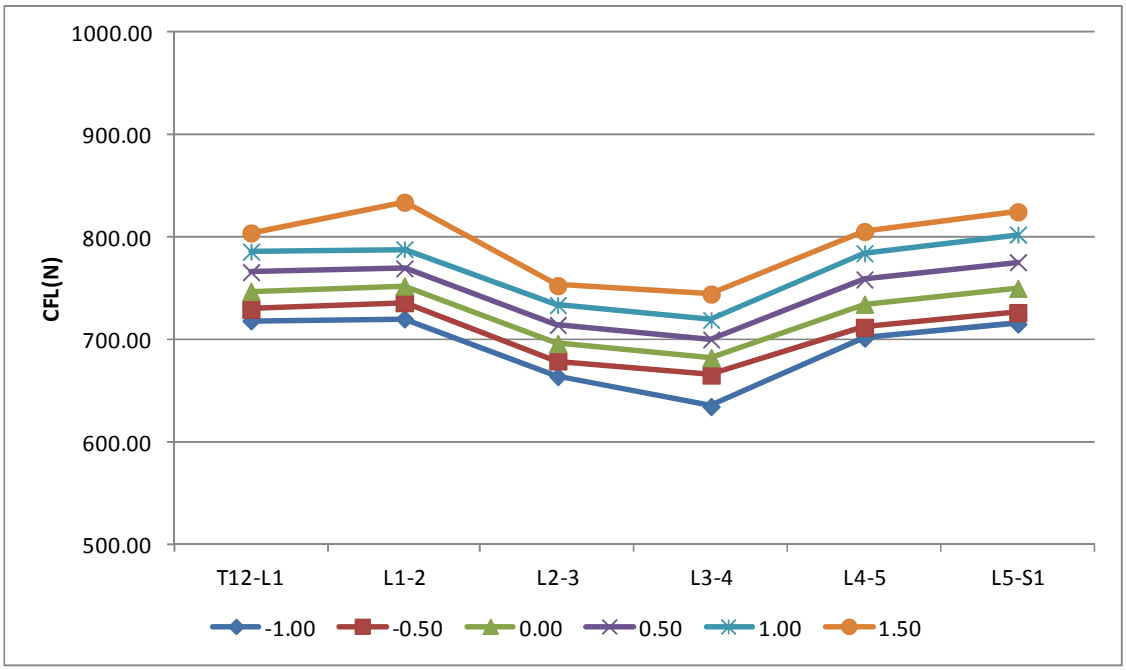

Figure 7-2 Comparison on CFLs in different levels to stabilize the lumbar spine

Figure 7-3 shows the predicted the sway of GC's of upper body resulting from the various MFs in response to FLP variation from η = -1 mm to η = 1.5 mm. MFs to create CFLs in FLP=0.5 mm under MFC 45 N/cm^2 produced the smallest sway of trunk CG among cases and the regression data showed that the lumbar spine was in its most stability near FLP at η = 0 mm. The lumbar spine model also showed that its range of stability under the criteria of less than 10 mm sway of the trunk CG was from FLP at η = -1mm to η = 1.5mm at the interval of 0.5mm investigation.

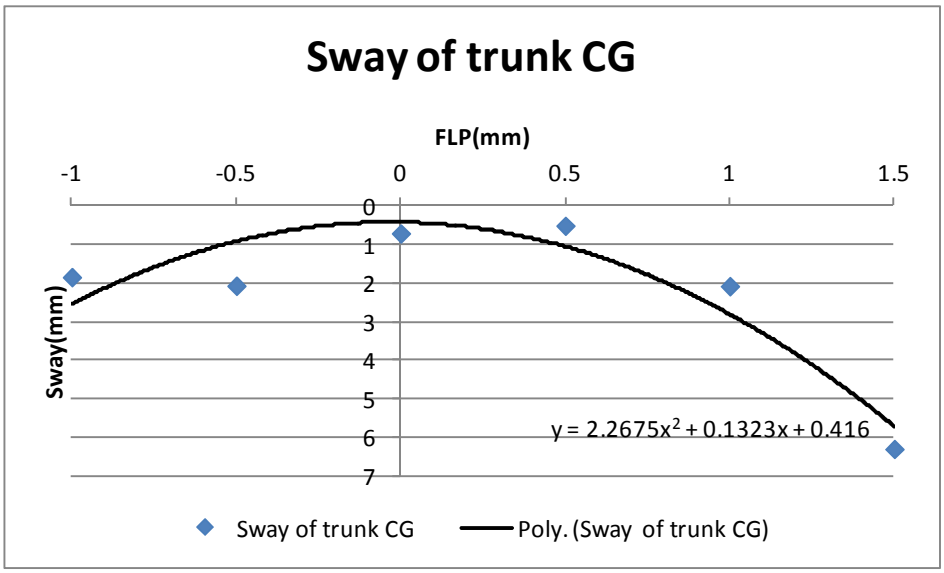

Figure 7-3 Range of FLP which stabilize the lumbar spine in a neutral posture under MFC 45 N/cm^2

7.4.2 Variation of MFC

The maximum muscle force of each muscle was generated by multiplying physiological cross section area (PCSA) of each muscle and muscle force capacity (MFC). In this study, the magnitude of MFC was proportional to maximum muscle force considering that PCSA of each muscle was constant and it represented the healthiness of back muscle. Previous study showed the feasibility that the CFL can be created by spinal muscles within the physiological range of MFC (0.1-0.9 N/cm^2) in all posture [5]. In a neutral standing posture, the relation between MFC (0.45 – 0.9 N/cm^2) and stability was evaluated.

The results of this study showed that the latissimus dorsi and the rectus abdominis were commonly activated on the thoracolumbar level to stabilize the upper body and

short muscles between L1 and L4 level played a crucial role in stabilizing the upper body in every case. Short muscles between L1 and L4 level might increase the stability of the lumbar spine by increasing the critical load on the lumbar spine. While, on L4 and L5 level of lumbar spine, the short fascicles of the longissimus seemed essential to creating the equilibrium of moment, since the lower part of the lumbar spine had a large spinal curvature.

This study also showed that the magnitude of CFL at each level decreased with greater MFC. However, the variation of the reaction forces at each level was less than 10%. Considering that FLPs on whole lumbar spine ran parallel to the curvature of the spine, CFL made compressive deformation on IVD and induced the sway of upper body. Thus CFLs in the case of MFC 90 N/cm^2 were smaller than those in the case of MFC 45N/cm^2 and the total sway of trunk CG in the case of MFC 90N/cm^2 induced by smaller MFCs was less than that of MFC 45N/cm^2. Since the MFC was an indicator of healthy muscle, a person who has stronger MFC could make the lumbar spine more stable based on the current study of the MFC variation.

On the other hands, since MFC is an indicator of healthy muscle and patients with low back pain have generally low MFCs, a study to explore the lowest limit of MFC in stabilizing the whole lumbar spine was also crucial to understanding the importance of the muscles. If indeed spinal muscles serve important stabilization functions, MFC within physiologic range should be adequate to control CFLs in all normal postures, including full flexion and extension.

The results of this study showed the feasibility that CFLs to stabilize the whole lumbar spine could be created by spinal muscles with the lowest limit of MFC 10 N/cm^2 in all flexed postures, although the minimum MFC required for CFL creating MFs resulting in a stable deformation of the lumbar spine was 30 N/cm^2 in neutral posture and 70 N/cm^2 in 5° extended posture. The stable deformation (trunk sway < 10 mm) of the lumbar spine from 40° flexed posture to 5° extended posture was found only CFLs along a FLP in the vicinity (about ± 2 mm) of the base spinal curve (FLP(η = 0 mm)) established by connecting the GCs of the vertebral bodies in the lowest limit of MFC in each posture.

In all flexed posture, the MFs could produce CFLs along a FLP located within a range from FLP at η = -1 mm to FLP at η = 2 mm and these MFs were found to produce stable deformation of the flexed lumbar spine. In contrast, there were no MFs to produce stable deformation of the extended lumbar spine under MFC 10 N/cm^2 in a neutral posture and all extension. However, when MFC limit was allowed to be or greater than 30 N/cm^2 in a neutral standing posture and 70 N/cm^2 in 5° extension, it was possible to find the MFs creating CFLs along FLP at η = 0.0 mm and FLP at η = -1.0 mm to produce a stable deformation in the lumbar spine in a neutral posture and 5° extension respectively.

Although not included in this result, it was possible to find, when MFC limit was allowed to be or greater than 135 N/cm^2, the MFs creating CFLs along FLP at η = -1.35 mm to produce a stable deformation in the lumbar spine even in 10° extension.

The minimum MFC for CFL creation with stability was much greater in extension than in flexion, even though the extension angles were only 1/4 of the flexion angles. This indicates that the CFL production for the stability demands greater short muscle strength in extension than in flexion. This seemed to occur mostly because all the short muscles are attached to the posterior aspect of the spine, which makes them much more effective in resisting the flexion moments than extension moments. Thus, the spinal musculature may be designed to maintain the stability of the flexed spine with greater mechanical efficiency than the extended spine. This may be beneficial as flexion occurs more than extension during normal activities. This may also be the reason why it is more difficult to maintain an extended posture than a flexed posture.

7.5 Summary

To achieve the goal of the normal function of the spinal stabilizing system *in vivo*, the passive system, active system and neutral system have to work together to provide sufficient stability to the spine to match the instantaneously varying stability demands due to changes in spinal posture [72]. Likewise, an optimization model and a 3-D FE model must be synchronized instantaneously due to the reason that the solution of the optimization was used as an input of the 3-D FE model. Furthermore, synchronization between the optimization and the 3-D FE model is essential to model verification.

Meanwhile, activated muscles were not always symmetric though the geometry of the 3-D FE model was sagittally symmetry. The trunk CG which was driven by applying moment on the trunk of a neutral posture was deviated from sagittal plane in flexed

postures and extended postures due to sagittally asymmetry of disc elements. For example, the trunk CG was deviated 0.7 mm from sagittal plane in 40° flexed posture and it produced lateral bending moment. However, such an asymmetry of the IVD is common in human physiology and the synchronization between the optimization and the FE model was still maintained even in the simulation of the spine with small lateral bending moment.

Considering verification is the process of gathering evidence to establish that computational implementation of the mathematical model and its associated solution is correct, the verification of the 3-D FE model was one of the key elements in biomechanical model development. Such a close match shown in 4.4 between the CFLs from the FE and optimization model predictions indicates that our optimization problems were formulated accurately without mathematical flaws.

In summary, comprehensive optimization and FE models of the spinal system incorporating the possible actions of 232 spinal muscles were introduced in this study. The results of this study support the hypothesis that the lumbar spine is stabilized *in vivo* by the CFLs created by the spinal muscles and the normal physiologic load in the spine is the CFL. A comprehensive 3-D static and dynamic analyses are required not only for the comprehensive test of the hypothesis but also for further investigation of the mechanical roles of spinal muscles *in vivo*, which is our long-term goal of our study.

CHAPTER 8

CONCLUSIONS

The optimization and FE models of the spinal system have been developed with various validations as shown in previous sections. The combined use of both models demonstrated that spinal muscle forces (MFs) predicted from the optimization model to create compressive follower loads (CFLs) along the optimum follower load path (FLP) can produce a large deformation of the lumbar spine inducing about 40 mm posterior translation of the trunk in a neutral standing posture. In fact, when the MFs to create CFLs along the optimum curve (FLP at η = -11.38 mm) were used in the FE model, both the directions and magnitudes of the FE predictions of CFLs were found to be substantially different from the optimization predictions due to a significant deformation of the lumbar spine as shown in the previous section. However, it was possible to predict from the optimization model the CFL-creating MFs that can produce almost no change in the lumbar lordosis. Particularly, the MFs producing CFLs along a base FLP (η = 0 mm, a spinal curve passing through the geometric centers (GCs) of the vertebral bodies) in the optimization model were found to result in a very minimal change in the lumbar lordosis and CFLs whose directions and magnitudes are almost the same as those from the optimization model. These results suggest the following conclusions:

- There exist the multiple combinations of spinal muscle forces (MFs) that can create CFLs in the lumbar spine.
- The lumbar spine in various postures can be stabilized by MFs that create CFLs in the lumbar spine.

- The CFLs may follow various FLPs, but the MFs resulting in CFLs along the FLP passing through the vicinity of GCs of the vertebral bodies ($\eta = 0$ mm) would be most physiological MFs to provide sufficient stability to the lumbar spine in various standing postures.
- The CFLs may vary in respond to different muscle force capacity (MFC), and the spinal muscles with larger MFC (healthier muscles) result in smaller CFLs could stabilize more extended posture even though the effect of MFC variation is less crucial in flexed posture.

These results support, at least in part, a hypothesis that the follower load mechanism may be a physiological motor control strategy of the spinal muscle recruitment patterns. Further studies are required to fully test the hypothesis. For example, the feasibility of CFL construction must be tested in motions out of sagittal plane, such as lateral bending or axial rotation (i.e., lateral bending, axial rotation, etc.). Dynamic analyses are also required to test the feasibility of CFL construction in the lumbar spine during the deformation for various tasks or daily activities.

REFERENCES

1. Nachemson A: **Lumbar intradiscal pressure. Experimental studies on post-mortem material.** *Acta Orthop Scand Suppl* 1960, **43:**1-104.

2. Crisco JJP, M.M.; Yamamoto, I.; Oxland, T.R.: **Euler stability of the human ligamentous spine. Part II: Experiment.** *Clin Biomech* 1992, **7:**27-32.

3. Patwardhan AG, Havey RM, Ghanayem AJ, Diener H, Meade KP, Dunlap B, Hodges SD: **Load-carrying capacity of the human cervical spine in compression is increased under a follower load.** *Spine* 2000, **25:**1548-1554.

4. Patwardhan AG, Havey RM, Meade KP, Lee B, Dunlap B: **A follower load increases the load-carrying capacity of the lumbar spine in compression.** *Spine* 1999, **24:**1003-1009.

5. Han K: **Biomechanical roles of spinal muscles in stabilizing the lumbar spine via follwer load mechanism.** *book.* University of Iowa, Biomedical engineering; 2008.

6. White AA, Panjabi MM: *Clinical Biomechanics of The Spine.* 2nd edn: Lippincott Williams & Wilkins; 1990.

7. Moore KL (Ed.). **Essential Clinical Anatomy**, Forth edition edition. Philadelpia, PA: Lippincott Williams & Wilkins; 2011.

8. Nachemson AL: **Disc pressure measurements.** *Spine (Phila Pa 1976)* 1981, **6:**93-97.

9. Wilke HJ, Neef P, Caimi M, Hoogland T, Claes LE: **New in vivo measurements of pressures in the intervertebral disc in daily life.** *Spine (Phila Pa 1976)* 1999, **24:**755-762.

10. Bean JC, Chaffin DB, Schultz AB: **Biomechanical model calculation of muscle contraction forces: a double linear programming method.** *J Biomech* 1988, **21:**59-66.

11. Stokes IA, Gardner-Morse M: **Lumbar spine maximum efforts and muscle recruitment patterns predicted by a model with multijoint muscles and joints with stiffness.** *J Biomech* 1995, **28:**173-186.

12. El-Rich M, Shirazi-Adl A, Arjmand N: **Muscle activity, internal loads, and stability of the human spine in standing postures: combined model and in vivo studies.** *Spine* 2004, **29:**2633-2642.

13. Cholewicki J, McGill SM: **EMG assisted optimization: a hybrid approach for estimating muscle forces in an indeterminate biomechanical model.** *J Biomech* 1994, **27:**1287-1289.

14. Gagnon D, Lariviere C, Loisel P: **Comparative ability of EMG, optimization, and hybrid modelling approaches to predict trunk muscle forces and lumbar spine loading during dynamic sagittal plane lifting.** *Clin Biomech (Bristol, Avon)* 2001, **16:**359-372.

15. Cholewicki J, McGill SM, Norman RW: **Comparison of muscle forces and joint load from an optimization and EMG assisted lumbar spine model: towards development of a hybrid approach.** *J Biomech* 1995, **28:**321-331.

16. Cholewicki J, McGill SM: **Mechanical stability of the in vivo lumbar spine: implications for injury and chronic low back pain.** *Clin Biomech (Bristol, Avon)* 1996, **11:**1-15.

17. Lucas DBB, B.: **Stability of the ligamentous spine.** San Francisco: University of Claifornia, Biomechanics Laboratory; 1961.

18. Knutsson F: **The instability associated with disc degeneration in the lumbar spine.** *Acta Radiol* 1944, **25:**593-609.

19. Hirsch CL, T.: **Lumbosacral synovial joints in flexion-extension.** *Acta Orthop Scand* 1968, **39:**303-311.

20. Kirkaldy-Willis WH, Wedge JH, Yong-Hing K, Reilly J: **Pathology and pathogenesis of lumbar spondylosis and stenosis.** *Spine* 1978, **3:**319-328.

21. Rosenberg NI: **Degenerative spondylolisthesis- predisposing factors.** *J Bone Joint Surg* 1975, **57:**467-474.

22. Frymoyer JWS, D.K.: **Segmental instability: rationale for treatment.** *Spine* 1979, **10:**280-286.

23. Kirkaldy-Willis WHF, H.F.: **Instability of the lumbar spine.** *Clin Orthop* 1982, **165:**110-121.

24. White AAIP, M.M.: *Clinical biomechanics of the spine.* 2 edn. Philadelphia, PA: Lippincott; 1990.

25. Weinstein JN, Gordon SL: *Low back pain and spinal instability.* Rosemont, IL: American Academy of Orthopaedic Surgeons; 1996.

26. Crisco JJ: **The biomechanical stability of the human lumbar spine: Experimental and theoretical investigations.** *Doctoral dissertation.* Yale University, 1992.

27. Gardner-Morse M, Stokes IA, Laible JP: **Role of muscles in lumbar spine stability in maximum extension efforts.** *J Orthop Res* 1995, **13:**802-808.

28. Gardner-Morse MG, Stokes IA: **The effects of abdominal muscle coactivation on lumbar spine stability.** *Spine* 1998, **23:**86-91; discussion 91-82.

29. Potvin JR, Brown SH: **An equation to calculate individual muscle contributions to joint stability.** *J Biomech* 2005, **38:**973-980.

30. Wilke HJ, Wolf S, Claes LE, Arand M, Wiesend A: **Stability increase of the lumbar spine with different muscle groups. A biomechanical in vitro study.** *Spine* 1995, **20:**192-198.

31. Bazant ZP, Cedolin L: *Stability of Structures.* Oxford University Press; 1991.

32. Timoshenko S, J G: *Theory of elastic stability.* New York: Mcgrow-Hill; 1961.

33. Aspden RM: **The spine as an arch. A new mathematical model.** *Spine (Phila Pa 1976)* 1989, **14:**266-274.

34. Patwardhan AG, Havey RM, Carandang G, Simonds J, Voronov LI, Ghanayem AJ, Meade KP, Gavin TM, Paxinos O: **Effect of compressive follower preload on the flexion-extension response of the human lumbar spine.** *J Orthop Res* 2003, **21:**540-546.

35. Goel VK, Grauer JN, Patel T, Biyani A, Sairyo K, Vishnubhotla S, Matyas A, Cowgill I, Shaw M, Long R, et al: **Effects of charite artificial disc on the implanted and adjacent spinal segments mechanics using a hybrid testing protocol.** *Spine (Phila Pa 1976)* 2005, **30:**2755-2764.

36. Goel VK, Panjabi MM, Patwardhan AG, Dooris AP, Serhan H: **Test protocols for evaluation of spinal implants.** *J Bone Joint Surg Am* 2006, **88 Suppl 2:**103-109.

37. Renner SM, Natarajan RN, Patwardhan AG, Havey RM, Voronov LI, Guo BY, Andersson GB, An HS: **Novel model to analyze the effect of a large compressive follower pre-load on range of motions in a lumbar spine.** *J Biomech* 2007, **40:**1326-1332.

38. Rohlmann A, Bauer L, Zander T, Bergmann G, Wilke HJ: **Determination of trunk muscle forces for flexion and extension by using a validated finite element model of the lumbar spine and measured in vivo data.** *J Biomech* 2006, **39:**981-989.

39. Rohlmann A, Neller S, Claes L, Bergmann G, Wilke HJ: **Influence of a follower load on intradiscal pressure and intersegmental rotation of the lumbar spine.** *Spine (Phila Pa 1976)* 2001, **26:**E557-561.

40. Wilke HJ, Rohlmann A, Neller S, Graichen F, Claes L, Bergmann G: **ISSLS prize winner: A novel approach to determine trunk muscle forces during flexion and extension: a comparison of data from an in vitro experiment and in vivo measurements.** *Spine* 2003, **28:**2585-2593.

41. Kim K, Kim YH: **Role of trunk muscles in generating follower load in the lumbar spine of neutral standing posture.** *J Biomech Eng* 2008, **130:**041005.

42. Zhou SH, McCarthy ID, McGregor AH, Coombs RR, Hughes SP: **Geometrical dimensions of the lower lumbar vertebrae--analysis of data from digitised CT images.** *Eur Spine J* 2000, **9:**242-248.

43. Brown T: **Some Mechanical Tests on the Lumbosacral Spine with Particular Reference to the Intervertebral Discs.** *JBJS* 1957, **39:**1135-1164.

44. Vena P, Franzoso G, Gastaldi D, Contro R, Dallolio V: **A finite element model of the L4-L5 spinal motion segment: biomechanical compatibility of an interspinous device.** *Comput Methods Biomech Biomed Engin* 2005, **8:**7-16.

45. An HS: *Chapter 1 : Anatomy of the Spine.* Lippincott Williams & Wilkins; 1998.

46. Bogduk N, Macintosh JE: **The applied anatomy of the thoracolumbar fascia.** *Spine* 1984, **9:**164-170.

47. Bogduk N, Macintosh JE, Pearcy MJ: **A universal model of the lumbar back muscles in the upright position.** *Spine* 1992, **17:**897-913.

48. Bogduk N, Pearcy M, Hadfield G: **Anatomy and biomechanics of psoas major.** *Clinical Biomechanics* 1992, **7:**109-119.

49. Gray H, Clemente CD: **Gray's Anatomy of the Human Body.** In *Gray's Anatomy of the Human Body.* Lippincott Williams & Wilkins; 1984

50. Macintosh JE, Bogduk N: **The biomechanics of the lumbar multifidus.** *Clinical Biomechanics* 1986, **1:**205-213.

51. Macintosh JE, Bogduk N: **1987 Volvo award in basic science. The morphology of the lumbar erector spinae.** *Spine* 1987, **12:**658-668.

52. Macintosh JE, Bogduk N: **The attachments of the lumbar erector spinae.** *Spine* 1991, **16:**783-792.

53. Macintosh JE, Valencia F, Bogduk N, Munro RR: **The morphology of the human lumbar multifidus.** *Clinical Biomechanics* 1986, **1:**196-204.

54. McGill SM, Patt N, Norman RW: **Measurement of the trunk musculature of active males using CT scan radiography: implications for force and moment generating capacity about the L4/L5 joint.** *J Biomech* 1988, **21:**329-341.

55. Rickenbacher J: **Chapter 4 : The Musculature of the Back.** In *Applied Anatomy of the Back.* Edited by Rickenbacher J: Springer; 1985: 54-100

56. Chaffin DB, Andersson GBJ, Martin BJ: **Anthropometry in Occupational Biomechanics.** In *Occupational Biomechanics.* 3rd Edition edition: Wiley-Interscience; 1999: 65-89

57. Adams MA, Dolan P, Hutton WC: **The lumbar spine in backward bending.** *Spine (Phila Pa 1976)* 1988, **13:**1019-1026.

58. Adams MA, Hutton WC, Stott JR: **The resistance to flexion of the lumbar intervertebral joint.** *Spine (Phila Pa 1976)* 1980, **5:**245-253.

59. Han KS, Rohlmann A, Yang SJ, Kim BS, Lim TH: **Spinal muscles can create compressive follower loads in the lumbar spine in a neutral standing posture.** *Med Eng Phys*.

60. Han JS: **Analysis of the internal mechanism of the spine in static and dynamic loading postures using optimization technique.** *PH. D.* The University of Iowa, Biomedical Engineering; 1991.

61. Marras WS, Jorgensen MJ, Granata KP, Wiand B: **Female and male trunk geometry: size and prediction of the spine loading trunk muscles derived from MRI.** *Clin Biomech (Bristol, Avon)* 2001, **16:**38-46.

62. Alexander L: **New dimensions in legal and ethical concepts for human research. 2. Special problems of medical disciplines. Psychiatry: methods and processes for investigation of drugs.** *Ann N Y Acad Sci* 1970, **169:**344-350.

63. An KN, Kaufman KR, Chao EY: **Physiological considerations of muscle force through the elbow joint.** *J Biomech* 1989, **22:**1249-1256.

64. Brand PW, Beach RB, Thompson DE: **Relative tension and potential excursion of muscles in the forearm and hand.** *J Hand Surg [Am]* 1981, **6:**209-219.

65. Haxton HA: **Absolute muscle force in the ankle flexors of man.** *J Physiol* 1944, **103:**267-273.

66. Ikai M, Fukunaga T: **Calculation of muscle strength per unit cross-sectional area of human muscle by means of ultrasonic measurement.** *Int Z Angew Physiol* 1968, **26:**26-32.

67. Kaufman KR, An KW, Litchy WJ, Chao EY: **Physiological prediction of muscle forces--I. Theoretical formulation.** *Neuroscience* 1991, **40:**781-792.

68. Wong KW, Leong JC, Chan MK, Luk KD, Lu WW: **The flexion-extension profile of lumbar spine in 100 healthy volunteers.** *Spine* 2004, **29:**1636-1641.

69. Stokes IA, Gardner-Morse M: **Spinal stiffness increases with axial load: another stabilizing consequence of muscle action.** *J Electromyogr Kinesiol* 2003, **13:**397-402.

70. Gardner-Morse MG, Stokes IA: **Physiological axial compressive preloads increase motion segment stiffness, linearity and hysteresis in all six degrees of freedom for small displacements about the neutral posture.** *J Orthop Res* 2003, **21:**547-552.

71. Lodygowski T, Kakor W, Marcin W: **Three-dimensional nonlinear finite element model of lumbar intervertebral disc.** *Acta of Bioengineering and Biomechanics* 2005, **vol. 7**.

72. Panjabi MM: **The stabilizing system of the spine. Part I. Function, dysfunction, adaptation, and enhancement.** *J Spinal Disord* 1992, **5:**383-389.

73. Bergmark A: **Stability of the lumbar spine: a study in mechanical engineering.** *Acta Orthop Scand* 1989, **60:**1-54.

74. Gardner-Morse MG, Stokes IA: **Structural behavior of human lumbar spinal motion segments.** *J Biomech* 2004, **37:**205-212.

75. Kiefer A, Shirazi-Adl A, Parnianpour M: **Synergy of the human spine in neutral postures.** *Eur Spine J* 1998, **7:**471-479.

76. Shirazi-Adl A, El-Rich M, Pop DG, Parnianpour M: **Spinal muscle forces, internal loads and stability in standing under various postures and loads--application of kinematics-based algorithm.** *Eur Spine J* 2005, **14:**381-392.

77. Shirazi-Adl A, Sadouk S, Parnianpour M, Pop D, El-Rich M: **Muscle force evaluation and the role of posture in human lumbar spine under compression.** *Eur Spine J* 2002, **11:**519-526.

78. Stokes IA, Gardner-Morse M: **Lumbar spinal muscle activation synergies predicted by multi-criteria cost function.** *J Biomech* 2001, **34:**733-740.

79. Rohlmann A, Neller S, Claes L, Bergmann G, Wilke HJ: **Influence of a follower load on intradiscal pressure and intersegmental rotation of the lumbar spine.** *Spine* 2001, **26:**E557-561.

80. Rohlmann A, Zander T, Rao M, Bergmann G: **Applying a follower load delivers realistic results for simulating standing.** *J Biomech* 2009, **42:**1520-1526.

81. Patwardhan AG, Meade KP, Lee B: **A frontal plane model of the lumbar spine subjected to a follower load: implications for the role of muscles.** *J Biomech Eng* 2001, **123:**212-217.

82. Kim K, Kim YH, Lee S: **Increase of load-carrying capacity under follower load generated by trunk muscles in lumbar spine.** *Proc Inst Mech Eng H* 2007, **221:**229-235.

83. Han KS, Rohlmann A, Yang SJ, Kim BS, Lim TH: **Spinal muscles can create compressive follower loads in the lumbar spine in a neutral standing posture.** *Med Eng Phys* 2011, **33:**472-478.

84. Han KS, Youn B, Yang SJ, Choi KK, Lim TH: **Follower compressive load can be produced during flexion and extension postures with muscle force capacity 40N.** In *Orthopaedic Research Society; San Francisco, CA*. 2008

85. Han KS: **Biomechanical roles of spinal muscles in stabilizing the lumbar spine via follower load mechanism.** *PhD Dissertation.* University of Iowa, Biomedical Engineering; 2008.

86. Dennison CR, Wild PM, Byrnes PW, Saari A, Itshayek E, Wilson DC, Zhu QA, Dvorak MF, Cripton PA, Wilson DR: **Ex vivo measurement of lumbar intervertebral disc pressure using fibre-Bragg gratings.** *J Biomech* 2008, **41:**221-225.

87. McNally DS, Adams MA: **Internal intervertebral disc mechanics as revealed by stress profilometry.** *Spine (Phila Pa 1976)* 1992, **17:**66-73.

APPENDIX A.116 SETS OF MUSCLES FOR THE 3-D FE MODEL OF *IN VIVO* SPINE

Table A-1 Classification of 116 sets of muscles for the 3-D FE model

		Superficial	Intermediate	Deep	Intrinsic	Long	Short
1	SerratusPI_L1_Rib11		√				√
2	SerratusPI_L2_Rib12		√			√	
3	LatissimusDorsi_Pel_RibHum	√				√	
4	LatissimusDorsi_L1_RibHum	√				√	
5	LatissimusDorsi_L2_RibHum	√				√	
6	LatissimusDorsi_L3_lr	√				√	
7	LatissimusDorsi_L3_lr	√				√	
8	LatissimusDorsi_L4_lr	√				√	
9	LatissimusDorsi_L4_lr	√				√	
10	ExternalOb_Pel_Rib10			√		√	
11	ExternalOb_Pel_Rib11			√		√	
12	ExternalOb_Pel_Rib12			√		√	
13	Iliocostalis_Sa_Rib5			√		√	
14	Iliocostalis_Sa_Rib6			√		√	
15	Iliocostalis_Sa_Rib7			√		√	
16	Iliocostalis_Sa_Rib8			√		√	
17	Iliocostalis_Sa_Rib9			√		√	
18	Iliocostalis_Sa_Rib10			√		√	
19	Iliocostalis_Sa_Rib11			√		√	
20	Iliocostalis_Sa_Rib12			√		√	
21	InternalOb_Pel_Rib10					√	
22	InternalOb_Pel_Rib11					√	
23	InternalOb_Pel_Rib12					√	
24	Longissimus_Sa_Rib6			√		√	
25	Longissimus_Sa_Rib7			√		√	
26	Longissimus_Sa_Rib8			√		√	
27	Longissimus_Sa_Rib9			√		√	
28	Longissimus_Sa_Rib10			√		√	
29	Longissimus_Sa_Rib11			√		√	
30	Longissimus_Sa_Rib12			√		√	

Table A-1 continued

31	Longissimus_L3_T3			√		√	
32	Longissimus_L4_T4			√		√	
33	Longissimus_L4_T5			√		√	
34	Longissimus_L5_T6			√		√	
35	Longissimus_Sa_T7			√		√	
36	Longissimus_Sa_T8			√		√	
37	Longissimus_Sa_T9			√		√	
38	Longissimus_Sa_T10			√		√	
39	Longissimus_Sa_T11			√		√	
40	Longissimus_Sa_T12			√		√	
41	PsoasMajor_Fe_T12			√		√	
42	QuadratusLum_Pel_Rib12			√		√	
43	RecAbdominis_Pel_Rib5					√	
44	RecAbdominis_Pel_Rib6					√	
45	RecAbdominis_Pel_Rib7					√	
46	RecAbdominis_Pel_Rib7					√	
47	SpinalisTho_L1_T6			√		√	
48	SpinalisTho_L2_T5			√		√	
49	SpinalisTho_Sa_T1			√		√	
50	Interspinales_L1_T12				√		√
51	Intertransversarii_L1_T12_La				√		√
52	Intertransversarii_L1_T12_Me				√		√
53	Rotatores_L1_T12				√		√
54	Rotatores_L2_T12				√		√
55	Longissimus_L2_T1			√		√	
56	Longissimus_L2_T2			√		√	
57	Iliocostalis_Sa_L1			√		√	
58	Longissimus_Sa_L1			√		√	
59	Multifidus_Sa_L1_F1			√		√	
60	Multifidus_Sa_L1_F2			√		√	
61	Multifidus_L5_L1_F3			√		√	
62	Multifidus_L4_L1_F4			√		√	
63	PsoasMajor_Fe_L1			√		√	
64	QuadratusLum_Pel_L1			√		√	
65	Interspinales_L2_L1				√		√
66	Intertransversarii_L2_L1_La				√		√
67	Intertransversarii_L2_L1_Me				√		√

Table A-1 continued

68	Rotatores_L2_L1				√		√
69	Rotatores_L3_L1				√		√
70	Iliocostalis_Sa_L2			√		√	
71	Longissimus_Sa_L2			√		√	
72	Multifidus_Sa_L2_F1			√		√	
73	Multifidus_Sa_L2_F2			√		√	
74	Multifidus_L5_L2_F3			√		√	
75	Multifidus_Sa_L2_F4			√		√	
76	PsoasMajor_Fe_L2			√		√	
77	QuadratusLum_Pel_L2			√		√	
78	Interspinales_L3_L2				√		√
79	Intertransversarii_L3_L2_La				√		√
80	Intertransversarii_L3_L2_Me				√		√
81	Rotatores_L3_L2				√		√
82	Rotatores_L4_L2				√		√
83	Iliocostalis_Sa_L3			√		√	
84	Longissimus_Sa_L3			√		√	
85	Multifidus_Sa_L3_F1			√		√	
86	Multifidus_Sa_L3_F2			√		√	
87	Multifidus_Sa_L3_F3			√		√	
88	Multifidus_Sa_L3_F4			√		√	
89	PsoasMajor_Fe_L3			√		√	
90	QuadratusLum_Pel_L3			√		√	
91	Interspinales_L4_L3				√		√
92	Intertransversarii_L4_L3_La				√		√
93	Intertransversarii_L4_L3_Me				√		√
94	Rotatores_L4_L3				√		√
95	Rotatores_L5_L3				√		√
96	Iliocostalis_Sa_L4			√			√
97	Longissimus_Sa_L4			√		√	
98	Multifidus_Sa_L4_F1			√			√
99	Multifidus_Sa_L4_F2			√			√
100	Multifidus_Sa_L4_F3			√			√
101	Multifidus_Sa_L4_F4			√			√
102	PsoasMajor_Fe_L4			√		√	
103	QuadratusLum_Pel_L4			√		√	
104	Interspinales_L5_L4				√		√

Table A-1 continued

105	Intertransversarii_L5_L4_La				√		√
106	Intertransversarii_L5_L4_Me				√		√
107	Rotatores_L5_L4				√		√
108	Rotatores_Sa_L4				√		√
109	Longissimus_Sa_L5			√			√
110	Multifidus_Sa_L5_F1			√			√
111	Multifidus_Sa_L5_F2			√			√
112	Multifidus_Sa_L5_F3			√			√
113	Multifidus_Sa_L5_F4			√			√
114	PsoasMajor_Fe_L5			√		√	
115	Interspinales_Sa_L5				√		√
116	Rotatores_Sa_L5				√		√

APPENDIX B. RECRUITED MUSCLES WHICH STABILIZED THE LUMBAR SPINE IN VARIOUS POSTURES UNDER MFC 45 N/CM^2

Table B-1 Activated muscles in various postures under MFC 45 N/cm^2

	Posture	NEUTRAL	FLEX10	FLEX20	FLEX40
	MFC	MFC 45 N/cm^2	MFC 45 N/cm^2	MFC 45 N/cm^2	MFC 45 N/cm^2
	FLP Location	0.00	-1.30	0.00	2.00
1	SerratusPI_L1_Rib11_L	0.00	25.52	0.25	0.00
2	SerratusPI_L1_Rib11_R	0.00	25.23	0.00	2.10
3	SerratusPI_L2_Rib12_L	0.00	12.86	0.00	0.00
4	SerratusPI_L2_Rib12_R	0.00	0.00	0.00	0.65
5	LatissimusDorsi_Pel_RibHum_L	0.00	0.00	0.00	0.00
6	LatissimusDorsi_Pel_RibHum_R	0.00	0.00	0.00	0.44
7	LatissimusDorsi_L1_RibHum_L	106.54	0.00	0.00	0.00
8	LatissimusDorsi_L1_RibHum_R	106.54	0.00	0.00	0.00
9	LatissimusDorsi_L2_RibHum_L	3.45	0.00	0.00	0.00
10	LatissimusDorsi_L2_RibHum_R	3.45	18.22	0.00	0.00
11	LatissimusDorsi_L3_L4_L3lr_L	0.00	0.00	0.00	0.00
12	LatissimusDorsi_L3_L4_L3lr_R	0.00	0.00	0.00	0.00
13	LatissimusDorsi_L3_RibHum_L3lr_L	0.00	0.00	0.00	0.00
14	LatissimusDorsi_L3_RibHum_L3lr_R	0.00	0.00	0.00	0.00
15	LatissimusDorsi_L4_L5_L4lr_L	0.00	0.00	0.00	0.00
16	LatissimusDorsi_L4_L5_L4lr_R	0.00	0.47	0.00	0.00
17	LatissimusDorsi_L4_RibHum_L4lr_L	0.00	0.00	0.00	0.00
18	LatissimusDorsi_L4_RibHum_L4lr_R	0.00	0.47	0.00	0.00
19	ExternalOb_Pel_Rib10_L	7.54	0.00	0.00	0.00
20	ExternalOb_Pel_Rib10_R	7.54	0.00	0.00	0.00
21	ExternalOb_Pel_Rib11_L	0.00	0.00	0.00	0.00
22	ExternalOb_Pel_Rib11_R	0.00	0.00	0.00	0.00
23	ExternalOb_Pel_Rib12_L	0.00	0.87	0.00	0.00
24	ExternalOb_Pel_Rib12_R	0.00	0.00	0.00	0.00
25	Iliocostalis_L1_Rib_SaRib5_L	0.00	0.00	0.00	0.00
26	Iliocostalis_L1_Rib_SaRib5_R	0.00	0.00	0.00	0.00
27	Iliocostalis_L1_Rib_SaRib6_L	0.00	0.00	0.00	0.00

Table B-1 continued

28	Iliocostalis_L1_Rib_SaRib6_R	0.00	0.00	0.00	0.00
29	Iliocostalis_L1_Rib_SaRib7_L	0.00	0.00	0.00	0.00
30	Iliocostalis_L1_Rib_SaRib7_R	0.00	0.00	0.00	0.00
31	Iliocostalis_L1_Rib_SaRib8_L	0.00	0.00	0.00	0.00
32	Iliocostalis_L1_Rib_SaRib8_R	0.00	0.00	0.00	0.00
33	Iliocostalis_L1_Rib_SaRib9_L	0.00	0.00	0.00	0.00
34	Iliocostalis_L1_Rib_SaRib9_R	0.00	0.00	0.00	0.00
35	Iliocostalis_L1_Rib_SaRib10_L	0.00	0.00	0.00	0.00
36	Iliocostalis_L1_Rib_SaRib10_R	0.00	0.00	0.00	0.00
37	Iliocostalis_L1_Rib_SaRib11_L	0.00	0.00	0.00	0.00
38	Iliocostalis_L1_Rib_SaRib11_R	0.00	0.00	0.00	0.00
39	Iliocostalis_L1_Rib_SaRib12_L	0.00	0.00	0.00	0.00
40	Iliocostalis_L1_Rib_SaRib12_R	0.00	0.00	0.00	0.00
41	InternalOb_Pel_Rib10_L	0.00	3.26	13.33	55.15
42	InternalOb_Pel_Rib10_R	0.00	3.11	12.88	54.00
43	InternalOb_Pel_Rib11_L	0.00	0.00	0.00	0.00
44	InternalOb_Pel_Rib11_R	0.00	0.00	0.00	0.00
45	InternalOb_Pel_Rib12_L	0.00	0.00	0.00	0.00
46	InternalOb_Pel_Rib12_R	0.00	0.00	0.00	0.00
47	Longissimus_L1_Rib_SaRib6_L	0.00	0.00	0.00	0.00
48	Longissimus_L1_Rib_SaRib6_R	0.00	0.00	0.00	0.00
49	Longissimus_L1_Rib_SaRib7_L	0.00	0.00	0.00	0.00
50	Longissimus_L1_Rib_SaRib7_R	0.00	0.00	0.00	0.00
51	Longissimus_L1_Rib_SaRib8_L	0.00	0.00	0.00	0.00
52	Longissimus_L1_Rib_SaRib8_R	0.00	0.00	0.00	0.00
53	Longissimus_L1_Rib_SaRib9_L	0.00	0.00	0.00	0.00
54	Longissimus_L1_Rib_SaRib9_R	0.00	0.00	0.00	0.00
55	Longissimus_L1_Rib_SaRib10_L	0.00	0.00	0.00	0.00
56	Longissimus_L1_Rib_SaRib10_R	0.00	0.00	0.00	0.00
57	Longissimus_L1_Rib_SaRib11_L	0.00	0.00	0.00	58.33
58	Longissimus_L1_Rib_SaRib11_R	0.00	0.00	0.00	11.79
59	Longissimus_L1_Rib_SaRib12_L	0.00	0.00	2.79	2.54
60	Longissimus_L1_Rib_SaRib12_R	0.00	0.00	0.00	58.33
61	Longissimus_L1_TR_L3T3_L	0.00	40.90	1.37	17.74
62	Longissimus_L1_TR_L3T3_R	0.00	38.58	24.57	79.56
63	Longissimus_L1_TR_L4T4_L	0.00	0.00	0.00	0.00

Table B-1 continued

64	Longissimus_L1_TR_L4T4_R	0.00	0.00	0.00	0.00
65	Longissimus_L1_TR_L4T5_L	0.00	0.00	0.00	0.00
66	Longissimus_L1_TR_L4T5_R	0.00	0.00	0.00	0.00
67	Longissimus_L1_TR_L5T6_L	0.00	0.52	31.46	10.28
68	Longissimus_L1_TR_L5T6_R	0.00	0.00	33.91	3.55
69	Longissimus_L1_TR_SaT7_L	0.00	0.00	0.00	0.00
70	Longissimus_L1_TR_SaT7_R	0.00	0.00	0.00	0.00
71	Longissimus_L1_TR_SaT8_L	0.00	0.00	0.00	0.00
72	Longissimus_L1_TR_SaT8_R	0.00	0.00	0.00	0.00
73	Longissimus_L1_TR_SaT9_L	0.00	0.00	0.00	0.00
74	Longissimus_L1_TR_SaT9_R	0.00	0.00	0.00	0.00
75	Longissimus_L1_TR_SaT10_L	0.00	0.00	0.00	0.00
76	Longissimus_L1_TR_SaT10_R	0.00	0.00	0.00	0.00
77	Longissimus_L1_TR_SaT11_L	0.00	0.00	0.00	58.33
78	Longissimus_L1_TR_SaT11_R	0.00	0.00	0.00	58.33
79	Longissimus_L1_TR_SaT12_L	0.00	0.00	45.27	58.33
80	Longissimus_L1_TR_SaT12_R	0.00	0.00	38.79	14.96
81	PsoasMajor_Fe_T12_L	0.00	0.00	0.00	0.00
82	PsoasMajor_Fe_T12_R	0.00	0.00	0.00	0.00
83	QuadratusLum_Pel_Rib12_L	0.00	0.00	0.00	0.00
84	QuadratusLum_Pel_Rib12_R	0.00	0.00	0.00	0.00
85	RecAbdominis_Pel_Rib5_L	0.00	0.00	0.00	0.00
86	RecAbdominis_Pel_Rib5_R	0.00	0.00	0.00	0.00
87	RecAbdominis_Pel_Rib6_L	0.00	0.00	0.00	0.00
88	RecAbdominis_Pel_Rib6_R	0.00	0.00	0.00	0.00
89	RecAbdominis_Pel_Rib7_CL	47.33	0.00	0.00	0.00
90	RecAbdominis_Pel_Rib7_CR	47.33	0.00	0.00	0.00
91	RecAbdominis_Pel_Rib7_L	0.00	0.00	0.00	0.00
92	RecAbdominis_Pel_Rib7_R	0.00	0.00	0.00	0.00
93	SpinalisTho_L1_T6_L	0.00	0.00	0.00	0.00
94	SpinalisTho_L1_T6_R	0.00	0.00	0.00	0.00
95	SpinalisTho_L2_T5_L	0.00	0.00	0.00	0.00
96	SpinalisTho_L2_T5_R	0.00	0.00	0.00	0.00
97	SpinalisTho_L1_TR_SaT1_L	0.00	0.00	0.00	0.00
98	SpinalisTho_L1_TR_SaT1_R	0.00	0.00	0.00	0.00
99	Interspinales_L1_T12_L	0.00	0.00	0.00	0.00

Table B-1 continued

100	Interspinales_L1_T12_R	0.00	0.00	0.00	0.00
101	Intertransversarii_L1_T12_La_L	0.00	0.00	0.00	0.00
102	Intertransversarii_L1_T12_La_R	0.00	2.05	0.00	0.00
103	Intertransversarii_L1_T12_Me_L	0.00	2.67	45.00	45.00
104	Intertransversarii_L1_T12_Me_R	0.00	0.00	44.71	45.00
105	Rotatores_L1_T12_L	45.00	0.00	0.00	0.00
106	Rotatores_L1_T12_R	45.00	0.00	0.00	0.00
107	Rotatores_L2_T12_L	45.00	0.00	0.00	0.00
108	Rotatores_L2_T12_R	45.00	0.00	0.00	0.00
109	Longissimus_L2_T1_L	0.00	0.00	0.00	0.00
110	Longissimus_L2_T1_R	0.00	0.00	1.40	0.00
111	Longissimus_L2_T2_L	0.00	0.00	0.00	0.00
112	Longissimus_L2_T2_R	0.00	0.00	0.00	3.18
113	Iliocostalis_L2_L1_SaL1_L	0.00	0.00	0.00	0.00
114	Iliocostalis_L2_L1_SaL1_R	0.00	0.00	0.00	0.00
115	Longissimus_L2_L1_SaL1_L	0.00	0.00	0.00	0.00
116	Longissimus_L2_L1_SaL1_R	0.00	0.00	0.00	0.00
117	Multifidus_L2_L1_SaL1_F1_L	0.00	0.00	0.00	0.00
118	Multifidus_L2_L1_SaL1_F1_R	0.00	0.00	0.00	0.00
119	Multifidus_L2_L1_SaL1_F2_L	0.00	0.00	0.00	0.00
120	Multifidus_L2_L1_SaL1_F2_R	0.00	0.00	0.00	0.00
121	Multifidus_L2_L1_L5L1_F3_L	0.00	0.00	0.00	0.00
122	Multifidus_L2_L1_L5L1_F3_R	0.00	0.00	0.00	0.00
123	Multifidus_L2_L1_L4L1_F4_L	39.10	0.00	0.00	0.00
124	Multifidus_L2_L1_L4L1_F4_R	39.10	0.00	0.00	0.00
125	PsoasMajor_Fe_L1_L	0.00	0.00	0.00	0.00
126	PsoasMajor_Fe_L1_R	0.00	0.00	0.00	0.00
127	QuadratusLum_Pel_L1_L	0.00	0.00	0.00	0.00
128	QuadratusLum_Pel_L1_R	0.00	0.00	0.00	0.00
129	Interspinales_L2_L1_L	6.62	21.23	25.30	8.03
130	Interspinales_L2_L1_R	6.62	18.12	3.57	22.62
131	Intertransversarii_L2_L1_La_L	0.00	0.00	0.00	0.00
132	Intertransversarii_L2_L1_La_R	0.00	0.00	0.00	0.00
133	Intertransversarii_L2_L1_Me_L	0.00	0.00	27.46	17.42
134	Intertransversarii_L2_L1_Me_R	0.00	0.00	29.74	15.28
135	Rotatores_L2_L1_L	45.00	0.00	0.00	0.00

Table B-1 continued

136	Rotatores_L2_L1_R	45.00	0.00	0.00	0.00
137	Rotatores_L3_L1_L	45.00	0.00	0.00	0.00
138	Rotatores_L3_L1_R	45.00	0.00	0.00	0.00
139	Iliocostalis_L3_L2_SaL2_L	0.00	0.00	0.00	0.00
140	Iliocostalis_L3_L2_SaL2_R	0.00	0.00	0.00	0.00
141	Longissimus_L3_L2_SaL2_L	0.00	0.00	0.00	0.00
142	Longissimus_L3_L2_SaL2_R	0.00	0.00	0.00	0.00
143	Multifidus_L3_L2_SaL2_F1_L	0.00	0.00	0.00	0.00
144	Multifidus_L3_L2_SaL2_F1_R	0.00	0.00	0.00	0.00
145	Multifidus_L3_L2_SaL2_F2_L	0.00	0.00	0.00	0.00
146	Multifidus_L3_L2_SaL2_F2_R	0.00	0.00	0.00	0.00
147	Multifidus_L3_L2_L5L2_F3_L	0.00	0.00	0.00	0.00
148	Multifidus_L3_L2_L5L2_F3_R	0.00	0.00	0.00	0.00
149	Multifidus_L3_L2_SaL2_F4_L	0.00	0.00	0.00	0.00
150	Multifidus_L3_L2_SaL2_F4_R	0.00	0.00	0.00	0.00
151	PsoasMajor_Fe_L2_L	0.00	0.00	0.00	0.00
152	PsoasMajor_Fe_L2_R	0.00	0.00	0.00	0.00
153	QuadratusLum_Pel_L2_L	0.00	0.00	0.00	0.00
154	QuadratusLum_Pel_L2_R	0.00	0.00	0.00	0.00
155	Interspinales_L3_L2_L	30.83	21.16	34.83	0.00
156	Interspinales_L3_L2_R	30.83	30.94	12.70	0.00
157	Intertransversarii_L3_L2_La_L	0.00	0.00	0.00	0.15
158	Intertransversarii_L3_L2_La_R	0.00	0.00	0.00	0.00
159	Intertransversarii_L3_L2_Me_L	0.00	13.75	14.66	0.00
160	Intertransversarii_L3_L2_Me_R	0.00	12.38	19.00	0.00
161	Rotatores_L3_L2_L	27.85	0.00	0.00	45.00
162	Rotatores_L3_L2_R	27.85	0.00	0.00	45.00
163	Rotatores_L4_L2_L	0.00	0.00	0.00	0.00
164	Rotatores_L4_L2_R	0.00	0.00	0.00	1.58
165	Iliocostalis_L4_L3_SaL3_L	0.00	0.00	0.00	0.00
166	Iliocostalis_L4_L3_SaL3_R	0.00	0.00	0.00	0.00
167	Longissimus_L4_L3_SaL3_L	0.00	22.39	11.68	0.00
168	Longissimus_L4_L3_SaL3_R	0.00	22.49	16.57	0.00
169	Multifidus_L4_L3_SaL3_F1_L	0.00	0.00	0.00	0.00
170	Multifidus_L4_L3_SaL3_F1_R	0.00	0.00	0.00	0.00
171	Multifidus_L4_L3_SaL3_F2_L	0.00	0.00	0.00	0.00

Table B-1 continued

172	Multifidus_L4_L3_SaL3_F2_R	0.00	0.00	0.00	0.00
173	Multifidus_L4_L3_SaL3_F3_L	0.00	0.00	0.00	0.00
174	Multifidus_L4_L3_SaL3_F3_R	0.00	0.00	0.00	0.00
175	Multifidus_L4_L3_SaL3_F4_L	0.00	0.00	0.00	0.00
176	Multifidus_L4_L3_SaL3_F4_R	0.00	0.00	0.00	0.00
177	PsoasMajor_Fe_L3_L	0.00	0.00	0.00	0.00
178	PsoasMajor_Fe_L3_R	0.00	0.00	0.00	0.00
179	QuadratusLum_Pel_L3_L	0.00	0.00	0.00	0.00
180	QuadratusLum_Pel_L3_R	0.00	0.00	0.00	0.00
181	Interspinales_L4_L3_L	32.80	45.00	16.61	45.00
182	Interspinales_L4_L3_R	32.80	45.00	22.69	45.00
183	Intertransversarii_L4_L3_La_L	0.00	0.70	0.00	0.00
184	Intertransversarii_L4_L3_La_R	0.00	0.00	0.00	0.62
185	Intertransversarii_L4_L3_Me_L	45.00	45.00	45.00	0.00
186	Intertransversarii_L4_L3_Me_R	45.00	45.00	44.34	7.18
187	Rotatores_L4_L3_L	0.00	0.00	0.00	40.31
188	Rotatores_L4_L3_R	0.00	0.00	0.00	35.38
189	Rotatores_L5_L3_L	0.00	0.00	0.00	0.00
190	Rotatores_L5_L3_R	0.00	0.00	0.00	0.00
191	Iliocostalis_Sa_L4_L	0.00	0.00	0.00	0.00
192	Iliocostalis_Sa_L4_R	0.00	0.00	0.00	0.00
193	Longissimus_Sa_L4_L	91.39	90.37	104.39	47.59
194	Longissimus_Sa_L4_R	91.39	89.60	104.39	52.46
195	Multifidus_Sa_L4_F1_L	0.00	0.00	0.00	0.00
196	Multifidus_Sa_L4_F1_R	0.00	0.00	0.00	0.00
197	Multifidus_Sa_L4_F2_L	0.00	0.00	0.00	0.00
198	Multifidus_Sa_L4_F2_R	0.00	0.00	0.00	0.00
199	Multifidus_Sa_L4_F3_L	0.00	0.00	0.00	0.00
200	Multifidus_Sa_L4_F3_R	0.00	0.00	0.00	0.00
201	Multifidus_Sa_L4_F4_L	0.00	0.00	0.00	0.00
202	Multifidus_Sa_L4_F4_R	0.00	0.00	0.00	0.00
203	PsoasMajor_Fe_L4_L	0.00	0.00	0.00	0.00
204	PsoasMajor_Fe_L4_R	0.00	0.00	0.00	0.00
205	QuadratusLum_Pel_L4_L	0.00	0.01	0.00	0.00
206	QuadratusLum_Pel_L4_R	0.00	0.00	0.00	0.00
207	Interspinales_L5_L4_L	18.30	12.93	0.00	0.52

Table B-1 continued

208	Interspinales_L5_L4_R	18.30	9.45	0.00	25.67
209	Intertransversarii_L5_L4_La_L	0.00	0.00	0.00	0.00
210	Intertransversarii_L5_L4_La_R	0.00	0.00	0.00	0.00
211	Intertransversarii_L5_L4_Me_L	45.00	44.11	0.35	45.00
212	Intertransversarii_L5_L4_Me_R	45.00	45.00	0.00	40.17
213	Rotatores_L5_L4_L	0.00	0.00	0.00	0.00
214	Rotatores_L5_L4_R	0.00	0.00	0.00	0.00
215	Rotatores_Sa_L4_L	0.00	0.00	0.00	0.00
216	Rotatores_Sa_L4_R	0.00	0.00	0.00	0.00
217	Longissimus_Sa_L5_L	84.31	72.20	69.06	104.25
218	Longissimus_Sa_L5_R	84.31	72.82	68.74	100.35
219	Multifidus_Sa_L5_F1_L	0.00	0.00	0.00	0.00
220	Multifidus_Sa_L5_F1_R	0.00	0.00	0.00	0.00
221	Multifidus_Sa_L5_F2_L	0.00	0.00	0.00	0.00
222	Multifidus_Sa_L5_F2_R	0.00	0.00	0.00	0.00
223	Multifidus_Sa_L5_F3_L	0.00	0.00	0.00	0.00
224	Multifidus_Sa_L5_F3_R	0.00	0.00	0.00	0.00
225	Multifidus_Sa_L5_F4_L	0.00	0.00	0.00	0.00
226	Multifidus_Sa_L5_F4_R	0.00	0.00	0.00	0.00
227	PsoasMajor_Fe_L5_L	0.00	0.00	0.00	0.00
228	PsoasMajor_Fe_L5_R	0.00	0.00	0.00	0.00
229	Interspinales_Sa_L5_L	0.00	0.00	0.00	0.00
230	Interspinales_Sa_L5_R	0.00	0.00	0.00	0.00
231	Rotatores_Sa_L5_L	0.00	0.00	0.00	0.00
232	Rotatores_Sa_L5_R	0.00	0.00	0.00	0.00

APPENDIX C. RECRUITED MUSCLES WHICH STABILIZED THE LUMBAR SPINE IN VARIOUS POSTURES UNDER THE LOWEST MFC

Table C-1 Activated muscles in various postures under the lowest MFC

	Posture	NEUTRAL	FLEX10	FLEX20	FLEX40	EXT05
	MFC	MFC 30 N/cm^2	MFC 10 N/cm^2	MFC 10 N/cm^2	MFC 10 N/cm^2	MFC 70 N/cm^2
	FLP Location	0.00	-1.30	0.00	2.00	-1.00
1	SerratusPI_L1_Rib11_L	0.00	14.57	3.34	57.78	0.00
2	SerratusPI_L1_Rib11_R	0.00	14.54	3.19	57.78	0.00
3	SerratusPI_L2_Rib12_L	0.00	4.06	0.00	0.78	0.00
4	SerratusPI_L2_Rib12_R	0.00	0.00	1.67	5.17	0.00
5	LatissimusDorsi_Pel_RibHum_L	0.00	0.00	0.00	0.00	0.00
6	LatissimusDorsi_Pel_RibHum_R	0.00	0.00	0.00	0.00	0.00
7	LatissimusDorsi_L1_RibHum_L	111.12	0.00	0.00	0.00	210.82
8	LatissimusDorsi_L1_RibHum_R	111.12	0.00	0.00	0.00	210.86
9	LatissimusDorsi_L2_RibHum_L	15.23	0.00	0.00	0.00	8.60
10	LatissimusDorsi_L2_RibHum_R	15.23	5.28	0.00	0.00	8.60
11	LatissimusDorsi_L3_L4_L3lr_L	55.21	39.16	0.00	0.00	0.00
12	LatissimusDorsi_L3_L4_L3lr_R	55.21	40.09	0.09	0.00	0.02
13	LatissimusDorsi_L3_RibHum_L3lr_L	55.21	39.16	0.00	0.00	0.00
14	LatissimusDorsi_L3_RibHum_L3lr_R	55.21	40.09	0.09	0.00	0.02
15	LatissimusDorsi_L4_L5_L4lr_L	6.84	34.39	0.00	0.00	0.00
16	LatissimusDorsi_L4_L5_L4lr_R	6.84	34.46	0.87	0.00	0.01
17	LatissimusDorsi_L4_RibHum_L4lr_L	6.84	34.39	0.00	0.00	0.00
18	LatissimusDorsi_L4_RibHum_L4lr_R	6.84	34.46	0.87	0.00	0.01
19	ExternalOb_Pel_Rib10_L	117.73	1.21	0.00	0.00	158.01
20	ExternalOb_Pel_Rib10_R	117.73	0.00	0.00	0.00	158.38
21	ExternalOb_Pel_Rib11_L	0.00	0.00	0.00	0.00	0.00
22	ExternalOb_Pel_Rib11_R	0.00	0.00	0.00	0.00	0.00
23	ExternalOb_Pel_Rib12_L	0.00	0.00	0.00	0.00	0.00
24	ExternalOb_Pel_Rib12_R	0.00	0.00	0.00	0.00	0.00
25	Iliocostalis_L1_Rib_SaRib5_L	0.00	0.00	0.00	12.96	0.00
26	Iliocostalis_L1_Rib_SaRib5_R	0.00	0.00	0.00	12.96	0.00
27	Iliocostalis_L1_Rib_SaRib6_L	0.00	0.00	0.00	12.96	0.00

Table C-1 continued

28	Iliocostalis_L1_Rib_SaRib6_R	0.00	0.00	0.00	12.96	0.00
29	Iliocostalis_L1_Rib_SaRib7_L	0.00	0.00	0.00	12.96	0.00
30	Iliocostalis_L1_Rib_SaRib7_R	0.00	0.00	0.00	12.96	0.00
31	Iliocostalis_L1_Rib_SaRib8_L	0.00	0.00	0.00	12.96	0.00
32	Iliocostalis_L1_Rib_SaRib8_R	0.00	0.00	0.00	5.76	0.00
33	Iliocostalis_L1_Rib_SaRib9_L	0.00	0.00	0.00	0.00	0.00
34	Iliocostalis_L1_Rib_SaRib9_R	0.00	0.00	0.00	0.00	0.00
35	Iliocostalis_L1_Rib_SaRib10_L	0.00	0.00	0.00	0.00	0.00
36	Iliocostalis_L1_Rib_SaRib10_R	0.00	0.00	0.00	0.00	0.00
37	Iliocostalis_L1_Rib_SaRib11_L	0.00	0.00	0.00	1.49	0.00
38	Iliocostalis_L1_Rib_SaRib11_R	0.00	0.00	0.00	0.00	0.00
39	Iliocostalis_L1_Rib_SaRib12_L	0.00	0.00	0.00	0.00	0.00
40	Iliocostalis_L1_Rib_SaRib12_R	0.00	0.00	0.00	0.00	0.00
41	InternalOb_Pel_Rib10_L	0.00	17.16	21.64	87.39	0.00
42	InternalOb_Pel_Rib10_R	0.00	16.79	21.35	84.86	0.00
43	InternalOb_Pel_Rib11_L	0.00	0.00	0.00	0.00	0.00
44	InternalOb_Pel_Rib11_R	0.00	0.00	0.00	0.00	0.00
45	InternalOb_Pel_Rib12_L	0.00	0.00	0.00	0.00	0.00
46	InternalOb_Pel_Rib12_R	0.00	0.00	0.00	0.00	0.00
47	Longissimus_L1_Rib_SaRib6_L	0.00	0.00	0.00	0.00	0.00
48	Longissimus_L1_Rib_SaRib6_R	0.00	0.00	0.00	0.00	0.00
49	Longissimus_L1_Rib_SaRib7_L	0.00	0.00	0.00	0.00	0.00
50	Longissimus_L1_Rib_SaRib7_R	0.00	0.00	0.00	0.00	0.00
51	Longissimus_L1_Rib_SaRib8_L	0.00	0.00	0.00	0.00	0.00
52	Longissimus_L1_Rib_SaRib8_R	0.00	0.00	0.00	0.00	0.00
53	Longissimus_L1_Rib_SaRib9_L	0.00	0.00	0.00	9.52	0.00
54	Longissimus_L1_Rib_SaRib9_R	0.00	0.00	0.00	12.96	0.00
55	Longissimus_L1_Rib_SaRib10_L	0.00	0.00	0.00	12.96	0.00
56	Longissimus_L1_Rib_SaRib10_R	0.00	0.00	0.00	12.96	0.00
57	Longissimus_L1_Rib_SaRib11_L	0.00	0.00	11.55	12.96	0.00
58	Longissimus_L1_Rib_SaRib11_R	0.00	0.00	12.96	12.96	0.00
59	Longissimus_L1_Rib_SaRib12_L	0.00	0.00	12.96	12.96	0.00
60	Longissimus_L1_Rib_SaRib12_R	0.00	0.00	12.96	12.96	0.00
61	Longissimus_L1_TR_L3T3_L	0.00	0.00	21.80	10.34	0.00
62	Longissimus_L1_TR_L3T3_R	0.00	1.83	25.93	22.24	0.00
63	Longissimus_L1_TR_L4T4_L	0.00	0.00	19.44	1.24	0.00

Table C-1 continued

64	Longissimus_L1_TR_L4T4_R	0.00	0.00	19.44	19.44	0.00
65	Longissimus_L1_TR_L4T5_L	0.00	0.76	19.44	19.44	0.00
66	Longissimus_L1_TR_L4T5_R	0.00	0.00	19.44	19.44	0.00
67	Longissimus_L1_TR_L5T6_L	0.00	0.00	15.56	15.56	0.00
68	Longissimus_L1_TR_L5T6_R	0.00	0.00	15.56	15.56	0.00
69	Longissimus_L1_TR_SaT7_L	0.00	0.00	0.00	0.00	0.00
70	Longissimus_L1_TR_SaT7_R	0.00	0.00	0.00	0.00	0.00
71	Longissimus_L1_TR_SaT8_L	0.00	0.00	0.00	0.00	0.00
72	Longissimus_L1_TR_SaT8_R	0.00	0.00	0.00	0.00	0.00
73	Longissimus_L1_TR_SaT9_L	0.00	0.00	0.00	12.96	0.00
74	Longissimus_L1_TR_SaT9_R	0.00	0.00	0.00	12.96	0.00
75	Longissimus_L1_TR_SaT10_L	0.00	0.00	0.00	12.96	0.00
76	Longissimus_L1_TR_SaT10_R	0.00	0.00	0.00	12.96	0.00
77	Longissimus_L1_TR_SaT11_L	0.00	0.00	12.96	12.96	0.00
78	Longissimus_L1_TR_SaT11_R	0.00	0.00	8.31	12.96	0.00
79	Longissimus_L1_TR_SaT12_L	0.00	0.00	12.96	12.96	0.00
80	Longissimus_L1_TR_SaT12_R	0.00	0.00	6.49	12.96	0.00
81	PsoasMajor_Fe_T12_L	0.00	0.00	0.00	0.00	0.00
82	PsoasMajor_Fe_T12_R	0.00	0.00	0.00	0.00	0.00
83	QuadratusLum_Pel_Rib12_L	0.00	0.00	0.00	0.00	0.00
84	QuadratusLum_Pel_Rib12_R	0.00	0.00	0.00	0.00	0.00
85	RecAbdominis_Pel_Rib5_L	0.00	0.00	0.00	0.00	0.00
86	RecAbdominis_Pel_Rib5_R	0.00	0.00	0.00	0.00	0.00
87	RecAbdominis_Pel_Rib6_L	0.00	0.00	0.00	0.00	0.00
88	RecAbdominis_Pel_Rib6_R	0.00	0.00	0.00	0.00	0.00
89	RecAbdominis_Pel_Rib7_CL	28.29	0.00	0.00	0.00	38.25
90	RecAbdominis_Pel_Rib7_CR	28.29	0.00	0.00	0.00	38.00
91	RecAbdominis_Pel_Rib7_L	0.00	0.00	0.00	0.00	1.28
92	RecAbdominis_Pel_Rib7_R	0.00	0.00	0.00	0.00	0.00
93	SpinalisTho_L1_T6_L	0.00	0.00	0.00	0.00	0.00
94	SpinalisTho_L1_T6_R	0.00	0.00	0.00	0.00	0.00
95	SpinalisTho_L2_T5_L	0.00	0.00	0.00	0.00	0.00
96	SpinalisTho_L2_T5_R	0.00	0.00	0.00	0.00	0.00
97	SpinalisTho_L1_TR_SaT1_L	0.00	0.00	0.00	9.44	0.00
98	SpinalisTho_L1_TR_SaT1_R	0.00	0.00	0.00	0.00	0.00
99	Interspinales_L1_T12_L	0.00	0.00	0.00	0.00	0.00

Table C-1 continued

100	Interspinales_L1_T12_R	0.00	0.00	0.00	0.00	0.00
101	Intertransversarii_L1_T12_La_L	0.00	0.00	0.00	0.00	0.00
102	Intertransversarii_L1_T12_La_R	0.00	3.76	0.00	0.00	0.00
103	Intertransversarii_L1_T12_Me_L	0.00	3.60	10.00	10.00	0.00
104	Intertransversarii_L1_T12_Me_R	0.00	0.00	9.16	10.00	0.00
105	Rotatores_L1_T12_L	30.00	0.00	0.00	0.00	70.00
106	Rotatores_L1_T12_R	30.00	0.00	0.00	0.00	70.00
107	Rotatores_L2_T12_L	30.00	0.00	0.00	0.00	70.00
108	Rotatores_L2_T12_R	30.00	0.00	0.00	0.00	70.00
109	Longissimus_L2_T1_L	0.00	0.00	0.00	0.00	0.00
110	Longissimus_L2_T1_R	0.00	0.00	0.00	0.00	0.00
111	Longissimus_L2_T2_L	0.00	0.00	0.00	0.00	0.00
112	Longissimus_L2_T2_R	0.00	0.00	0.00	0.00	0.00
113	Iliocostalis_L2_L1_SaL1_L	0.00	0.00	0.00	0.00	0.00
114	Iliocostalis_L2_L1_SaL1_R	0.00	0.00	0.00	0.00	0.00
115	Longissimus_L2_L1_SaL1_L	0.00	0.00	0.00	0.00	0.00
116	Longissimus_L2_L1_SaL1_R	0.00	0.00	0.00	0.00	0.00
117	Multifidus_L2_L1_SaL1_F1_L	0.00	0.00	0.00	0.00	0.00
118	Multifidus_L2_L1_SaL1_F1_R	0.00	0.00	0.00	0.00	0.00
119	Multifidus_L2_L1_SaL1_F2_L	0.00	0.00	0.00	0.00	0.00
120	Multifidus_L2_L1_SaL1_F2_R	0.00	0.00	0.00	0.00	0.00
121	Multifidus_L2_L1_L5L1_F3_L	0.00	0.00	0.00	11.67	0.00
122	Multifidus_L2_L1_L5L1_F3_R	0.00	0.00	0.00	11.67	0.00
123	Multifidus_L2_L1_L4L1_F4_L	46.67	0.00	0.00	0.00	21.81
124	Multifidus_L2_L1_L4L1_F4_R	46.67	0.00	0.00	0.00	21.69
125	PsoasMajor_Fe_L1_L	0.00	0.00	0.00	0.00	0.00
126	PsoasMajor_Fe_L1_R	0.00	0.00	0.00	0.00	0.00
127	QuadratusLum_Pel_L1_L	0.00	0.00	0.00	0.00	0.00
128	QuadratusLum_Pel_L1_R	0.00	0.00	0.00	0.73	0.00
129	Interspinales_L2_L1_L	2.65	0.00	5.81	10.00	37.94
130	Interspinales_L2_L1_R	2.65	10.00	1.46	10.00	38.02
131	Intertransversarii_L2_L1_La_L	30.00	0.00	0.00	10.00	70.00
132	Intertransversarii_L2_L1_La_R	30.00	0.00	0.00	10.00	70.00
133	Intertransversarii_L2_L1_Me_L	0.00	0.00	0.00	9.96	0.00
134	Intertransversarii_L2_L1_Me_R	0.00	0.00	0.00	8.72	0.00
135	Rotatores_L2_L1_L	30.00	10.00	5.66	10.00	70.00

Table C-1 continued

136	Rotatores_L2_L1_R	30.00	10.00	7.46	10.00	70.00
137	Rotatores_L3_L1_L	30.00	6.33	2.92	6.75	70.00
138	Rotatores_L3_L1_R	30.00	5.20	0.00	8.50	70.00
139	Iliocostalis_L3_L2_SaL2_L	0.00	0.00	0.00	0.00	0.00
140	Iliocostalis_L3_L2_SaL2_R	0.00	0.00	0.00	0.00	0.00
141	Longissimus_L3_L2_SaL2_L	0.00	0.00	0.00	0.00	0.00
142	Longissimus_L3_L2_SaL2_R	0.00	0.00	0.00	0.00	0.00
143	Multifidus_L3_L2_SaL2_F1_L	0.00	0.00	0.00	0.00	0.00
144	Multifidus_L3_L2_SaL2_F1_R	0.00	0.00	0.00	0.00	0.00
145	Multifidus_L3_L2_SaL2_F2_L	0.00	0.00	0.00	0.00	0.00
146	Multifidus_L3_L2_SaL2_F2_R	0.00	0.00	0.00	0.00	0.00
147	Multifidus_L3_L2_L5L2_F3_L	0.00	0.00	0.00	0.00	0.00
148	Multifidus_L3_L2_L5L2_F3_R	0.00	0.00	0.00	0.00	0.00
149	Multifidus_L3_L2_SaL2_F4_L	0.00	0.00	0.00	0.00	0.00
150	Multifidus_L3_L2_SaL2_F4_R	0.00	0.00	0.00	0.00	0.00
151	PsoasMajor_Fe_L2_L	0.00	0.00	0.00	0.00	0.00
152	PsoasMajor_Fe_L2_R	0.00	0.00	0.00	4.96	0.00
153	QuadratusLum_Pel_L2_L	0.00	0.00	0.00	34.02	0.00
154	QuadratusLum_Pel_L2_R	0.00	0.00	0.00	30.75	0.00
155	Interspinales_L3_L2_L	30.00	10.00	0.00	0.00	70.00
156	Interspinales_L3_L2_R	30.00	10.00	0.00	0.00	70.00
157	Intertransversarii_L3_L2_La_L	7.60	0.03	0.00	0.00	23.41
158	Intertransversarii_L3_L2_La_R	7.60	0.00	0.00	0.00	23.35
159	Intertransversarii_L3_L2_Me_L	30.00	1.16	0.00	0.00	45.16
160	Intertransversarii_L3_L2_Me_R	30.00	2.89	3.53	0.00	45.30
161	Rotatores_L3_L2_L	5.60	0.00	10.00	10.00	70.00
162	Rotatores_L3_L2_R	5.60	0.00	10.00	9.62	69.98
163	Rotatores_L4_L2_L	0.00	0.00	0.00	10.00	0.00
164	Rotatores_L4_L2_R	0.00	0.00	0.03	7.30	0.00
165	Iliocostalis_L4_L3_SaL3_L	0.00	0.00	0.00	0.00	0.00
166	Iliocostalis_L4_L3_SaL3_R	0.00	0.00	0.00	0.00	0.00
167	Longissimus_L4_L3_SaL3_L	53.58	28.09	19.95	0.00	19.36
168	Longissimus_L4_L3_SaL3_R	53.58	29.59	22.81	0.00	19.43
169	Multifidus_L4_L3_SaL3_F1_L	0.00	0.00	0.00	0.00	0.00
170	Multifidus_L4_L3_SaL3_F1_R	0.00	0.00	0.00	0.00	0.00
171	Multifidus_L4_L3_SaL3_F2_L	0.00	0.00	0.00	0.00	0.00

Table C-1 continued

172	Multifidus_L4_L3_SaL3_F2_R	0.00	0.00	0.00	0.00	0.00
173	Multifidus_L4_L3_SaL3_F3_L	0.00	0.00	0.00	0.00	0.00
174	Multifidus_L4_L3_SaL3_F3_R	0.00	0.00	0.00	0.00	0.00
175	Multifidus_L4_L3_SaL3_F4_L	0.00	0.00	0.00	0.00	0.00
176	Multifidus_L4_L3_SaL3_F4_R	0.00	0.00	0.00	0.00	0.00
177	PsoasMajor_Fe_L3_L	0.00	0.00	0.00	0.00	0.00
178	PsoasMajor_Fe_L3_R	0.00	0.00	0.00	0.00	0.00
179	QuadratusLum_Pel_L3_L	0.00	0.00	0.00	0.00	0.00
180	QuadratusLum_Pel_L3_R	0.00	0.00	0.00	0.00	0.00
181	Interspinales_L4_L3_L	30.00	10.00	10.00	10.00	70.00
182	Interspinales_L4_L3_R	30.00	10.00	10.00	10.00	70.00
183	Intertransversarii_L4_L3_La_L	30.00	0.00	8.38	0.00	70.00
184	Intertransversarii_L4_L3_La_R	30.00	0.00	7.08	0.18	70.00
185	Intertransversarii_L4_L3_Me_L	30.00	9.89	10.00	0.00	70.00
186	Intertransversarii_L4_L3_Me_R	30.00	10.00	10.00	4.14	70.00
187	Rotatores_L4_L3_L	0.00	0.00	0.00	10.00	0.00
188	Rotatores_L4_L3_R	0.00	0.59	0.00	10.00	0.04
189	Rotatores_L5_L3_L	0.00	0.00	0.00	10.00	0.00
190	Rotatores_L5_L3_R	0.00	0.00	0.00	10.00	0.00
191	Iliocostalis_Sa_L4_L	0.00	3.45	9.10	0.00	0.00
192	Iliocostalis_Sa_L4_R	0.00	3.83	8.72	0.00	0.00
193	Longissimus_Sa_L4_L	139.11	77.78	77.78	67.97	186.39
194	Longissimus_Sa_L4_R	139.11	77.78	77.78	70.31	186.17
195	Multifidus_Sa_L4_F1_L	0.00	0.00	0.00	0.00	0.00
196	Multifidus_Sa_L4_F1_R	0.00	0.00	0.00	0.00	0.00
197	Multifidus_Sa_L4_F2_L	0.00	0.00	0.00	0.00	0.00
198	Multifidus_Sa_L4_F2_R	0.00	0.00	0.00	0.00	0.00
199	Multifidus_Sa_L4_F3_L	0.00	0.00	0.00	0.00	0.00
200	Multifidus_Sa_L4_F3_R	0.00	0.00	0.00	0.00	0.00
201	Multifidus_Sa_L4_F4_L	0.00	0.35	0.00	0.00	0.00
202	Multifidus_Sa_L4_F4_R	0.00	0.00	0.00	0.00	0.00
203	PsoasMajor_Fe_L4_L	0.00	0.00	0.00	0.00	0.00
204	PsoasMajor_Fe_L4_R	0.00	0.00	0.00	0.00	0.00
205	QuadratusLum_Pel_L4_L	0.00	0.00	0.00	0.00	0.00
206	QuadratusLum_Pel_L4_R	0.00	0.00	0.00	0.00	0.00
207	Interspinales_L5_L4_L	30.00	10.00	10.00	10.00	49.76

Table C-1 continued

208	Interspinales_L5_L4_R	30.00	10.00	10.00	10.00	33.86
209	Intertransversarii_L5_L4_La_L	30.00	0.00	8.85	2.45	0.00
210	Intertransversarii_L5_L4_La_R	30.00	0.24	8.54	3.05	1.30
211	Intertransversarii_L5_L4_Me_L	30.00	10.00	10.00	10.00	70.00
212	Intertransversarii_L5_L4_Me_R	30.00	10.00	10.00	10.00	70.00
213	Rotatores_L5_L4_L	0.00	0.00	0.00	0.27	0.00
214	Rotatores_L5_L4_R	0.00	0.00	0.50	0.00	0.00
215	Rotatores_Sa_L4_L	0.00	0.00	0.00	0.00	0.00
216	Rotatores_Sa_L4_R	0.00	0.00	0.00	0.00	0.00
217	Longissimus_Sa_L5_L	126.88	68.72	73.93	77.78	155.19
218	Longissimus_Sa_L5_R	126.88	68.98	74.00	77.78	155.34
219	Multifidus_Sa_L5_F1_L	0.00	0.00	0.00	0.00	0.00
220	Multifidus_Sa_L5_F1_R	0.00	0.00	0.00	0.00	0.00
221	Multifidus_Sa_L5_F2_L	0.00	0.00	0.00	0.00	0.00
222	Multifidus_Sa_L5_F2_R	0.00	0.00	0.00	0.00	0.00
223	Multifidus_Sa_L5_F3_L	0.00	0.00	0.00	0.00	0.00
224	Multifidus_Sa_L5_F3_R	0.00	0.00	0.00	0.00	0.00
225	Multifidus_Sa_L5_F4_L	0.00	0.00	0.00	16.64	0.00
226	Multifidus_Sa_L5_F4_R	0.00	0.00	0.00	19.68	0.00
227	PsoasMajor_Fe_L5_L	0.00	0.00	0.00	0.00	0.00
228	PsoasMajor_Fe_L5_R	0.00	0.00	0.00	0.00	0.00
229	Interspinales_Sa_L5_L	0.00	0.00	0.00	0.00	0.00
230	Interspinales_Sa_L5_R	0.00	0.00	0.00	0.00	0.00
231	Rotatores_Sa_L5_L	0.00	0.00	0.00	0.00	0.00
232	Rotatores_Sa_L5_R	0.00	0.00	0.00	0.00	0.00

APPENDIX D. THE ROLE OF SHORT MUSCLES IN STABILIZING THE WHOLE LUMBAR SPINE

The studies of the main section showed that spinal muscles were able to create CFLs and stabilize the lumbar spine in different MFCs and FLPs. However, the biomechanical roles of short intrinsic muscles (SIMs) in stabilizing the lumbar spine as well as in creating CFLs remain unclear.

To investigate the biomechanical roles of SIMs, such as rotatores, interspinales and intertransversarii, in controlling the deformation and the stability of the whole lumbar spine *via* a follower load mechanism. For this purpose, the optimization and the 3-D FE model with and without 54 SIMs at all levels were used simultaneously in order to determine the spinal MFs creating CFL in the lumbar spine in a neutral standing posture and the deformation of the lumbar spine resulting from the upper body weight of 350N and such MFs.

The optimization analyses predicted that CFLs can be created by spinal muscles without SIMs from FLP at η = -30.0 mm to FLP at η = -4.0 mm. However, the FE predictions in the case of FLP at η = -4.0 mm as shown in Figure D-1 clearly demonstrated that the CFL creating MFs predicted from the model without SIMs produce a large deformation particularly at the T12-L1-L2 segments (unstable deformation) regardless of FLP variation, whereas such MFs predicted from the model with SIMs produced stable deformation of the lumbar spine (resulting in the trunk sway <10 mm, see section 5.1).

The predicted CFLs in this case were 2277 N at T12-L1, 2288 N at L1-L2, 2405 N at L2-L3, 2565 N at L3-L4, 2818 N at L4-L5 and 2859 N at L5-Sac. The CFLs created by spinal muscles without contribution of SIMs were higher (300% or more) than those

with the contribution of SIMs. These higher CFLs and the lack of MFs in diversified directions that used to be provided by SIMs seemed to result in greater (or more unstable) deformation of the lumbar spine. Thus, this result clearly showed that SIMs were essential to stabilizing the spine via a CFL mechanism.

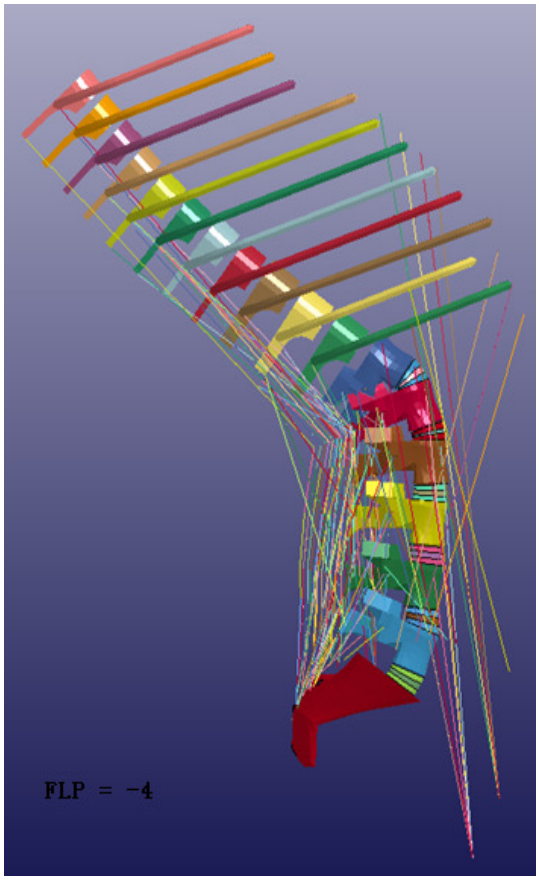

Figure D-1 Deformation of the lumbar spine without SIMs (MFC = 45 N/cm^2 , FLP at η = -4.0 mm)